5-2022

Theoretical studies of benzoquinone reactivity in acidic and basic environments

Natali Majoras
University of Tennessee at Chattanooga, rjq339@mocs.utc.edu

THEORETICAL STUDIES OF BENZOQUINONE REACTIVITY IN ACIDIC AND BASIC ENVIRONMENTS

Natali Kei Majoras

Departmental Honors Thesis
The University of Tennessee at Chattanooga
Chemistry and Physics

Examination Date:
4 April 2022

Titus V. Albu
Professor of Chemistry
Thesis Director

Jared Pienkos
Assistant Professor of Chemistry
Department Examiner

ABSTRACT

Quinones are a class of organic compounds containing a six-membered unsaturated ring with two carbonyl groups. They are biologically relevant mostly due to their ability to participate in redox reactions. Prior experiments in our lab showed that quinones can induce protein modifications that are pH dependent. In an acidic environment the modifications were less significant than in a basic environment. Previous computational studies have also been carried out to model, in neutral solutions, the reaction between various quinones and various amines. Various amine groups are used as a model for the amino group of lysine to represent protein modification. The theoretical study presented here will extend previous work by looking at the reaction between benzoquinone and methylamine in both acidic and basic media. All theoretical calculations were performed using a hybrid density functional theory method, MPW1K, in conjunction with the 6-31+G(d,p) basis set.

TABLE OF CONTENTS

Page

ABSTRACT……... ii
TABLE OF CONTENTS……...iii
LIST OF TABLES…….vii
LIST OF FIGURES……ix
LIST OF ACRONYMS……....xiv

Chapter 1

1. INTRODUCTION.....1

1.1 Quinones……..... 1

1.1.1 Brief description of quinones ……..……1

1.1.2 Selected experimental studies of quinones… ……..2

1.1.3 Selected theoretical studies of quinones……..3

1.2 Prior studies in our laboratory….. ….....…….....4

1.2.1 Prior experimental studies on protein modification by quinones….. ……..4

1.2.2 Prior theoretical studies of quinones and their reactivity toward amines…….....7

1.3 Research objective for the current study……..9

1.4 Computational methodologies…….9

Chapter 2

2. REACTION STUDIES IN NEUTRAL ENVIRONMENTS…….12

2.1 Introduction……12

2.2 Reactants and Products…….……....14

2.2.1 Reactants……14

2.2.2 Product of the 1,4-addition reaction…..……..17

2.2.3 Product of the 1,2-addition reaction.....…….19

2.3 Reactant and Product Complexes …….……21

2.3.1 Reactant complex ……..21

2.3.2 Product complex for the 1,4-addition reaction……..23

2.3.3 Product complex for the 1,2-addition reaction …….....…….....24

2.4 Transition States…….……...26

2.4.1 Transition states for the 1,4-addition reaction…….. ……..…..……..26

2.4.2 Transition states for the 1,2-addition reaction……...…….…..……..28

2.5 Energy Profile for Reaction Pathways in Neutral Environment……..…..33

Chapter 3

3. REACTION STUDIES IN BASIC ENVIRONMENTS……...…….35

3.1 Introduction ……..…….……..…..35

3.2 Basic-Modeled Reactants and Products ……..……...…..37

3.2.1 Basic-modeled reactants……37

3.2.2 Basic-modeled product of the 1,4-addition reaction……..…...38

3.2.3 Basic-modeled product of the 1,2-addition reaction……..…...40

3.3 Basic-Modeled Reactant and Product Complexes ……..……...…..42

3.3.1 Basic-modeled reactant complexes……..……..…...42

3.3.2 Basic-modeled product complex for the 1,4-addition reaction……..…...44

3.3.3 Basic-modeled product complex for the 1,2-addition reaction……..…...46

3.4 Basic-Modeled Transition States……..……...…..47

3.5 Energy Profile for the Reaction Pathways in Basic Environment……...…..49

Chapter 4

4. REACTION STUDIES IN ACIDC ENVIRONMENTS……..…..…….51

4.1 Introduction……51

4.2 Acidic-Modeled Reactants and Products……...53

4.2.1 Acidic-modeled reactants…….……...……...53

4.2.2 Acidic-modeled product of the 1,4-addition reaction.……..…….54

4.2.3 Acidic-modeled product of the 1,2-addition reaction...…….56

4.3 Acidic-Modeled Reactant and Product Complexes…….....…..58

4.3.1 Acidic-modeled reactant complexes……...……..…….58

4.3.2 Acidic-modeled product complex for the 1,4-addition reaction……...…….59

4.3.3 Acidic-modeled product complex for the 1,2-addition reaction……...…….61

4.4 Acidic-Modeled Transition State…….....…..62

4.5 Analysis of Acidic-Modeled Reaction Pathway……64

Chapter 5

5. ANALYSIS OF REACTION IN DIFFERENT ENVIRONMENTS……...67

5.1 Introduction……67

5.2 Reaction Path Energies……..67

5.2.1 Barrier heights…….…….……...……...67

5.2.2 Energies of reaction determined from reactants and products…..……...……...68

5.2.3 Energies of reaction determined from reactant and product complexes…..……...69

5.3 The Effect of Ionized Species on the Transition State of 1,4-Addition Reaction..71

5.3.1 Ionized species in cubic positions……..71

5.3.2 Ionized species in special positions…….……..79

5.4 Future Work and Concluding Remarks…….....81

BIBLIOGRAPHY ……83

APPENDICES ……85

APPENDIX A − Supplementary Information for Chapter 2, 3, 4, and 5……..85

APPENDIX B − Sample Gaussian Input Files ……98

LIST OF TABLES

Page

Table 2.1 Species labeling and chemical formulas for various stages of the reaction pathway in neutral environments……..14

Table 2.2 Gas-phase barrier heights (kcal/mol) and imaginary frequencies (cm^{-1}) for transition states for 1,2-addition of methylamine to benzoquinone……...31

Table 2.3 Selected internuclear distances (Å) for transition states for 1,2-addition of methylamine to benzoquinone……...32

Table 3.1 Species labeling and chemical formulas for various stages of the reaction pathway in basic environments……36

Table 4.1 Species labeling and chemical formulas for various stages of the reaction pathway in acidic environments……...52

Table 5.1 Relative energy difference for the reactants to products reaction of the 1,4-addition of MA to PBQ……..69

Table 5.2 Relative energy difference for the reactants to products reaction of the 1,2-addition of MA to PBQ……..69

Table 5.3 Relative energy difference for the reactant complex to product complex reaction of the 1,4-addition of MA to PBQ……70

Table 5.4 Relative energy difference for the reactant complex to product complex reaction of the 1,2-addition of MA to PBQ……71

Table 5.5 Distances between O_{26} and the N_{14}, O_{17}, and O_{20} atoms that are involved in hydrogen transfer process of the transition state……76

Table 5.6 Distances between O_{26} and the H_{13}, H_{19}, and H_{16} atoms that are involved in hydrogen transfer process of the transition state……77

Table 5.7 Energetic effect on **TSA1** from the influencing species (H_2O, OH^-, H_3O^+) in cubic positions……78

Table 5.8 Energetic effect on **TSA1** from the influencing species (H_2O, OH^-, H_3O^+) in special positions……81

LIST OF FIGURES

Page

Figure 1.1 Chemical structures of selected quinones: a) 1,4-benzoquinone, b) 1,4-naphthoquinone, and c) 9,10-anthraquinone……2

Figure 1.2 Schematic of p-Benzoquinone protein modification……...5

Figure 1.3 SDS-PAGE results for concentration- and time-dependent modifications of RNase upon exposure to PBQ at 0.5 mM and 5.0 mM……...6

Figure 1.4 pH dependent fluorescence intensity for Lysozyme modified by PBQ……...7

Figure 1.5 A sample potential energy surface with examples of first and second order saddle points……..10

Figure 2.1 The first step of the reaction of benzoquinone with methylamine leading to the 1,4-addition product (top) and 1,2-addition product (bottom)……...12

Figure 2.2 Ten possible orientations of water dimers. Adapted from Anderson and Tschumper, 2006……15

Figure 2.3 Lowest-energy structures of water dimer (left) and methylamine (right)……..15

Figure 2.4 Lowest-energy conformation for methylamine trimer……...16

Figure 2.5 Two other low-energy conformations for methylamine trimer…….17

Figure 2.6 Lowest-energy conformation for the product of the 1,4-addition of methylamine to benzoquinone (**PA1**)……..18

Figure 2.7 Two other low-energy conformations for the product of the 1,4-addition of methylamine to benzoquinone (**PA2** and **PA3**)…….18

Figure 2.8 Lowest-energy conformation for the product of the 1,2-addition of methylamine to benzoquinone (**PB1**)……..20

Figure 2.9 Other low-energy conformations for the product of the 1,2-addition of methylamine to benzoquinone **PB2** and **PB3**……..……..20

Figure 2.10 Lowest-energy conformation of the reactant complex……..22

Figure 2.11 Three other low-energy conformations for the reactant complex: **RC2**, **RC3**, and RC4……22

Figure 2.12 Lowest-energy conformation of the product complex for the 1,4-addition of methylamine to benzoquinone **PCA1**……24

Figure 2.13 Three other low-energy conformations for the product complexes for the 1,4-addition of methylamine: **PCA2**, **PCA3**, **PCA4**……...24

Figure 2.14 Lowest-energy conformation of the product complex for the 1,2-addition of methylamine to benzoquinone **PCB1**……25

Figure 2.15 Three other low-energy conformations for the product complexes for the 1,2-addition of methylamine: **PCB2, PCB3,** and **PCB4**…….26

Figure 2.16 Lowest-energy transition state for the 1,4-addition of methylamine to benzoquinone **TSA1**……..27

Figure 2.17 Next three low-energy transition states for the 1,4-addition of methylamine to benzoquinone: **TSA2**, **TSA3**, **TSA4**……..27

Figure 2.18 Lowest-energy transition state for the 1,2-addition of methylamine to benzoquinone **TSB1**……...29

Figure 2.19 Other transition states for 1,2-addition of methylamine to benzoquinone: **TSB2**-**TSB5**……..30

Figure 2.20 Labels for the 1,2-addition transition state distances…….31

Figure 2.21 Energy diagram for the reaction of methylamine with benzoquinone in neutral environments……..33

Figure 3.1 The first step of the reaction of benzoquinone with deprotonated MA leading to the basic-modeled 1,4-addition product (top) and 1,2-addition product……...36

Figure 3.2 Lowest energy basic-modeled trimer **BR1**……38

Figure 3.3 Next three lowest-energy basic-modeled trimers: **BR2**, **BR3**, **BR4**……..38

Figure 3.4 Lowest-energy conformation for the basic-modeled product of the 1,4-addition of methylamine to benzoquinone (**BPA1**)…….39

Figure 3.5 Other low-energy conformations for the basic-modeled product of the 1,4-addition of methylamine to benzoquinone: **BPA2, BPA3, BPA4**……..40

Figure 3.6 Lowest-energy conformation for the basic-modeled product of the 1,2-addition of methylamine to benzoquinone (**BPB1**)…….41

Figure 3.7 Other low-energy conformations for the basic-modeled product of the 1,2-addition of methylamine to benzoquinone: **BPB2**, and **BPB3**……..41

Figure 3.8 Lowest-energy conformation for the basic-modeled reactant complex **BRC1**….43

Figure 3.9 Next low-energy basic-modeled reactant complexes: **BRC2** and **BRC3**……..43

Figure 3.10 Lowest-energy conformation of the basic-modeled product complex for the 1,4-addition of methylamine to benzoquinone **BPCA1**……...45

Figure 3.11 Other low-energy conformations for the basic-modeled product complexes for the 1,4-addition of methylamine: **BPCA2**, **BPCA3**, **BPCA4**…….45

Figure 3.12 Lowest-energy conformation of the basic-modeled product complex for the 1,2-addition of methylamine to benzoquinone **BPCB1**……...46

Figure 3.13 Other low-energy conformations for the basic-modeled product complexes for the 1,2-addition of methylamine: **BPCB2, BPCB3,** and **BPCB4**……...47

Figure 3.14 Trials for basic-modeled transition state for the 1,4-addition of MAT to BQ…...48

Figure 3.15 Basic-modeled energy diagram calculated with deprotonated species……..49

Figure 4.1 The first step of the reaction of benzoquinone with protonated MA leading to the acidic-modeled 1,4-addition product (top) and 1,2-addition product (bottom)….52

Figure 4.2 Lowest-energy acidic-modeled trimer **AR1**……..54

Figure 4.3 Two other low-energy acidic-modeled trimers **AR2** and **AR3**…….54

Figure 4.4 Lowest-energy conformation for the acidic-modeled product of the 1,4-addition of methylamine to benzoquinone (**APA1**)…….55

Figure 4.5 Another low-energy conformation for the acidic-modeled product of the 1,4-addition of methylamine to benzoquinone: **APA2**……56

Figure 4.6 Lowest-energy conformation for the acidic-modeled product of the 1,2-addition of methylamine to benzoquinone (**APB1**)…….57

Figure 4.7 Other low-energy conformation for the acidic-modeled product of the 1,2-addition of methylamine to benzoquinone (**APB2**)…….58

Figure 4.8 Lowest-energy conformation for the acidic-modeled reactant complex **ARC1**…59

Figure 4.9 Lowest-energy conformation of the acidic-modeled product complex for the 1,4-addition of methylamine to benzoquinone **APCA1**……...60

Figure 4.10 Other low-energy conformations for the acidic-modeled product complexes for the 1,4-addition of methylamine: **APCA2**, **APCA3**, **APCA4**……...61

Figure 4.11 Lowest-energy conformation of the acidic-modeled product complex for the 1,2-addition of methylamine to benzoquinone **APCB1**……...62

Figure 4.12 Acid-modeled variations of **TSA1** starting geometries: **A**, **B**, **C**, and corresponding output geometries **D**, **E**, **F**, respectively…….63

Figure 4.13 Acidic-modeled energy diagram calculated with protonated species……65

Figure 5.1 Geometric positioning of H_2O, H_3O^+, or HO^- species in the corners of the cubic model……..72

Figure 5.2 Another representation of the geometric positioning of H_2O, H_3O^+, or HO^- species in the corners of the cubic model……..73

Figure 5.3 Representation of all geometric (corners, edges, and faces) positioning of H_2O, H_3O^+, or HO^- species in the cubic model……..74

Figure 5.4 Lowest energy neutral transition state with oxygen, nitrogen, and hydrogens numbered for reference of Table 5.5 and Table 5.8 **TSA1**……75

Figure 5.5 Special positioning of influencing species and their linear relationship with the main atoms involved in hydrogen transfer process, where X is the "center" of the **TSA1**……..80

LIST OF ACRONYMS

DFT	Density functional theory
HDFT	Hybrid density functional theory
HF	Hartree-Fock
MPW1B95	Modified Perdew-Wang exchange functional and Beck's correlation functional method
MPWB1K	Modified Perdew-Wang exchange functional and Beck's correlation functional method
PBQ	Para-benzoquinone
MAT	Methylamine trimer
SDS-PAGE	Sodium Dodecyl Sulfate Polyacrylamide Gel Electrophoresis
UV-Vis	Ultraviolet-Visible

CHAPTER 1

INTRODUCTION

1.1 Quinones

1.1.1 Brief description of quinones

Quinones are a class of organic compounds containing a six-membered unsaturated cyclic ring with two carbonyl groups that are either adjacent to each other or separated by a double bond. Quinones have been studied as chemical entities for over a hundred years and have a rich and diverse chemistry that can be used to influence a synthetic route. Quinone-type compounds are frequently included in commercial and industrial chemicals of many broad and attractive applications. Quinone compounds are utilized as synthetic intermediates and are used as building blocks in organic chemistry studies. Quinones are also studied in the application of the Diels-Alder reaction for the synthesis of natural products [Nawrat and Moody, 2014] [Dohi *et al*., 2012].

Some common quinones are shown in Figure 1.1. Benzoquinones are the simplest form of quinone only containing two carbonyl groups configured in *para*- or *ortho*- positions on a six-membered ring. They are universally found in diverse organisms as free quinones, protein cofactors, or a necessary tool for the mitochondrial electron transport chain. Many benzoquinones are identified as environmental toxins derived from modern industrial processes as the metabolites of polycyclic aromatic hydrocarbons, contributing to bioaccumulation. It is of current study in epidemiology and animal experimentation that quinone derivatives of benzene metabolites serves as a source of inducing abnormal cell behavior leading to cancer or triggering immune response. It is known that benzoquinones are a factor in potential toxins whether

environmentally or biologically except in some limited cases. The mechanism of their toxicity is thought to occur via the combination of oxidative damage intervened by redox-cycling, adduct formation with DNA and proteins, and protein cross-linkage/ protein conformation change [Kim, 2013].

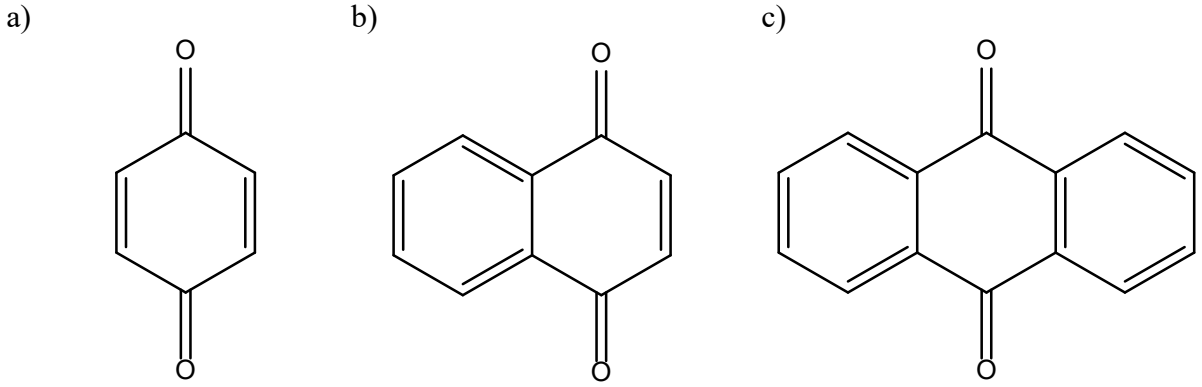

Figure 1.1 Chemical structures of selected quinones: a) 1,4-benzoquinone, b) 1,4-naphthoquinone, and c) 9,10-anthraquinone

1.1.2 Selected experimental studies of quinones

Recently, an experimental study investigating the electrochemical reduction of a series of substituted benzoquinones have been examined in ethylene. The significance of this experiment shows the importance of hydrogen bonding between the quinones or its intermediates and the solvent. Analysis of reduction potentials, amplitude of stabilization, donor character of the substituent, and electron transfer kinetics determined the hydrogen-bonding interections of the mentioned species. The results concluded the redox behavoir of quinones in ethylene that is highly dependent on the nature of the quinone, displayed many similarities from what is observed in a solvent similar to acetonitrile. However, there were noticeable differences in potential between the first and second charge transfer. The observations reflect the effect of

hydrogen bonding in ethylene resulting in stabilization of electrogenerated quinone intermediates [Zhen and Hapiot, 2022].

In another recent organic study, quinones are considered to be a privileged structure and serve as a useful template for the design of new compounds with potential pharmacological activity. The study details developments of quinones in the fields of antitumor, antibacterial, antifungal, anitviral, anti-Alzheimer's disease and antimalarial, investigating biological activity, structural modification, and mechanism of action. From this study, it is determined that quinones serve as a multi-functioning building block in drug discovery available in a wide range of biological activity and different structural modification possibilities that help develop selective drug candidates. The results of the study concluded three main pharmacological advances of quinones: (1) serve as building blocks to locate dependent functional groups to optimize engagement with binding pockets, (2) act as key pharmacophore elements to carry out aromatic interactions or hydrogen bonds, and (3) play a role in electron transport in metabolic pathways [Zhang *et al*., 2021].

1.1.3 Selected theoretical studies of quinones

Recently, a theoretical study investigating the hydration of quinones as catholytes in aqueous redox flow batteries has been studied. The significance of this is due to the quinone ability to carry both electrons and protons in aqueous solutions. Out of a large library of quinones, a multiscale procedure to predict the hydration free energies was employed. The experiment found that introduction of –CHO, –$COOCH_3$, –COOH, –PO_3H_2, and –SO_3H cause a higher hydration free energy. With this, a thermodynamic model is presented as a "first step"

toward molecular screening and design of catholytes for future battery applications [Li *et al*., 2021].

Another recent study was conducted to investigate the redox reaction mechanism of quinone compounds in industrial processes. The experiment involves the oxidation of H_2S by 1,4-naphthoquinone-2-sulfonic acid (NQS), which itself is reduced to 1,4-dihydroxynaphthalene-2-sulfonic acid ($NQSH_2$). From multiple DFT calculations, it is determined that the rate determining step is the initial step in each process that corresponds to the net hydrogen-atom transfer. The essential reactions are characterized as PCET (proton-coupled electron transfer) because the electron and proton are transferred through different pathways. Analysis of transition states resulted in electron transfer precedes proton transfer to a significant extent. This work is significant in the development of new catalysts [Tarumi *et al*., 2019].

In another recent study, electronic structure calculation methods were employed to systematically explore the microscopic mechanism of related light-induced reactions and deactivation pathways. The study obtained accurate potential energy profiles, minimum energy pathways, and absorption spectra that observe the light-induced tetrazole-quinone 1,3-dipolar cycloaddition mechanism at the atomic level. The significance of this study involves the rational design of related photoinduced reactions for future work [He *et al*., 2021].

1.2 Prior studies in our laboratoy

1.2.1 Prior experimental studies of protein modifications by quinones

The neutral reaction modeled computationally in the current thesis is based on previous experiments involving p-benzoquinone. Specifically, *Modifications of ribonuclease A induced by p-benzoquinone* paper [Kim *et al*. 2012] is an experimental study used as foundation for

modeling the neutral reaction pathway between methylamine and benzoquinone. In the experimental study, SDS-PAGE experiments revealed that PBQ was efficient in producing oligomers and polymeric aggregates when RNase was incubated with PBQ. Fluorescence behavior and anisotropic changes of the modified RNase were monitored for a series of incubation reactions, where RNase was incubated with PBQ in phosphate buffer. The modified RNase exhibited less intense fluorescence and slightly higher anisotropy than the unmodified RNase. UV-Vis spectroscopy indicated that PBQ formed covalent bonds to the modified RNase. A proposed mechanism of PBQ action in protein modification can be seen in Figure 1.2.

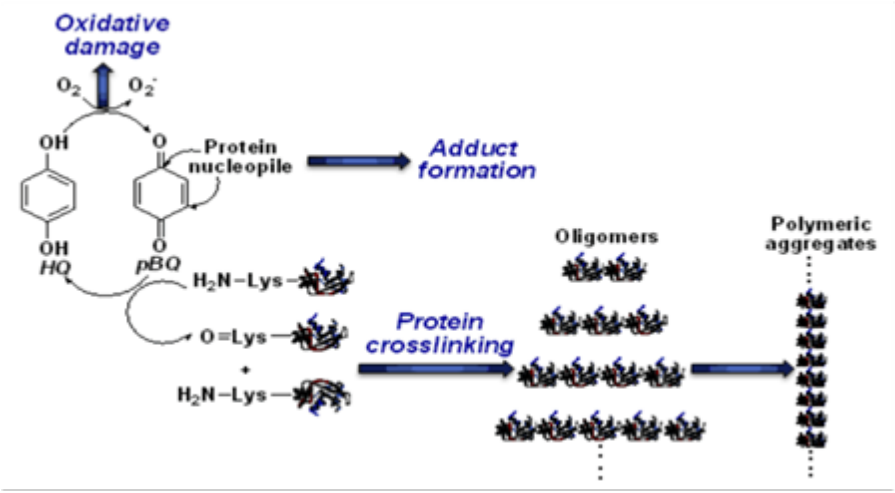

Figure 1.2 Schematic of p-Benzoquinone protein modification

Further, the details related to the SDS-PAGE are useful in identifying changes in molecular weight of modified RNase by the presence of PBQ [Kim *et al*., 2012]. To explore the structural and morphological changes of RNase, fluorescence spectroscopic measurements were coupled with UV-Vis spectroscopy and confocal microscopy. The results of SDS-PAGE showed the extent of RNase modification intensified as the concentration of PBQ increased. At the highest level of concentration used in this study, specifically 5.0 mM of PBQ, multiple protein bands appeared as early as 10 minutes in regions of 33, 53, and 70 kDa. Further, a smearing band

also appeared at the higher molecular weight region (around 100 kDa) as incubation time increased to 30 minutes or longer. The control RNase experiment showed no modification in a 24-hour incubation period at the same experimental temperature of 37°C. A visual of the modified protein bands can be seen in Figure 1.3.

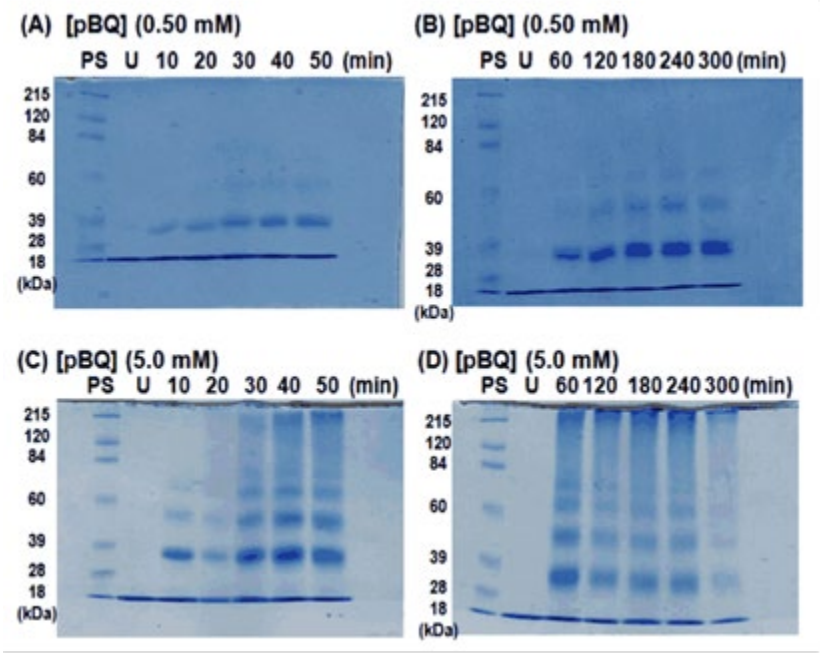

Figure 1.3 SDS-PAGE results for concentration- and time-dependent modifications of RNase upon exposure to PBQ at 0.5 mM and 5.0 mM

Additionally, the modification of Lysozyme by PBQ under pH dependence was investigated through fluorescent experiments [Kim *et al.*, 2012], and selected results are presented in Figure 1.4. The results in Figure 1.4 shows the fluorescence spectra of the modified Lysozyme after 24-hour incubation at various pH values. Acidic conditions are represented in the blue peak, neutral in red, and basic in green. The fluorescence intensity was found to be dependent on the pH value of the environment. Acidic conditions resulted in the highest fluorescence intensity, with a peak intensity of about 125,000 a.u. at 340 nm. A high fluorescence intensity represents less modifications of the protein during the reaction, therefore

less reactivity. The neutral conditions peak intensity is about 25,000 a.u. less than acidic conditions, implying slightly more reactive reaction conditions. The basic conditions peak is about 50,000 a.u. less than the neutral peak and about 75,000 a.u. less than the acidic peak. Overall, the basic conditions of lysozyme modification by PBQ is the most favorable reaction environment, with the lowest peak intensity.

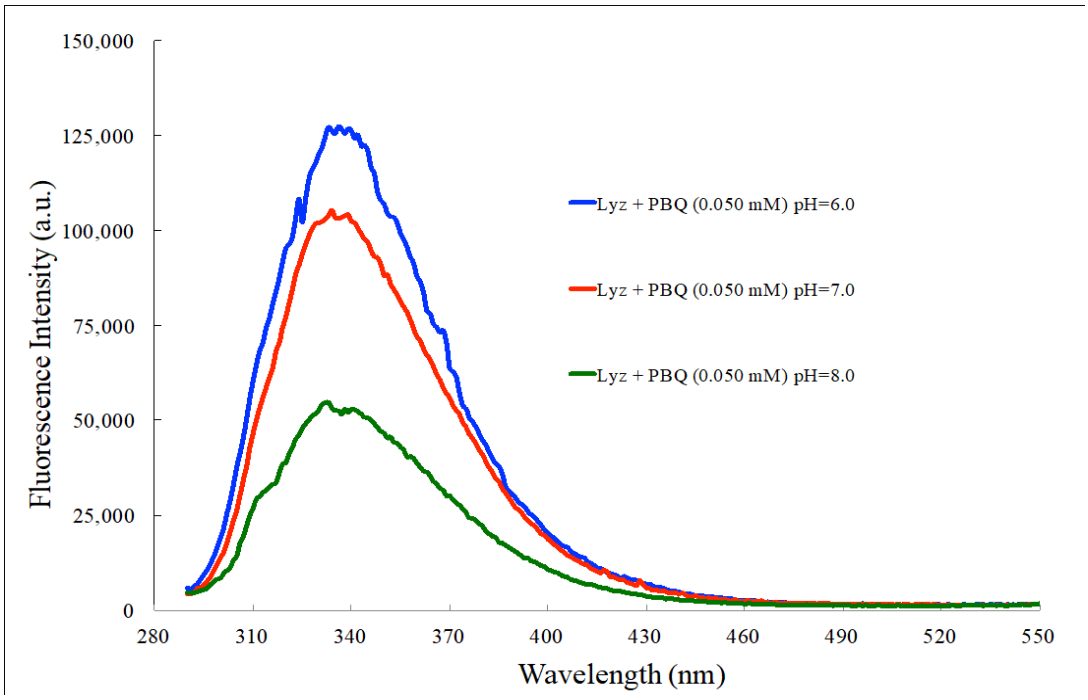

Figure 1.4 pH dependent fluorescence intensity for Lysozyme modified by PBQ

1.2.2 Prior theoretical studies of quinones and their reactivity toward amines

In an initial study, the reactivity of quinones toward N-containing nucleophiles was investigated. Nucleophilic addition reactions at the carbonyl bonds with NH_3 and CH_3NH_2 nucleophiles were studied for four different quinones (para-benzoquinone, 2-chloro-para-benzoquinone, 2-methyl-para-benzoquinone, and ortho-benzoquinone). The reactions were investigated under three different pathways: a direct hydrogen transfer, and two pathways of

hydrogen transfer through water and methanol. The results showed that solvent-assisted pathways have lower barrier height and are more favorable [Fernando, 2009].

Following the initial study, a more specified study involving three different quinone*s* (*p*-benzoquinone, chloro-*p*-benzoquinone, and methyl-*p*-benzoquinone) and their reactivities towards N-containing nucleophiles (ammonia, methylamine, and ethylamine) was investigated. Most of the saddle points for the chosen pathways were located and optimized. Possible reactant complexes were identified and about 25 these complexes were optimized. From these calculations, minimum reaction pathways were identified from the investigated reactions [Rathnayake, 2013].

Next, an investigation into naphthoquinone reactivity towards amino groups was conducted. The reactions between three naphthoquinones, 1,2-naphthoquinone (ONQ), 1,4-naphthoquinone (PNQ), and 2-hydroxy-1,4-naphthoquinone (HNQ), and methylamine, an N-containing nucleophile were investigated. It was found that both ONQ and HNQ favored 1,2-addition reactions while PNQ favored the 1,4-addition reaction. Computational analysis showed that ONQ is predicted to be the most reactive, followed by HNQ, and lastly PNQ [Lee, 2019].

To investigate the protein modification determined experimentally, the theoretical model for the current thesis is that of benzoquinone reacting with methylamine with reaction pathways to form a 1,2-addition and a 1,4-addition product. Between naphthoquinones, anthraquinones, and benzoquinones, benzoquinone is the easiest quinone to study theoretically the protein modifications. Likewise, methylamine is the simplest N-containing compound to substitute and model a protein. This way the reaction between nitrogen and carbon can be observed without having to configure larger parts of an actual protein.

1.3 Research objective for the current study

The current project continues the study of the reactivity of quinones towards N-containing nucleophiles. The primary goal of the current study is to computationally investigate the influence of pH on the reaction between benzoquinone and methylamine. There will be two distinct approaches to do that. The first approach involves creating energy profiles for the reaction in neutral, acidic and basic environments and using these profiles to predict how the pH will influence the reactivity. These results will be quantitatively compared to the previously studied neutral reaction pathway for the addition of methylamine to benzoquinone. The energy diagram for the neutral reaction between benzoquinone and methylamine allows for comparison of favorability among the three pH-dependent pathways. Energy comparative analysis with be discussed at the end of each chapter for each environment: neutral, basic, and acidic.

The second approach involves investigating the influence of either a water moelcule or a charged species (H_3O^+ and OH^-) on the energy of a transition state. This will allow for an averaged energy comparison due to different ionic effects on a constant transition state.

1.4 Computational Methodologies

The utilization of a potential energy profiles is used for visualization of barrier heights among the three pH-dependent reactions. All atoms within a molecular system contain their individual coordinates that will define the internuclear distances between one another. The relative position for each group of three atoms also contains an angle. For each distance or angle defining the geometry of the system, an electronic energy of the system can be obtained. Representations of the electronic energy as a function of geometric parameters of the system is known to be as a potential energy surface. Mathematically, a general potential energy surface can

be characterized by its stationary points, the points whose derivative is zero. These stationary points can be classified as a maximum, minimum, or a saddle point. In a first-order saddle point, the function (i.e., the energy) is at a maximum in one of the $(3N - 6)$ internal coordinates and at a minimum in the remaining $(3N - 7)$ coordinates, where N is number of atoms in the system. The minimum-energy path that converts reactants into products, passes through a first-order saddle point, and defines the reaction coordinates. The molecular state that corresponds to the maximum energy along the reaction coordinate is the transition state. An example of a potential energy surface can be found below in Figure 1.5 [Teixeira-Dias, 2019].

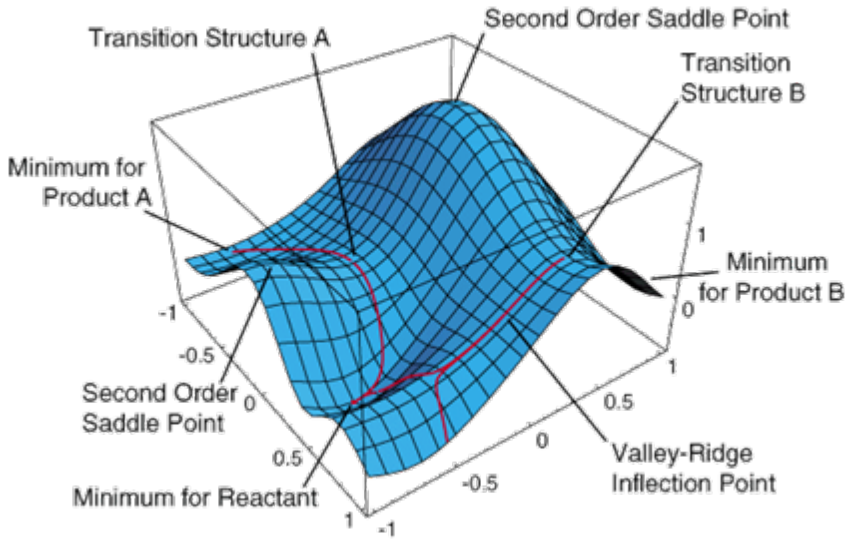

Figure 1.5 A sample potential energy surface with examples of first and second order saddle points

In the current study, all electronic structure calculations were carried out using hybrid density functional theory (HDFT) method of mPW1B95-44 in conjunction with the 6-31+G(d,p) basis set, which was determined to give good results for transition state geometries [Zhao and Truhlar, 2004; Albu and Mikel, 2007]. The mPW1B95-44 functional uses the modified Perdew-Wang (mPW) exchange functional [Adamo and Barone, 1998], followed by 1 indicating one

parameter method, the B95 correlation functional [Becke, 1996], and a Hartree-Fock exchange contribution of 44%. This method was labeled as MPW1K in the original study and was shown to give significant results in obtaining barrier heights [Zhao and Truhlar, 2004].

All the gas-phased geometry optimizations of products, reactants, and intermediate complexes including transition states were performed using a very tight convergence criterion and an ultrafine integration grid for numerical integrations. All the calculations were performed using Gaussian 09 software [Frisch *et al.*, 2009]. The Gaussian keywords used to carry out the calculations are exemplified in the appendix. For visualization of structures, ball and stick rendering is obtained by the Chemcraft software. In these structures, balls of white, gray, red, and blue represent hydrogen, carbon, oxygen, and nitrogen atoms, respectively. The connectivities between atoms are represented by sticks or cylinders, and intermolecular attractions like hydrogen bonding or van der Waals interactions are represented by dashed lines between the atoms.

CHAPTER 2

REACTION STUDIES IN NEUTRAL ENVIRONMENTS

2.1 Introduction

The results of the study of the reaction between benzoquinone (BQ) and methylamine (MA) in neutral environments are presented in this chapter. The first step of this reaction can lead to an 1,2-addition or an 1,4-addition as presented in Figure 2.1 below. Both reactions involve creation of a N–C bond between the N atom of methylamine and a C atom of benzoquinone. Additionally, a proton is transfer between the N atom of the amine and an O atom of benzoquinone. In previous studies [Fernando, 2009; Rathnayake, 2013; Lee, 2019], it was found that the H transfer is done through the intermediacy of one or two water molecules. Accordingly, modeling the reactions requires the inclusion of two water molecules in computations.

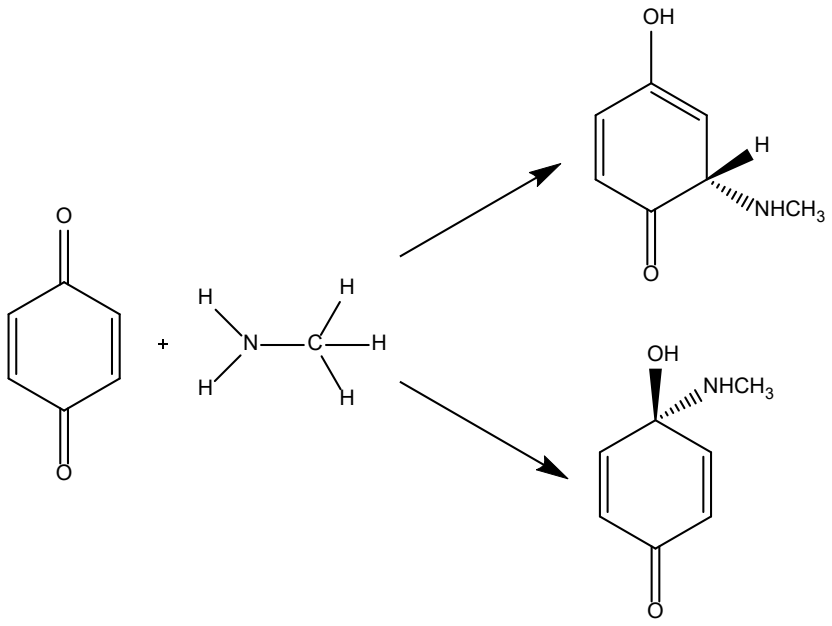

Figure 2.1 The first step of the reaction of benzoquinone with methylamine leading to the 1,4-addition product (top) and 1,2-addition product (bottom)

To create an energy profile for the reaction, energies are necessary for all five stages of the reaction: the reactants, the reactant complex, the transition state, the product complex, and, finally, the products. These energies will be obtained by optimizing the geometries for all relevant species along the reaction pathway. Some of these relevant species have been investigated previously but the most important results were reoptimized to verify their accuracy and will be presented here, with the appropriate references to previous work. The labels and chemical formulas of these relevant species are listed in Table 2.1. The label A is used for species along the 1,4-addition pathway, while label B is used for species along the 1,2-addition pathway. Also, for most of these species, multiple conformations are possible, so a number is added to the label to indicate the ranking of increasing energy. For example, **RC1** will represent the lowest-energy reactant complex while **PA3** will represent the third lowest energy conformation of the 1,4-product.

Table 2.1 Species labeling and chemical formulas for various stages of the reaction pathway in neutral environments

Formula	Name/Description & Label
$H_2O\cdots H_2O\cdots CH_3NH_2$	Methylamine trimer (MAT) (**R**)
$C_6H_4O_2$	Benzoquinone (**BQ**)
$H_2O\cdots H_2O\cdots CH_3NH_2\cdots C_6H_4O_2$	Reactant complex (**RC**)
$H_2O\cdots H_2O\cdots CH_3NH\cdots H\cdots C_6H_4O_2$	1,4-Transition state (**TSA**)
$H_2O\cdots H_2O\cdots CH_3NH\cdots H\cdots C_6H_4O_2$	1,2-Transition state (**TSB**)
$H_2O\cdots H_2O\cdots CH_3NH–C_6H_4O_2H$	1,4-Product complex (**PCA**)
$H_2O\cdots H_2O\cdots CH_3NH–C_6H_4O_2H$	1,2-Product complex (**PCB**)
$CH_3NH–C_6H_4O_2H$	1,4-Product (**PA**)
$CH_3NH–C_6H_4O_2H$	1,2-Product (**PB**)
$H_2O\cdots H_2O$	Water dimer (**P**)

2.2 Reactants and Products

2.2.1 Reactants

One of the reactants is 1,4-benzoquinone or *p*-benzoquinone that has only one conformation as rotation around any bond is restricted due to all carbons being double bonded. The other reactant is the trimer formed between methylamine and two water molecules. This trimer can be seen as being formed from methylamine and water dimer so a careful investigation on both these species was carried out.

Ten various conformations of water dimer complexes were investigated by Anderson and Tschumper [Anderson and Tschumper, 2006] with ten different density functional theory (DFT) methods. Figure 2.2 shows these ten water dimer conformations. All ten conformations were also optimized to determine the lowest-energy geometry with the level of theory used in the

current study, and this lowest-energy geometry is shown in Figure 2.3 along with lowest-energy geometry of methylamine.

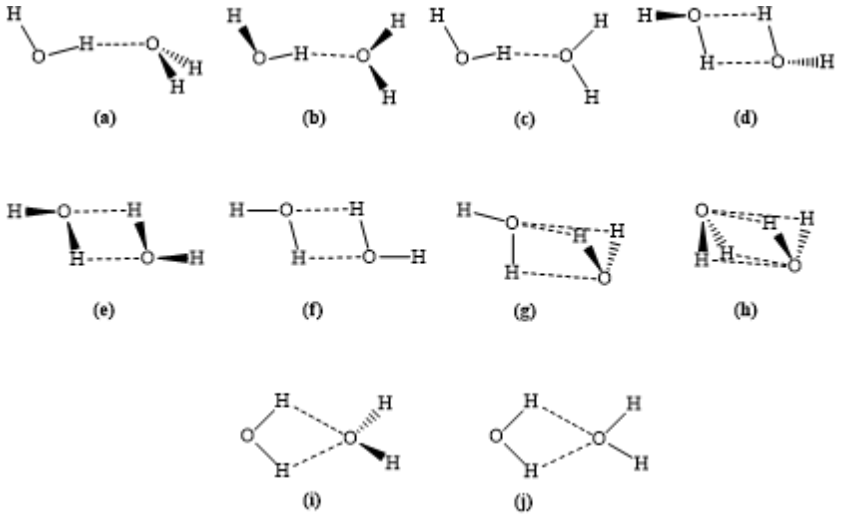

Figure 2.2 Ten possible orientations of water dimers. Adapted from Anderson and Tschumper, 2006.

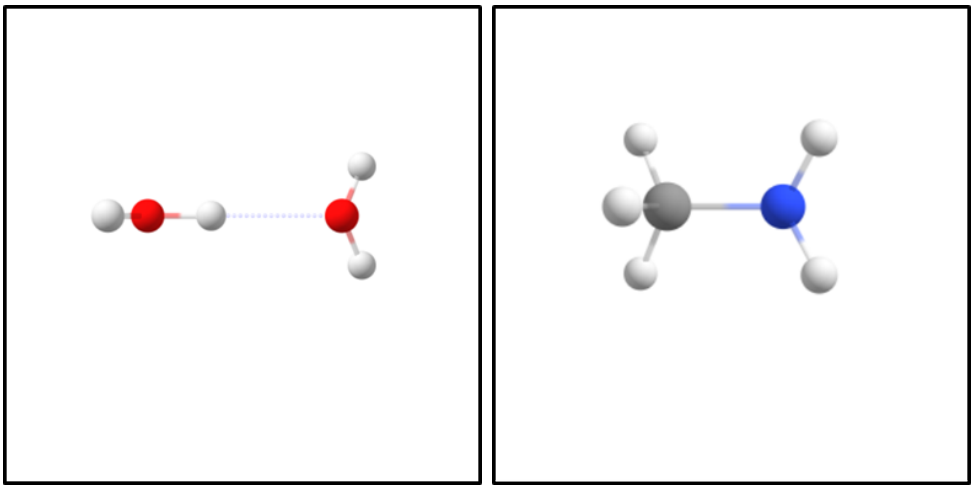

Figure 2.3 Lowest-energy structures of water dimer (left) and methylamine (right)

A methylamine molecule and a water dimer can combine to form a methylamine trimer (MAT), which is considered to be the starting point of reaction along with benzoquinone. To find the lowest-energy complex for MAT, multiple starting geometries were studied. The interactions (i.e., the hydrogen bonding) between the water molecules and the amine group of MA varies

greatly in these initial geometries. Through these multiple optimization calculations, the three lowest-energy MAT structures were obtained. These structures are presented in Figures 2.4 and 2.5.

For all low energy conformations of MAT, a triangular geometry between the O atoms of water and the N atom of methylamine is obtained. This triangular arrangement is preferred because it maximizes the number of hydrogen bonds to three. The variation between these low-energy conformations comes from the different orientations of H atoms of water molecules and the methyl group of MA. The lowest-energy conformation (**R1**) is 12.09 kcal/mol lower in energy than separated methylamine and water dimer. The other two low-energy conformations, **R2** and **R3**, are 0.05 kcal/mol and 0.07 kcal/mol, respectively, higher in energy than **R1**.

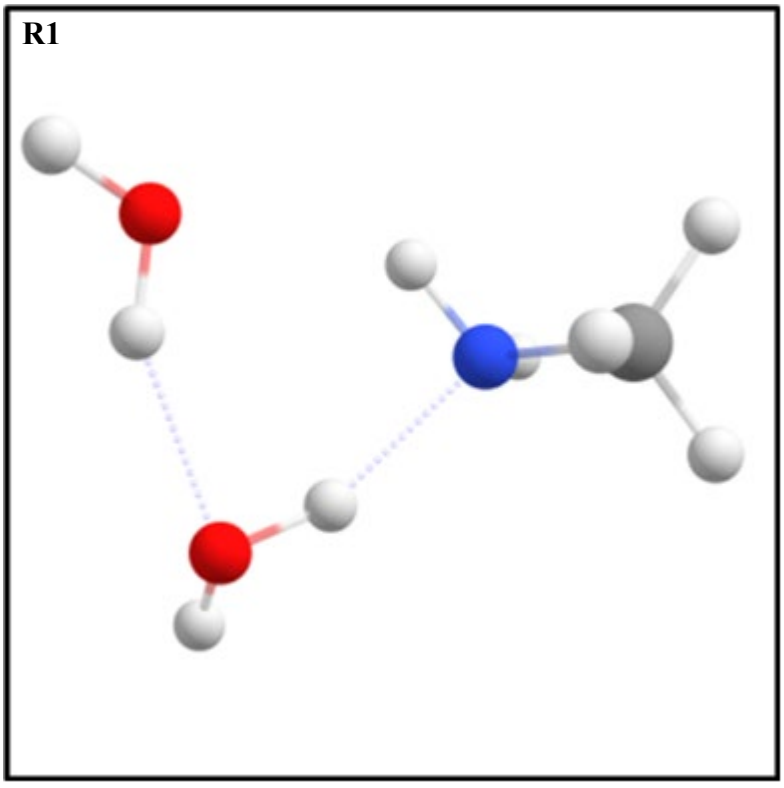

Figure 2.4 Lowest-energy conformation for methylamine trimer

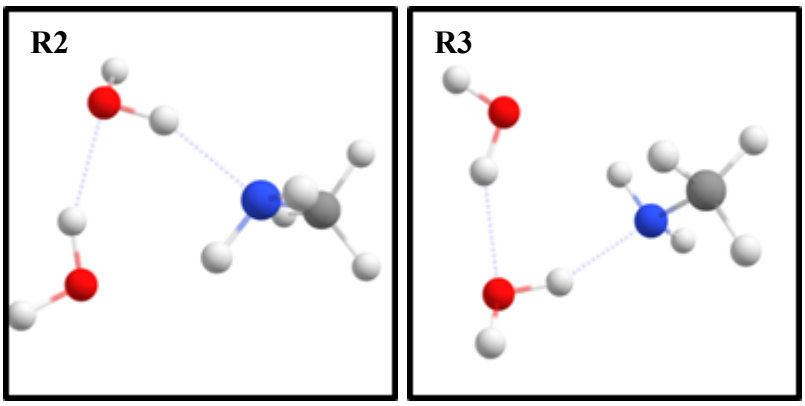

Figure 2.5 Two other low-energy conformations for methylamine trimer

2.2.2 Product of the 1,4-addition reaction

The product of the 1,4-addition reaction is a compound that has a new N–C bond and has a H atom connected to an O atom of benzoquinone as shown in Figure 2.1. The N–C bond is two C atoms away from the new OH group. Multiple conformations are possible due to the rotation around the C–N bond, rotation around the C–OH bond, and flipping the bond orientation around trigonal pyramidal N atom. The complete conformational analysis was previously reported [Rathnayake, 2013]. The lowest-energy product conformation is shown in Figure 2.6 and the next two low-energy conformations are shown in Figure 2.7. For **PA1**, the H atom of OH is orienting towards the amine group and the methyl group is facing away from C=O group. The two low-energy conformations in Figure 2.7, **PA2** and **PA3**, are 3.54 kcal/mol and 4.53 kcal/mol, respectively, higher in energy than **PA1**.

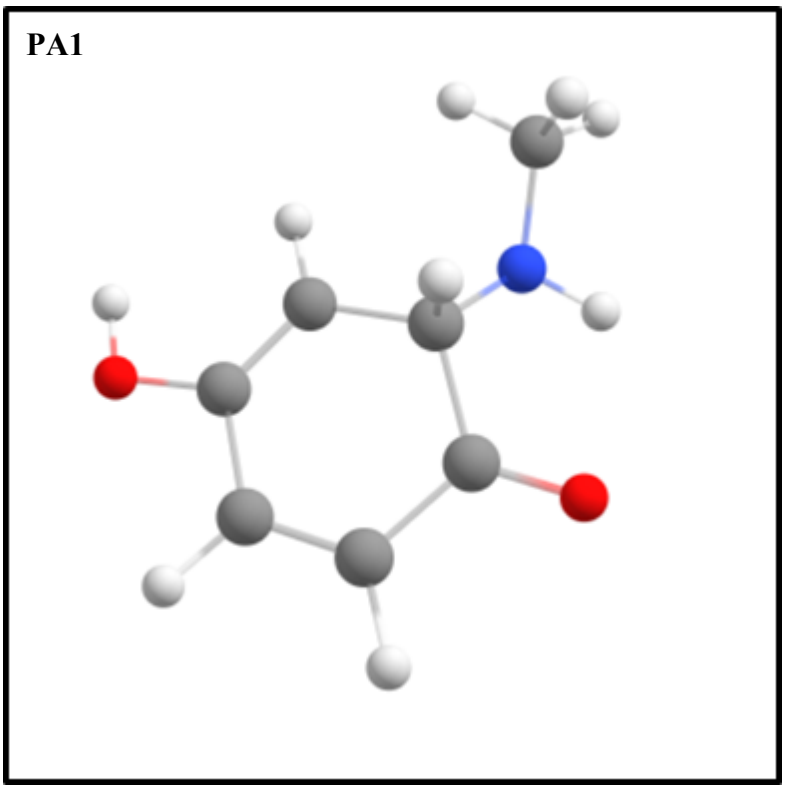

Figure 2.6 Lowest-energy conformation for the product of the 1,4-addition of methylamine to benzoquinone (**PA1**)

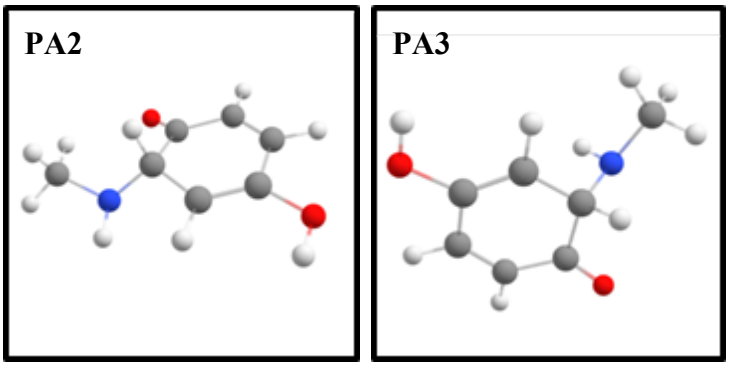

Figure 2.7 Two other low-energy conformations for the product of the 1,4-addition of methylamine to benzoquinone (**PA2** and **PA3**)

2.2.3 Product of the 1,2-addition reaction

The product of the 1,2-addition reaction is a compound that has a new N–C bond and has a H atom connected to an O atom of benzoquinone as shown in Figure 2.1. The N–C bond is now next to the new OH group. Multiple conformations are possible due to the rotation around the C–N bond, rotation around the C–OH bond, and flipping the bond orientation around trigonal pyramidal N atom. The complete conformational analysis was previously reported [Fernando, 2009]. The lowest-energy product conformation of the 1,2-addition product (**PB1**) is shown in Figure 2.8. Other low-energy 1,2-addition products can be seen in Figure 2.9. For this conformation, the H atom of OH is orienting towards the amine group, the methyl group is pointing away from C–OH group, and the lone pair of N atom is pointing toward the H atom of the OH group. The next two low-energy conformations of **PB2** and **PB3**, are 0.77 kcal/mol and 3.46 kcal/mol, respectively, higher in energy than **PB1**. Comparing the 1,2-addition product to the 1,4-addition product, the **PB1** is 0.15 kcal/mol lower in energy than **PA1**.

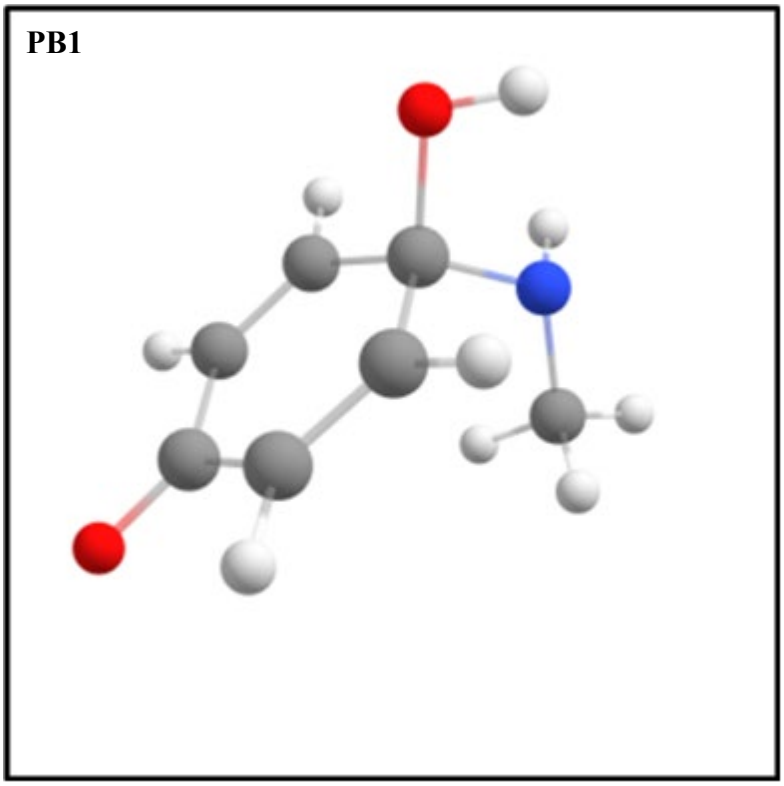

Figure 2.8 Lowest-energy conformation for the product of the 1,2-addition of methylamine to benzoquinone (**PB1**)

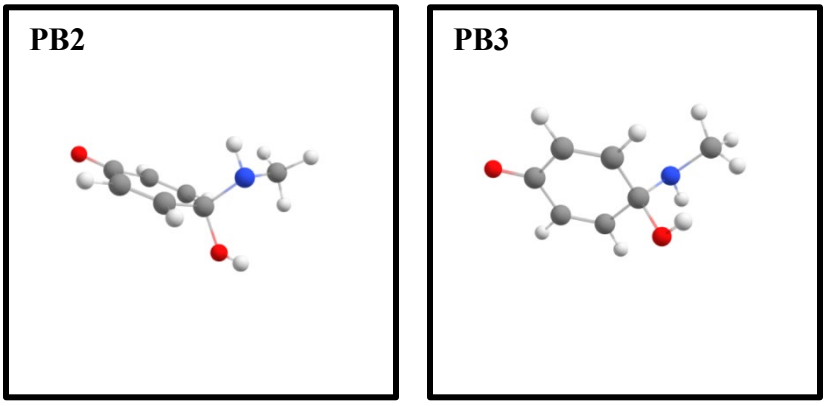

Figure 2.9 Other low-energy conformations for the product of the 1,2-addition of methylamine to benzoquinone **PB2** and **PB3**

2.3 Reactant and Product Complexes

2.3.1 Reactant complex

The reactant complex is a tetramer containing methylamine, *p*-benzoquinone and two water molecules interacting with each other through non-covalent interactions, mainly hydrogen bonding. Several such complexes were investigated earlier [Rathnayake, 2013], and the lowest energy conformations of that study were recalculated for this study. In addition, few additional optimization calculations for this tetramer were carried out and a new lower-energy structure was obtained. The lowest-energy conformation for the reactant complex, **RC1**, is shown in Figure 2.10, and a few additional low-energy conformations are shown in Figure 2.11. In the current study, eighteen different starting geometries of the neutral reactant complexes were optimized but only four reached optimized conformations. Finding optimized reactant complex structures, as well as finding optimized product complex structures, requires multiple optimization attempts to try to include as many conformations as possible.

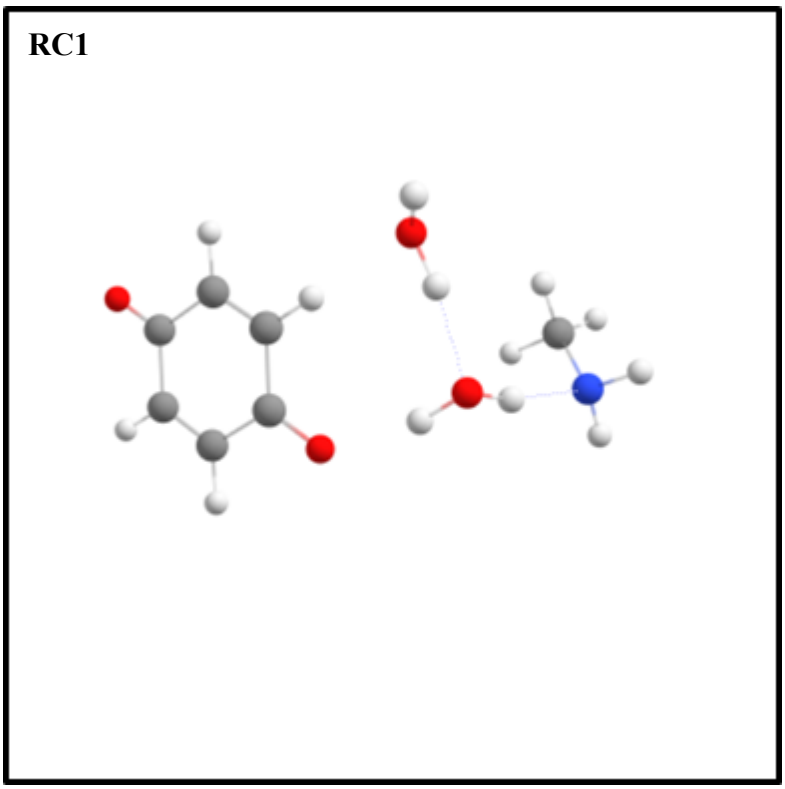

` **Figure 2.10** Lowest-energy conformation of the reactant complex

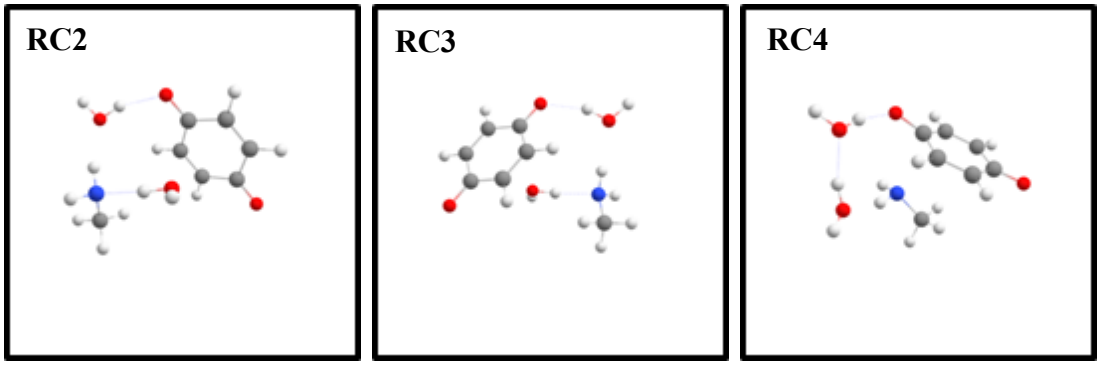

Figure 2.11 Three other low-energy conformations for the reactant complex: **RC2**, **RC3**, and **RC4**

For **RC1**, the tetramer structure appears to be formed as a MAT interacting with the BQ, with MA away from BQ such that an interaction between a H atom of one water molecule and the O atom of a carbonyl group of BQ is possible. Also, both amine hydrogens are pointing away from benzoquinone. The three other low-energy reactant complex conformation (**RC2**, **RC3**, and

RC4) appear to have a circular arrangement among the two water molecules, MA and BQ. The lowest-energy conformation (**RC1**) is 6.17 kcal/mol lower in energy than separated MAT and BQ. The other three low-energy conformations, **RC2**, **RC3**, and **RC4**, are 1.15 kcal/mol, 1.34 kcal/mol, and 1.45 kcal/mol, respectively, higher in energy than **RC1**.

2.3.2 Product complex for the 1,4-addition reaction

Another stage of the reaction pathway is the product complex stage that follows the transition state and precedes the separated product stage. The product complex stage contains the product of the reaction (either 1,2 addition or 1,4 addition) and two water molecules with structures that maximize the interactions among these species therefore reducing its energy. The lowest-energy product complex geometry for the 1,4-addition of methylamine to benzoquinone is shown in Figure 2.12, and three other low-energy conformations are shown in Figure 2.13.

For **PCA1**, the arrangement of the two water molecules is similar to their location in the transition state, where their positions were facilitating the H atom transfer, but the C–N bond and the O–H bond are completely formed. There are three H bond interactions in PCA1, in a circular pattern, which appear to be energetically preferred because this pattern does not appear in **PCA2**, **PCA3** or **PCA4**. Also, in **PCA2**, **PCA3** or **PCA4** conformations there appear to be three H-bond interactions as well. The lowest-energy conformation (**PCA1**) is 17.81 kcal/mol lower in energy than separated products (i.e., the 1,4-addition product **PA1** and water dimer). The other three low-energy conformations, **PCA2**, **PCA3**, and **PCA4**, are 6.45 kcal/mol, 8.46 kcal/mol, and 9.01 kcal/mol, respectively, higher in energy than **PCA1**.

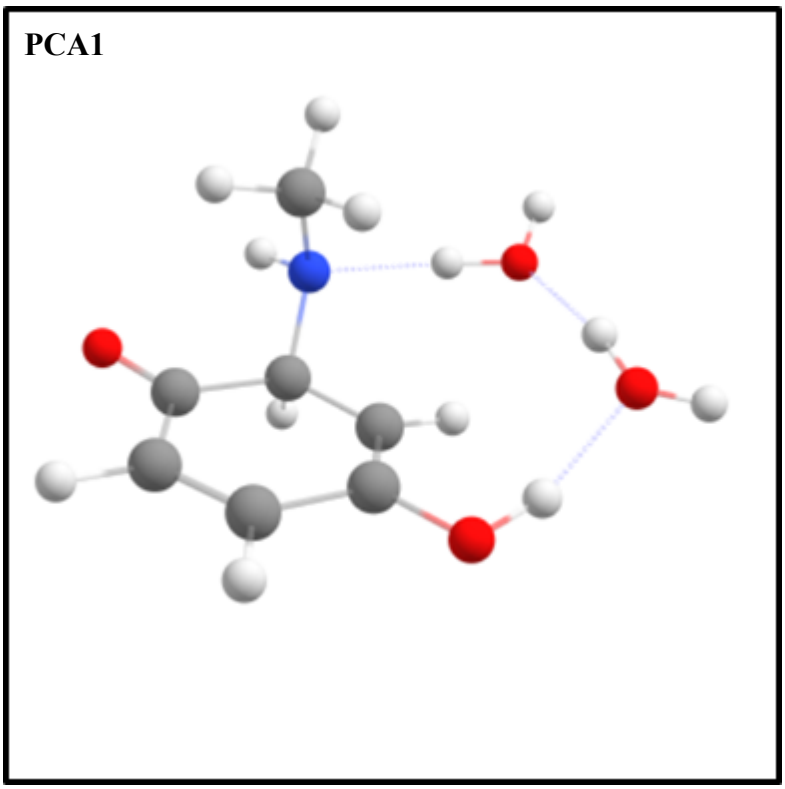

Figure 2.12 Lowest-energy conformation of the product complex for the 1,4-addition of methylamine to benzoquinone **PCA1**

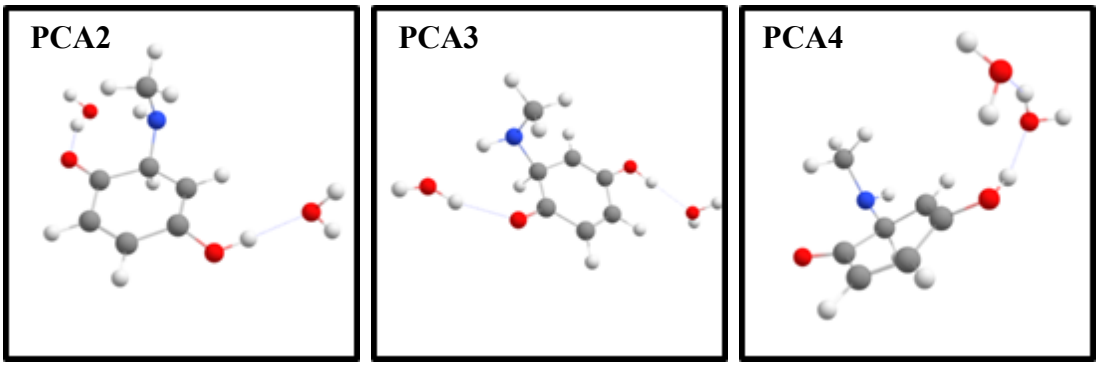

Figure 2.13 Three other low-energy conformations for the product complexes for the 1,4-addition of methylamine: **PCA2**, **PCA3**, **PCA4**

2.3.3 Product complex for the 1,2-addition reaction

The lowest-energy product complex geometry for the 1,2-addition of methylamine to benzoquinone is shown in Figure 2.14, and three other low-energy conformations are shown in

Figure 2.15. For **PCB1**, both water molecules interact with the OH group of the BQ but do not interact directly with each other. Also, one water molecule interacts with amino group of BQ. The lowest-energy conformation (**PCB1**) is 13.75 kcal/mol lower in energy than separated products (i.e., the 1,2-addition product **PB1** and water dimer). The other three low-energy conformations, **PCB2**, **PCB3**, and **PCB4**, are 0.14 kcal/mol, 3.22 kcal/mol, and 6.11 kcal/mol, respectively, higher in energy than **PCB1**.

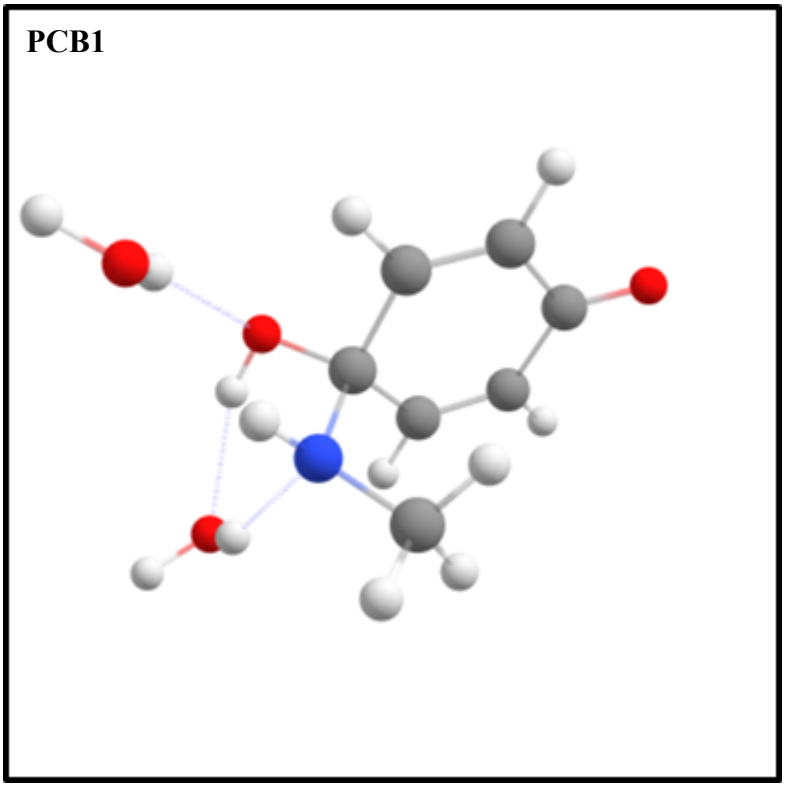

Figure 2.14 Lowest-energy conformation of the product complex for the 1,2-addition of methylamine to benzoquinone **PCB1**

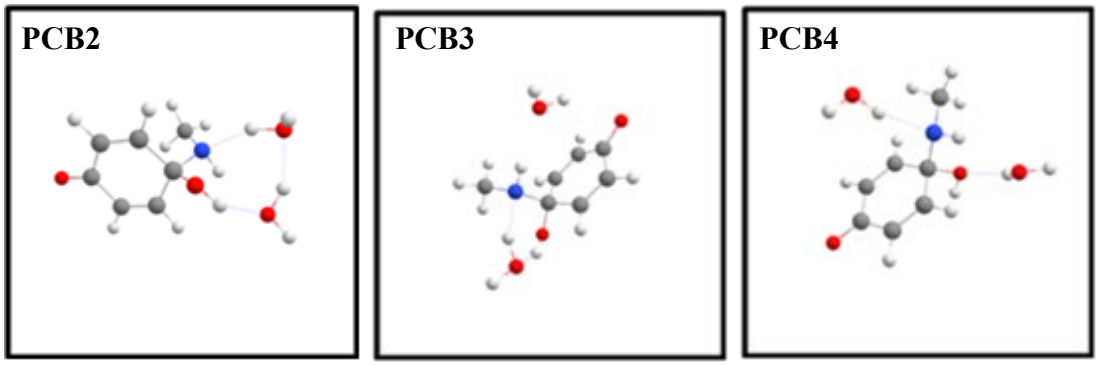

Figure 2.15 Three other low-energy conformations for the product complexes for the 1,2-addition of methylamine: **PCB2, PCB3,** and **PCB4.**

2.4 Transition States

2.4.1 Transition states for the 1,4-addition reaction

A transition state along a reaction pathway, better described as the saddle point along that reaction pathway, is the geometry or structure that corresponds to the maximum energy along the reaction pathway. A transition state is an intermediate between the reactants and products and is also known as the activated complex. By identifying transition states for various reaction pathways, one can determine the energetically favored pathway, which probably is the most likely reaction as well. The transition states for the 1,4-addition of methylamine to benzoquinone through the intermediacy of two water molecules has been studied previously [Rathnayake, 2013], and the most important structures were verified for the current study. The lowest-energy transition state structure for the 1,4-addition of methylamine to benzoquinone is shown in Figure 2.16, and three other low-energy structures are shown in Figure 2.17. The lowest-energy 1,4 addition transition state (**TSA1**) is 6.56 kcal/mol higher in energy than separated reactants (i.e., the optimized MAT and BQ). The other three low-energy transition state geometries, **TSA2**,

TSA3, and **TSA4**, are 0.24 kcal/mol, 5.34 kcal/mol, and 5.99 kcal/mol, respectively, higher in energy than **TSA1**.

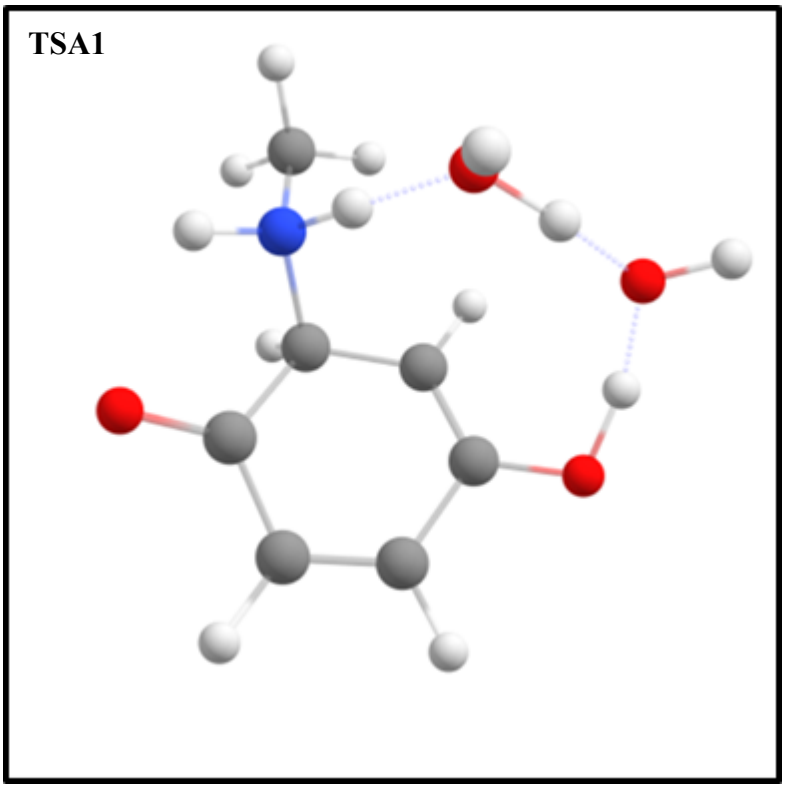

Figure 2.16 Lowest-energy transition state for the 1,4-addition of methylamine to benzoquinone **TSA1**

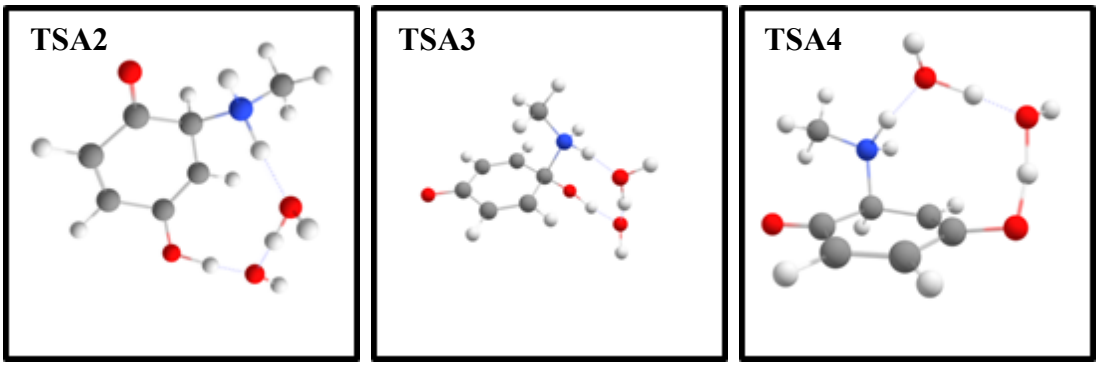

Figure 2.17 Next three low-energy transition states for the 1,4-addition of methylamine to benzoquinone: **TSA2**, **TSA3**, **TSA4**

2.4.2 Transition states for the 1,2-addition reaction

The transition states for the 1,2-addition of methylamine to benzoquinone through the intermediacy of two water molecules has not been studied previously so the results in this section are all original results. Five distinct transitions states were identified. The lowest-energy transition state structure for the 1,2-addition of methylamine to benzoquinone is shown in Figure 2.18, and all other structures are shown in Figure 2.19. A summary of some important parameters of the transition states are given in Tables 2.2 and 2.3. The symbols $V^{\ddagger}$ and $\omega^{\ddagger}$ are gas-phase barrier height in kcal/mol and imaginary frequency in cm^{-1}, respectively. The gas-phase barrier heights in the table are relative to energy of the individual BQ and MAT separated. An imaginary frequency indicates a local maximum on the potential energy surface, along the reaction coordinate. A larger imaginary frequency value is indicative to a narrow barrier while a lower imaginary frequency value is indicative to a wider barrier. The geometric parameter listed in Table 2.3 are presented in Figure 2.20.

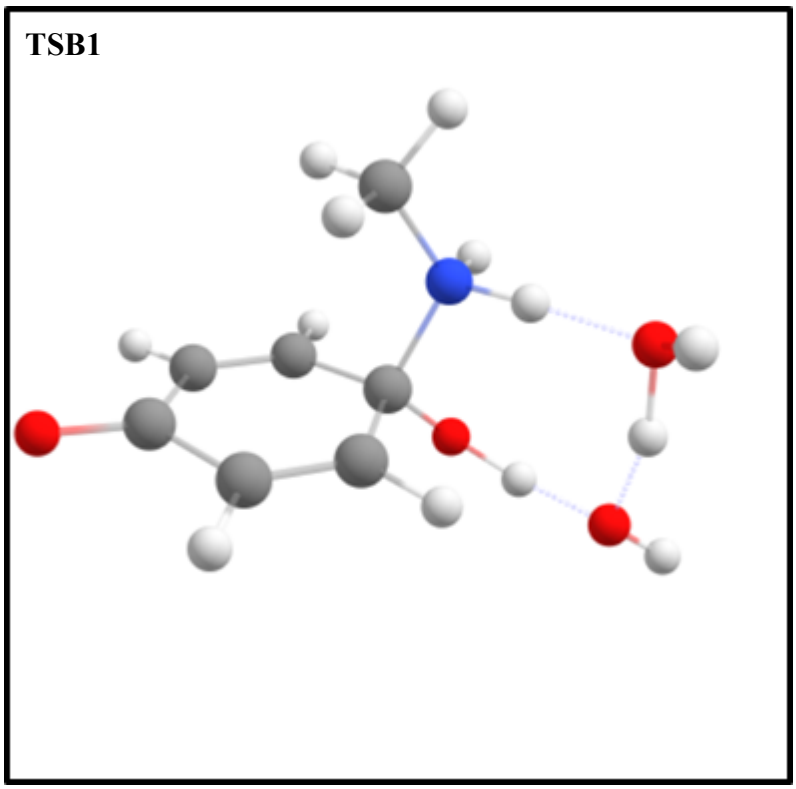

Figure 2.18 Lowest-energy transition state for the 1,2-addition of methylamine to benzoquinone **TSB1**

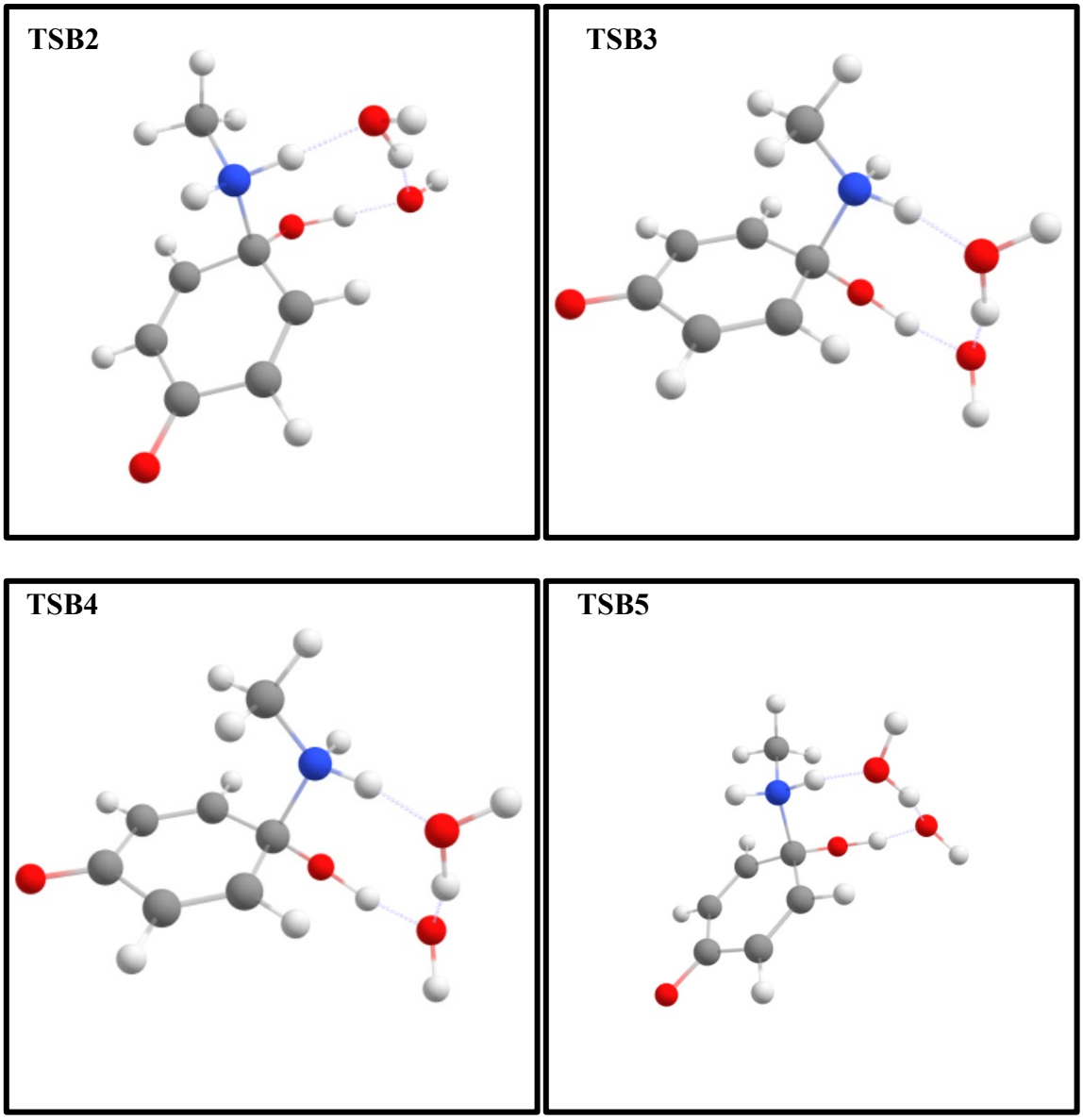

Figure 2.19 Other transition states for 1,2-addition of methylamine to benzoquinone: **TSB2-TSB5**

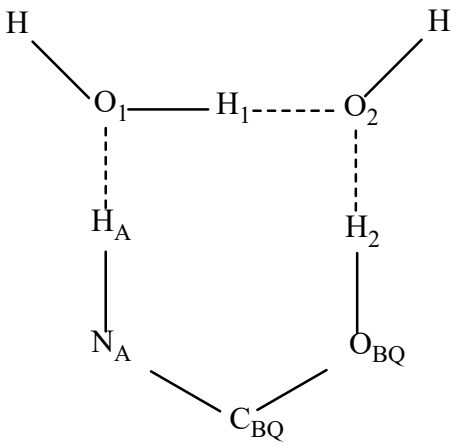

Figure 2.20 Labels for the 1,2-addition transition state distances

Table 2.2 Gas-phase barrier heights (kcal/mol) and imaginary frequencies (cm^{-1}) for transition states for 1,2-addition of methylamine to benzoquinone

Transition State	$V^{\ddagger}$ (kcal/mol)	$\omega^{\ddagger}$ (cm^{-1})
TSB1	7.77	677*i*
TSB2	7.84	664*i*
TSB3	8.18	757*i*
TSB4	8.26	681*i*
TSB5	8.38	751*i*

Table 2.3 Selected internuclear distances (Å) for transition states for 1,2-addition of methylamine to benzoquinone

Transition State	C_{BQ}–N_A (Å)	N_A–H_A (Å)	O_1–H_1 (Å)	O_{BQ}–H_2 (Å)	C_{BQ}–O_{BQ} (Å)	$N_A\cdots O_1$ (Å)	$O_1\cdots O_2$ (Å)	$O_2\cdots O_{BQ}$ (Å)
TSB1	1.545	1.096	1.114	1.097	1.345	1.467	1.290	1.327
TSB2	1.553	1.096	1.118	1.090	1.341	1.469	1.285	1.338
TSB3	1.543	1.097	1.122	1.102	1.345	1.474	1.275	1.311
TSB4	1.545	1.094	1.117	1.093	1.346	1.473	1.288	1.330
TSB5	1.553	1.097	1.127	1.096	1.341	1.471	1.269	1.320

As seen in Table 2.2, the transition state **TSB1** was the lowest gas-phase barrier height of 7.7 kcal/mol, when compared to that of the reactants. The next two transition states **TSB2** and **TSB3** had gas-phase barrier heights of 7.84 kcal/mol and 8.18 kcal/mol, respectively, which only have a less than 1 kcal/mol difference to the **TSB1**. The remaining transition states in Table 2.2 are very similar in energy, with transition state **TSB5** having the highest gas-phase barrier at 8.38 kcal/mol. This is still less than 1 kcal/mol difference between all structures. As seen in Table 2.2, the imaginary frequencies that were observed ranges from 677*i* cm^{-1} to 751*i* cm^{-1}. Also, when visualizing atom movements associated with these imaginary frequencies, the most significant motions are seen for H_a, H_w, and H_x atoms showing that reaction pathways are mostly H transfer processes at the top of the energy barrier.

In **TSB1** as well as other transition states, the carbon-nitrogen bond appear to be mostly already formed while the two water molecules are in positions facilitating the transfer of H atoms. As shown in Table 2.3, intermolecular distances C_{BQ}–N_A, N_A–H_A, O_1–H_1, O_{BQ}–H_2, and C_{BQ}–O_{BQ} have fairly consistent values around 1.55 Å, 1.10 Å, 1.12 Å, 1.10 Å, and 1.34 Å,

respectively. The remaining intermolecular distances shown in Table 2.3 have enough variation that there does not appear to be a trend.

2.5 Energy Profile for Reaction Pathways in Neutral Environment

Once all reactants, transition states, and products are optimized to their lowest energy geometries, an overall energy diagram can be created for the neutral reaction pathway for the addition of methylamine to benzoquinone. This diagram is presented in Figure 2.21. The zero of energy is considered to be the electronic energy of separated BQ and MAT.

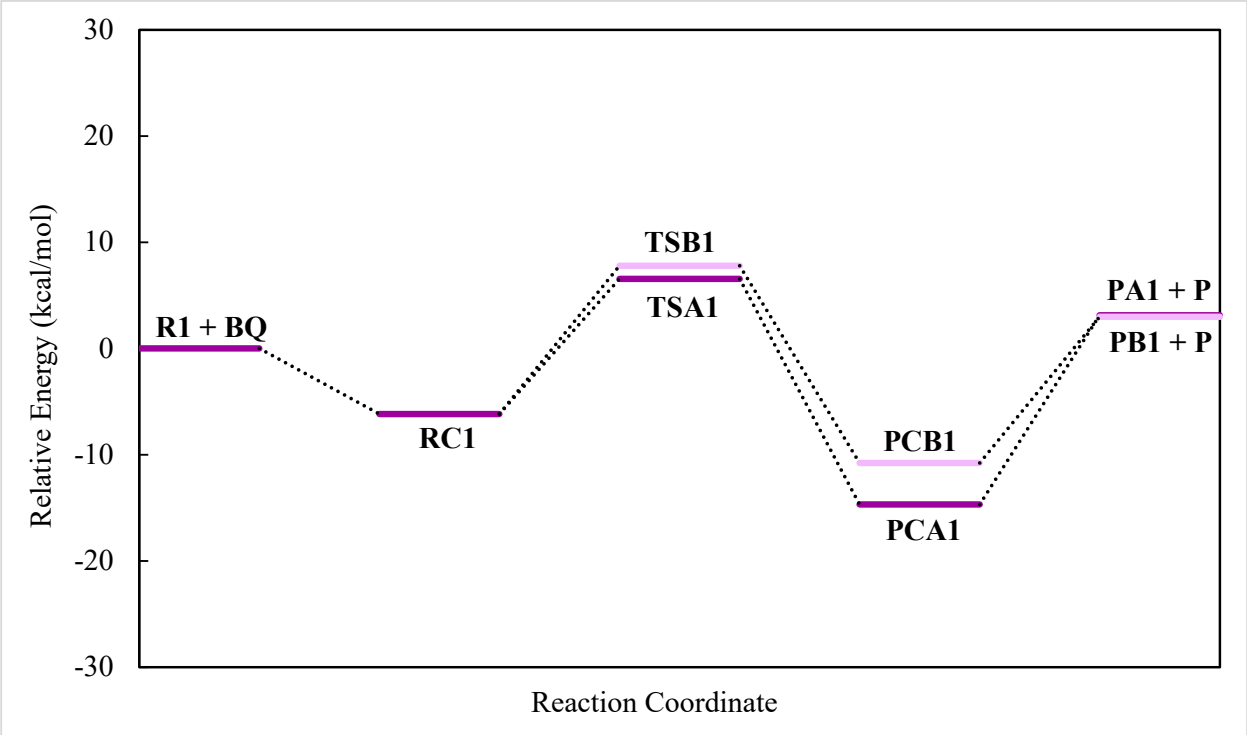

Figure 2.21 Energy diagram for the reaction of methylamine with benzoquinone in neutral environments

Although the main purpose of this diagram is to be used as a benchmark for comparison to similar diagrams in acidic and basic environments, certain comparisons between 1,2-addition reaction and 1,4-addition reactions can be made. Both of these reactions initiate from the same

reaction stage, but the initial stage of the reaction can be considered to be either the stage of separated reactants or the stage of reactant complex, in which the two reactants are interacting with each other. Typically, for reactions in gas phase, the separated reactant stage is considered to be the starting point of the reaction. However, the reactant complex stage is probably a better representation for the reaction occurring in aqueous solutions. Accordingly, the barrier height (i.e., the barrier necessary to be overcome for the reaction to occur) can be determined either with respect to separated reactant stage or the reactant complex stage. With respect to separated reactants, the 1,4-addition reaction has a barrier height of 6.56 kcal/mol while the 1,2-addition reaction has a barrier height of 7.77 kcal/mol. With respect to the reactant complex, the 1,4-addition reaction has a barrier height of 12.73 kcal/mol while the 1,2-addition reaction has a barrier height of 13.94 kcal/mol. Independent of how the barrier height is determined, the 1,4-addition pathway is calculated to be preferred by about 1 kcal/mol over the 1,2-addition pathway. Consistently, the 1,4-addition product complex is 3.91 kcal/mol lower in energy than the 1,2-addition product complex. However, the product of the 1,4-addition reaction is 0.15 kcal/mol higher in energy than the product of the 1,2-addition reaction.

CHAPTER 3

REACTION STUDIES IN BASIC ENVIRONMENTS

3.1 Introduction

The results of the study of the reaction between benzoquinone (BQ) and methylamine (MA) in basic environments are presented in this chapter. The basic environment is modeled by considering a deprotonated system although, in reality, even in the most basic environments, a deprotonated system is not expected to be actually present in aqueous solutions. Like the neutral system, the first step of the reaction can lead to an 1,2-addition or an 1,4-addition, as presented in Figure 3.1 below. The abbreviations for the basic-modeled species can be found in Table 3.1 below, as well. Both reactions involve creation of a N–C bond between the N atom of methylamine and a C atom of benzoquinone. In the basic-modeled reaction, an H atom is not transferred between the N atom of the amine and an O atom of benzoquinone, resulting in an anionic oxygen on BQ. Like the neutral system, modeling the reactions requires the inclusion of two water molecules in computations.

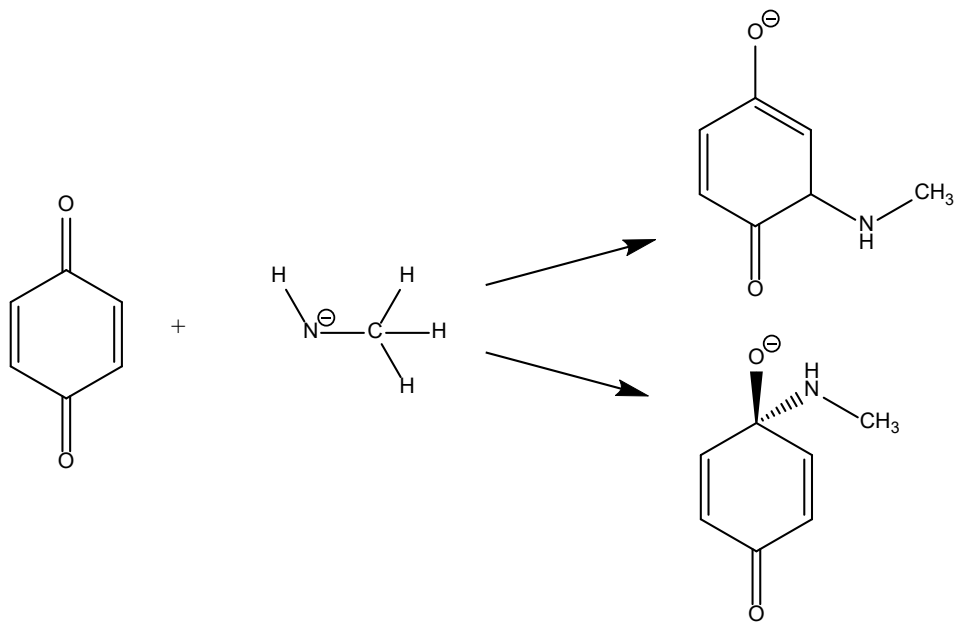

Figure 3.1 The first step of the reaction of benzoquinone with deprotonated MA leading to the basic-modeled 1,4-addition product (top) and 1,2-addition product (bottom)

Table 3.1 Species labeling and chemical formulas for various stages of the reaction pathway in basic environments

Formula	Name/Description & Label
$H_2O\cdots\ CH_3NH^-\cdots H_2O$	Deprotonated methylamine trimer (BMAT) (**BR**)
$C_6H_4O_2$	Benzoquinone (**BQ**)
$H_2O\cdots HO^-\cdots CH_3NH_2\cdots C_6H_4O_2$	Reactant complex (**BRC**)
$H_2O\cdots H_2O\cdots CH_3NH\cdots C_6H_4O_2^-$	Transition state (**BTS**)
$H_2O\cdots H_2O\cdots CH_3NH–C_6H_4O_2^-$	1,4-Product complex (**BPCA**)
$H_2O\cdots H_2O\cdots CH_3NH–C_6H_4O_2^-$	1,2-Product complex (**BPCB**)
$CH_3NH–C_6H_4O_2^-$	1,4-Product (**BPA**)
$CH_3NH–C_6H_4O_2^-$	1,2-Product (**BPB**)
$H_2O\cdots H_2O$	Water dimer (**P**)

3.2 Basic-Modeled Reactants and Products

3.2.1 Basic-modeled reactants

The basic-modeled (i.e., deprotonated) MAT contains the methylamine group, a water molecule and a hydroxide ion. Various starting geometries of BMAT were considered, some that were deprotonated at the amine group and some that were deprotonated at water. When the starting geometry is deprotonated at the amine, the optimized structure has the proton transferred from the center water to the amine group. For all low-energy conformations of BMAT a triangular geometry between the O atoms of water and hydroxide and the N atom of methylamine is obtained. This triangular arrangement is preferred because it maximizes the number of hydrogen bonds to three. The variation between these low-energy conformations comes from the different orientations of H atoms of water molecule, hydroxide group, and the methyl group of MA. The lowest-energy conformation (**BR1**) is 53.17 kcal/mol lower in energy than the separated deprotonated MA and water dimer and 14.11 kcal/mol lower in energy that separated MA and deprotonated water dimer. The other low-energy conformations, **BR2**, **BR3**, and **BR4** are 0.49 kcal/mol, 0.63 kcal/mol, and 0.66 kcal/mol respectively, higher in energy than **BR1**. **BR1** and **BQ** together form the reactant state, which is considered the zero of energy for the other stages of the reaction pathway in basic environments.

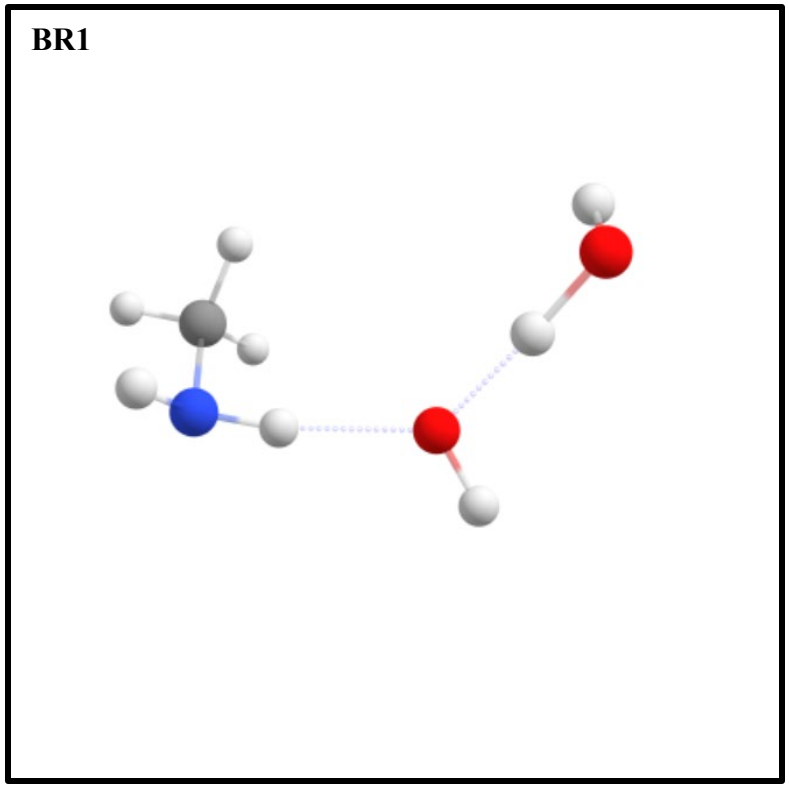

Figure 3.2 Lowest energy basic-modeled trimer **BR1**

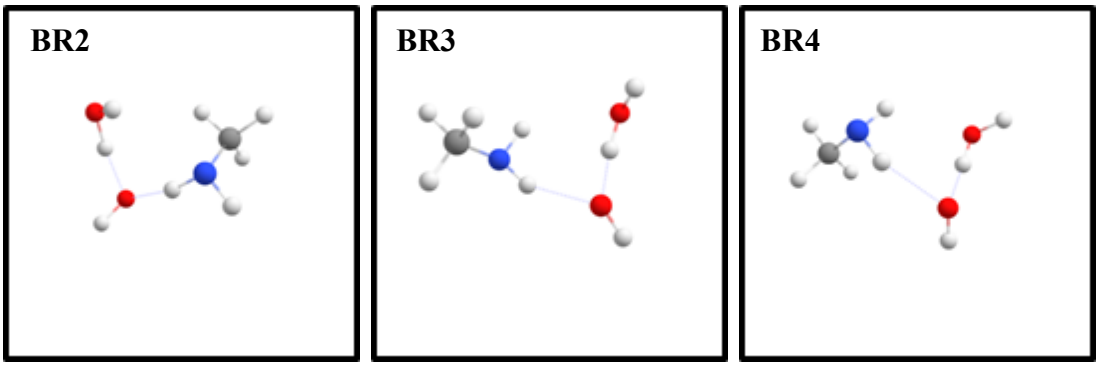

Figure 3.3 Next three lowest-energy basic-modeled trimers: **BR2**, **BR3**, **BR4**

3.2.2 Basic-modeled product of the 1,4-addition reaction

The product of the 1,4-addition reaction is a compound that has a new N–C bond. Due to the deprotonation at the amine in the reactant, no hydrogen atom needs to be transferred to the oxygen of BQ. The negative charge of the system is formally located on one oxygen atom of BQ.

Multiple conformations are possible due to the rotation around the C–N bond and flipping the bond orientation around trigonal pyramidal N atom. The lowest-energy product conformation for the basic-modeled 1,4-addition step is shown in Figure 3.4 and the next low-energy conformations are shown in Figure 3.5. For **BPA1**, the H atom of the amine group is orienting towards the anionic oxygen, the methyl group is pointing towards the C=O group, and the lone pair of N orients away from the neighboring C=O. The next low-energy conformations in Figure 3.5, **BPA2**, **BPA3**, and **BPA4**, are 0.16 kcal/mol, 0.52 kcal/mol, and 1.52 kcal/mol respectively, higher in energy than **BPA1**.

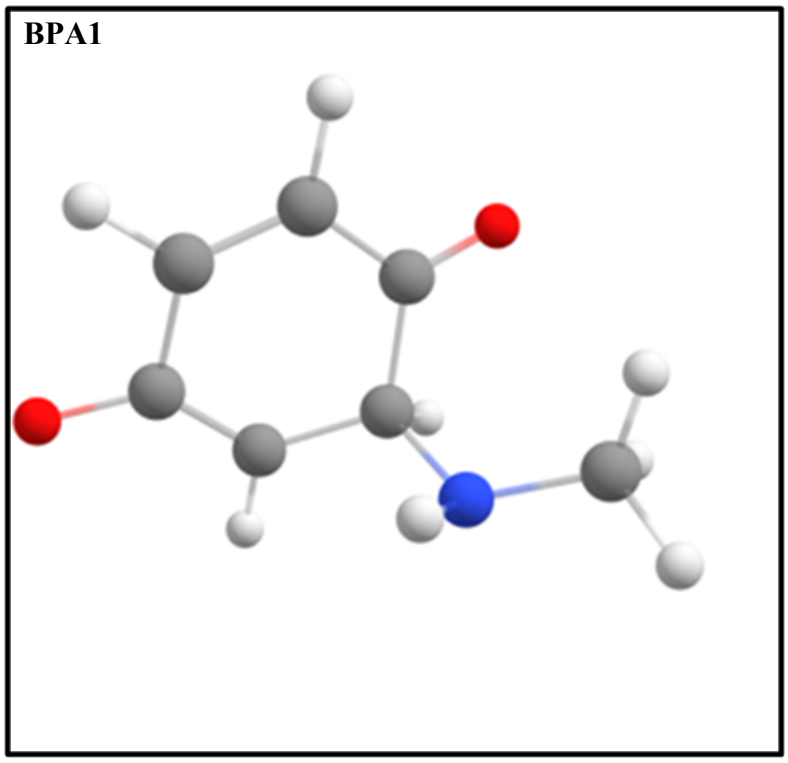

Figure 3.4 Lowest-energy conformation for the basic-modeled product of the 1,4-addition of methylamine to benzoquinone (**BPA1**)

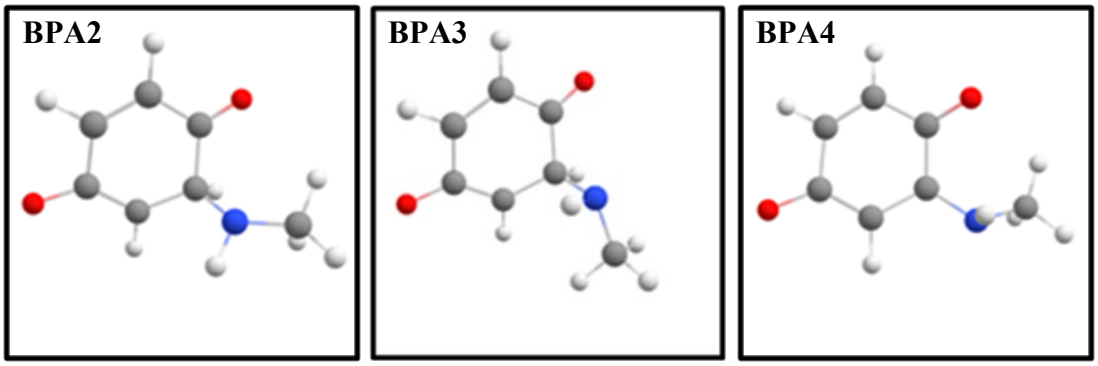

Figure 3.5 Other low-energy conformations for the basic-modeled product of the 1,4-addition of methylamine to benzoquinone: **BPA2, BPA3, BPA4**

3.2.3 Basic-modeled product of the 1,2-addition reaction

Like the product of the 1,4-addition reaction, the product of the 1,2-addition reaction is a compound that has a new N–C bond and a formal negative charge on an oxygen atom of BQ. Multiple conformations are possible due to the rotation around the C–N bond and flipping the bond orientation around trigonal pyramidal N atom. The lowest-energy product conformation of the basic-modeled 1,2-addition product (**BPB1**) is shown in Figure 3.6. For this conformation, the H atom of the amine group is orienting away from the anionic oxygen, the methyl group is pointing towards the anionic oxygen, and the lone pair of N is pointing away from both the anionic oxygen and the methyl group. The next low-energy conformations of **BPB2** and **BPB3**, are 0.10 kcal/mol and 0.30 kcal/mol respectively, higher in energy than **BPB1**. Comparing the 1,2-addition product to the 1,4-addition product, the **BPB1** is 8.88 kcal/mol higher in energy than **BPA1**.

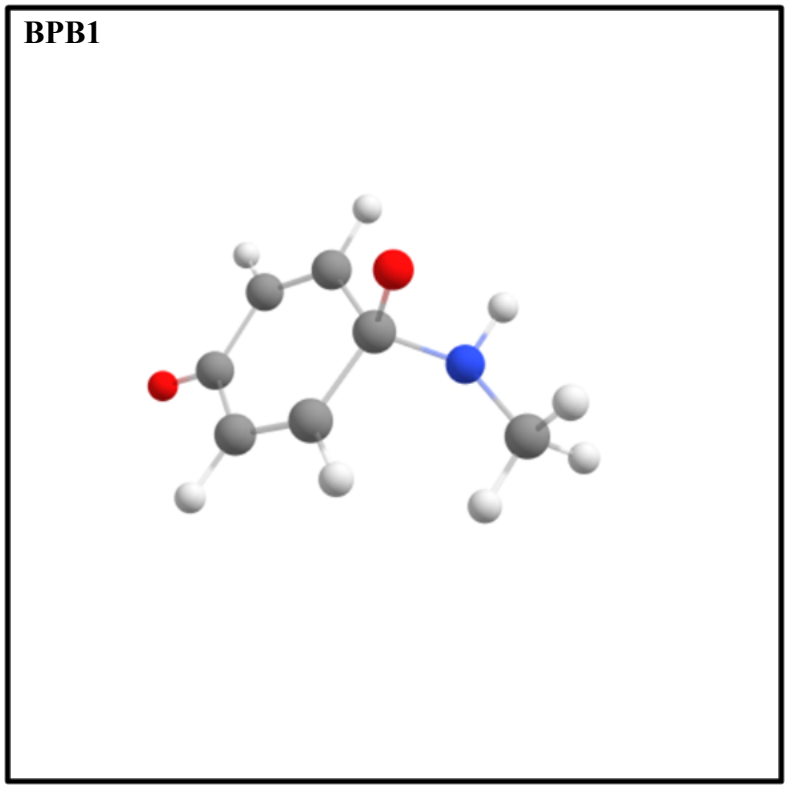

Figure 3.6 Lowest-energy conformation for the basic-modeled product of the 1,2-addition of methylamine to benzoquinone (**BPB1**)

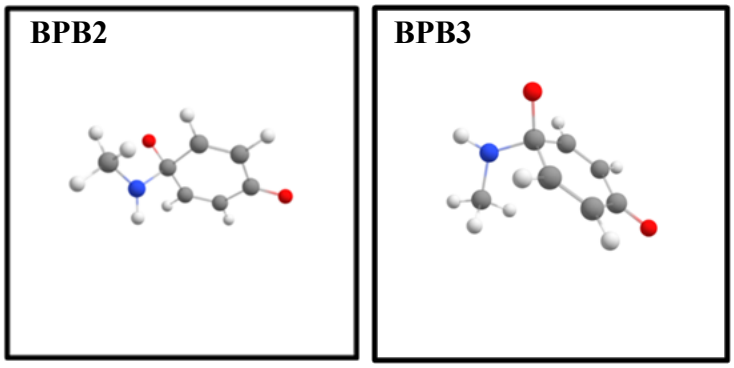

Figure 3.7 Other low-energy conformations for the basic-modeled product of the 1,2-addition of methylamine to benzoquinone: **BPB2**, and **BPB3**

3.3 Basic-Modeled Reactant and Product Complexes

3.3.1 Basic-modeled reactant complexes

The reactant complex is a deprotonated tetramer containing methylamine, *p*-benzoquinone and two water molecules interacting with each other through non-covalent interactions, mainly H bonding. Optimization calculations for this tetramer under basic-modeled conditions (i.e., deprotonated) were carried out and few optimized structures were obtained. Finding optimized reactant complex structures, as well as finding optimized product complex structures, requires multiple optimization attempts to try to include as many conformations as possible. In the current study, more than thirty different starting geometries of the deprotonated reactant complexes were optimized but only four reached optimized reactant complex conformations. Other trials resulted in the formation of a product complex. The lowest-energy conformation for the reactant complex, **BRC1**, is shown in Figure 3.8, and two additional low-energy conformations are shown in Figure 3.9.

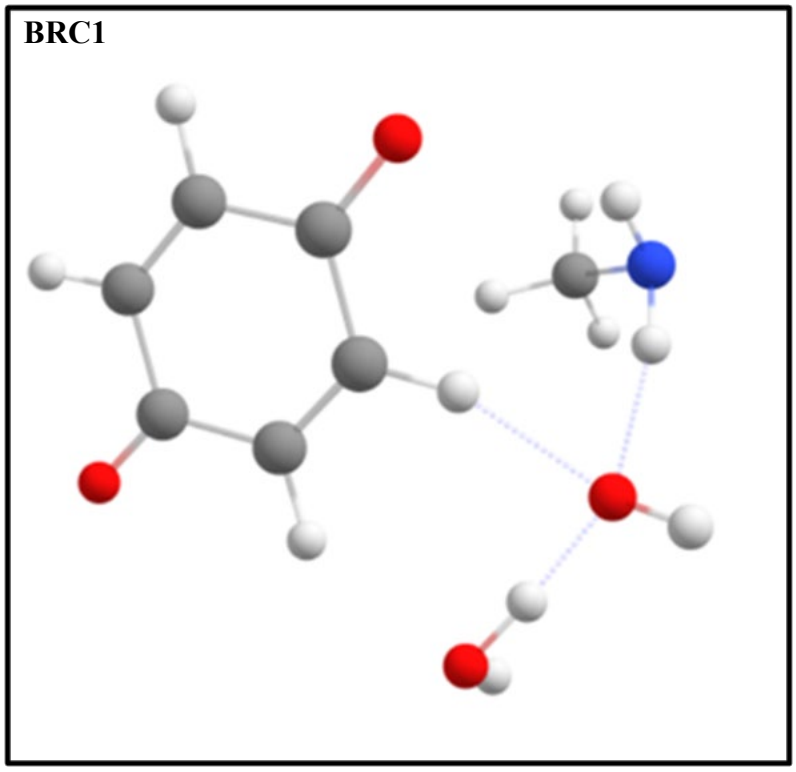

Figure 3.8 Lowest-energy conformation for the basic-modeled reactant complex **BRC1**

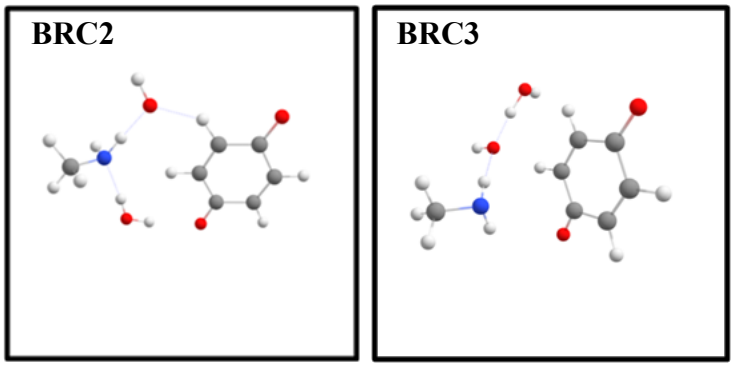

Figure 3.9 Next low-energy basic-modeled reactant complexes: **BRC2** and **BRC3**

For **BRC1**, the tetramer structure appears to be formed as a BMAT interacting with the BQ. The BMAT is deprotonated at one water molecule creating a hydroxyl anion. The MA is positioned out of the way from BQ such that an interaction between the OH^- ion and an H atom of BQ is possible. The lowest-energy reactant complex, **BRC1**, has the OH^- ion involved in all hydrogen bonding. The other two optimized reactant complex conformations (**BRC2**, and

BRC3) appear to have a circular arrangement among the OH^- ion, the water molecule, MA and BQ. The lowest-energy conformation (**BRC1**) is 17.44 kcal/mol lower in energy than separated BMAT and BQ. The other two low-energy conformations, **BRC2** and **BRC3**, are 1.82 kcal/mol, and 6.21 kcal/mol, respectively, higher in energy than **BRC1**.

3.3.2 Basic-modeled product complex for the 1,4-addition reaction

The product complex stage contains the product of the reaction (either 1,2 addition or 1,4 addition) and two water molecules with structures that maximize the interactions among these species therefore reducing its energy. The lowest-energy basic-modeled product complex geometry for the 1,4-addition of methylamine to benzoquinone (**BPCA1**) is shown in Figure 3.10, and three other low-energy conformations are shown in Figure 3.11.

For **BPCA1**, the two water molecules arrange such both form hydrogen bonds with the anionic oxygen. There are three hydrogen bond interactions in **BPCA1**, in a triangular pattern, which appear to be preferred because this pattern appears also in **BPCA2** and **BPCA3**. **BPCA4**, however, form more of a linear relationship between both water molecules, resulting in higher energy. The lowest-energy conformation (**BPCA1**) is 28.59 kcal/mol lower in energy than separated products (i.e., the 1,4-addition product **BPA1** and water dimer). The other three low-energy conformations, **BPCA2**, **BPCA3**, and **BPCA4**, are 0.11 kcal/mol, 0.42 kcal/mol, and 1.58 kcal/mol, respectively, higher in energy than **BPCA1**.

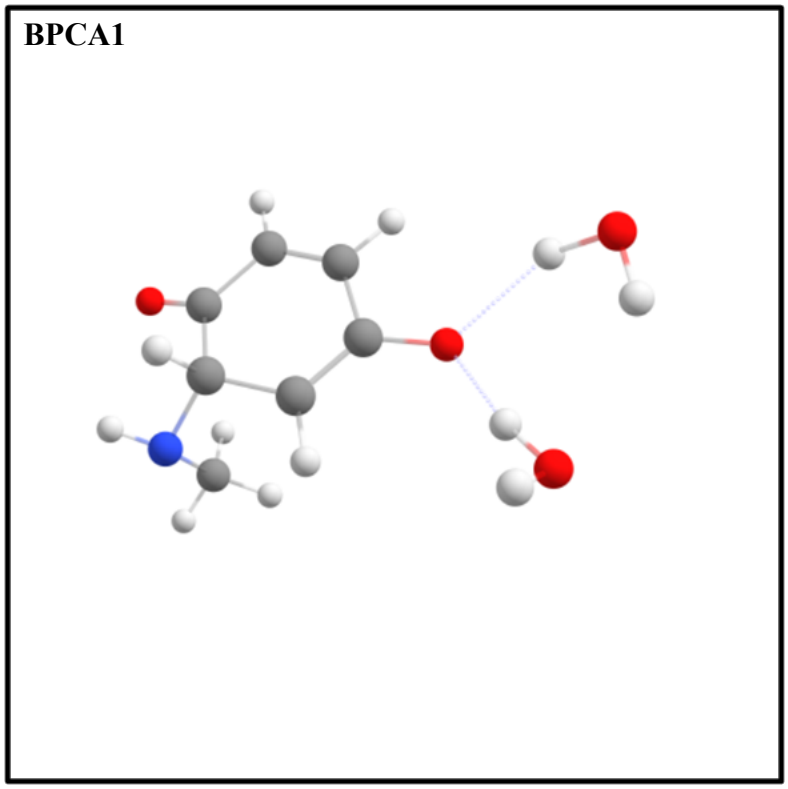

Figure 3.10 Lowest-energy conformation of the basic-modeled product complex for the 1,4-addition of methylamine to benzoquinone **BPCA1**

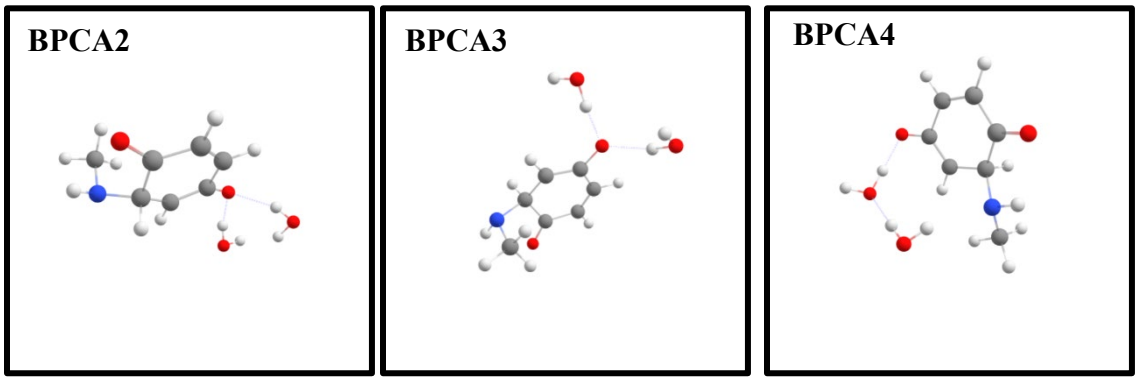

Figure 3.11 Other low-energy conformations for the basic-modeled product complexes for the 1,4-addition of methylamine: **BPCA2**, **BPCA3**, **BPCA4**

3.3.3 Basic-modeled product complex for the 1,2-addition reaction

The lowest-energy product complex geometry for the 1,2-addition of methylamine to benzoquinone is shown in Figure 3.12, and three other low-energy conformations are shown in Figure 3.13. For **BPCB1**, both water molecules interact with the O^- group of the **BPB,** similar to the triangular interaction in all product complexes for the 1,4-addition of MA. The lowest-energy conformation (**BPCB1**) is 31.84 kcal/mol lower in energy than separated products (i.e., the 1,2-addition product **BPB1** and water dimer). The other three low-energy conformations, **BPCB2**, **BPCB3**, and **BPCB4**, are 2.32 kcal/mol, 2.32 kcal/mol, and 2.94 kcal/mol, respectively, higher in energy than **BPCB1**.

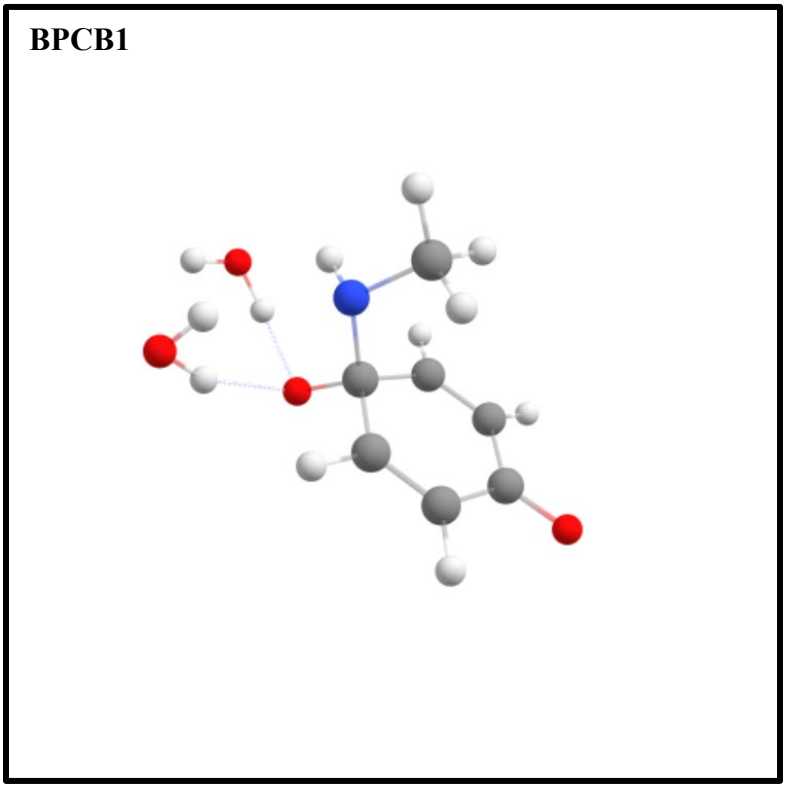

Figure 3.12 Lowest-energy conformation of the basic-modeled product complex for the 1,2-addition of methylamine to benzoquinone **BPCB1**

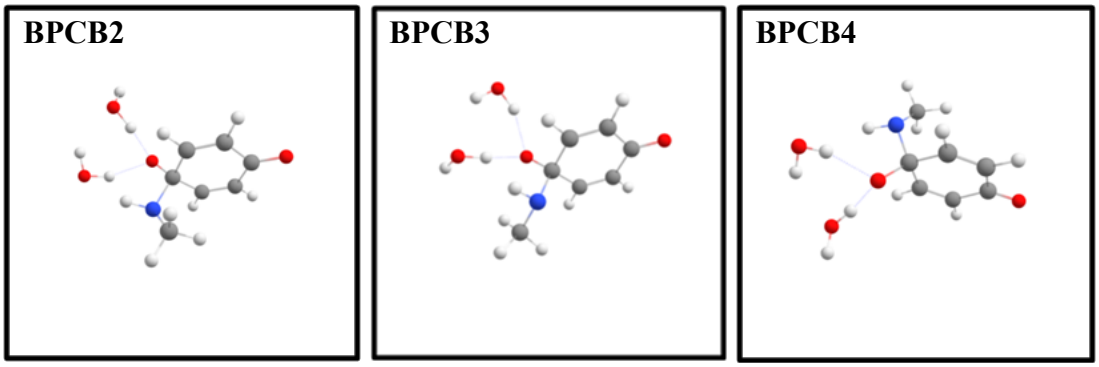

Figure 3.13 Other low-energy conformations for the basic-modeled product complexes for the 1,2-addition of methylamine: **BPCB2, BPCB3,** and **BPCB4.**

3.4 Basic-Modeled Transition States

No transition states for either the 1,2-addition reaction or the 1,4-addition reaction were obtained in this study. Many computations were pursued but none of them optimized to the desired transition state. The starting geometries for some of these computations were obtained from the transition state for the 1,4-addition reaction in neutral environment (**TSA1**) by removing a proton. These computations moved toward either the product complex area of the potential energy surface or the reactant complex area and were not finalized. Two examples of unoptimized trial this can be seen in Figure 3.14.

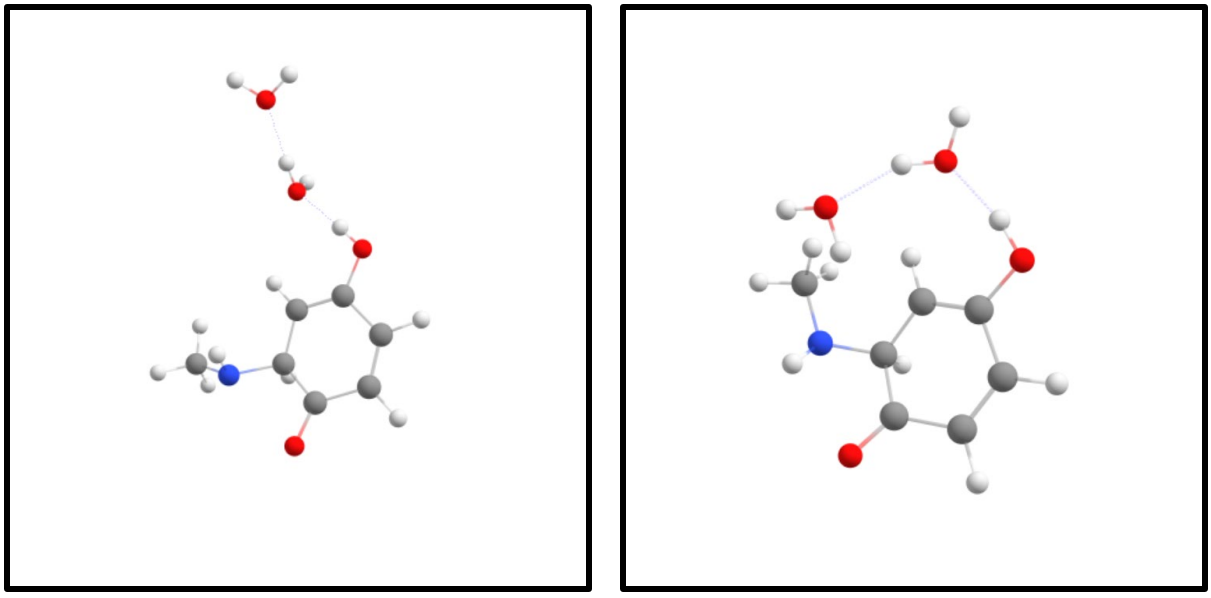

Figure 3.14 Trials for basic-modeled transition state for the 1,4-addition of MAT to BQ

The transition states for either the 1,2-addition reaction or the 1,4-addition reaction are saddle points connecting the reactant complex valley to the product complex valley on the potential energy surface for the system. For the deprotonated system studied in the chapter, the transition between the reactant complex and the product complex involves only creating the C–N bond and reorganization of the two water molecules but not the H transfer that was necessary for the neutral system. Because the making of the C–N bond is lowering the energy of the system, the reorganization of the two water molecules will be the only process that can lead to an increase in energy therefore a barrier height. As this reorganization process is not expected to require high amounts of energy, the barrier height for either the 1,2-addition reaction or the 1,4-addition reaction is expected to be quite low. Determining the actual barrier height values by finding the transition states for these reactions was proven to be very difficult due to the large flexibility of water molecule orientations and the likelihood of the system moving toward either the product complex or the reactant complex.

3.5 Energy Profile for Reaction Pathways in Basic Environment

Even though no transition state has been identified for the basic-modeled addition of MA to BQ, based on the energies of optimized reactants, products, and complexes, an overall energy diagram can be created for the reaction pathway for the addition of methylamine to benzoquinone in basic environments. This diagram is presented in Figure 3.15. The zero of energy is considered to be the electronic energy of separated BQ and BMAT.

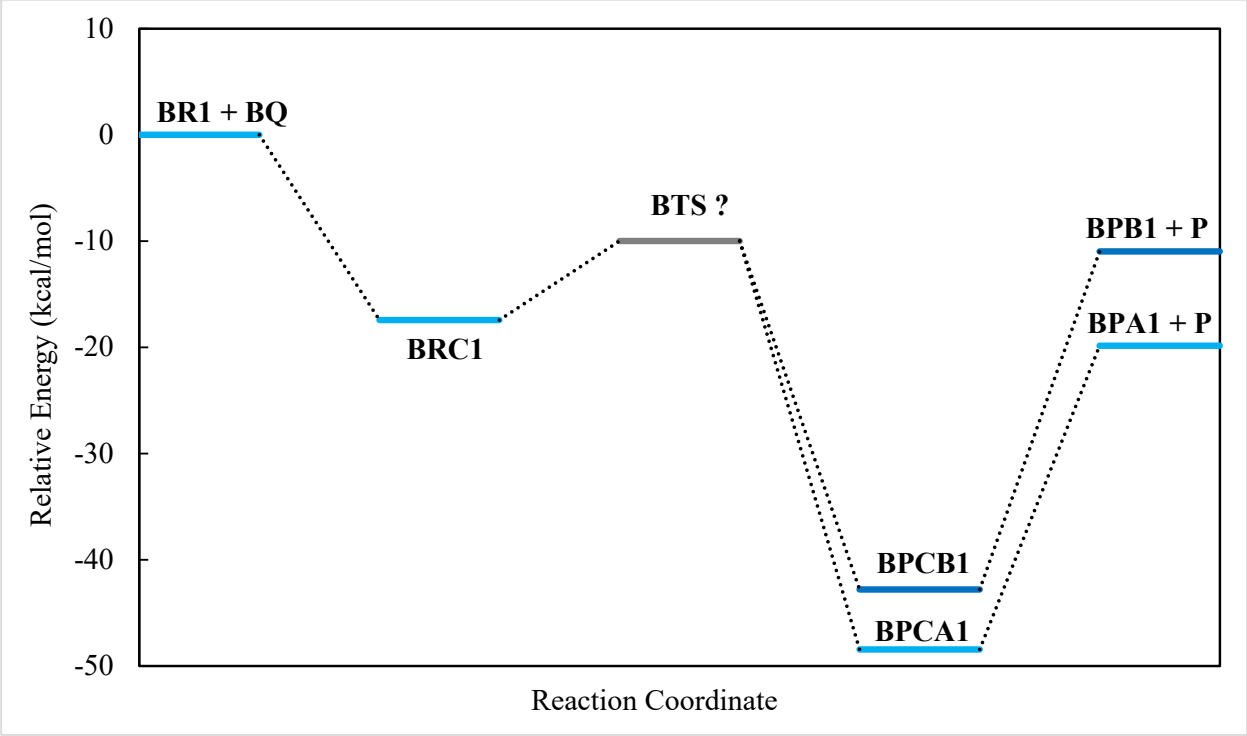

Figure 3.15 Basic-modeled energy diagram calculated with deprotonated species

Considering that moving from the reactant complex to either one of product complexes involves only formation of the C–N bond and reorganization of water molecules but no bond breaking, the barrier heights are not expected to be very large. They are estimated to be around 5-10 kcal/mol, the approximate energy value of a hydrogen bond. Also, based on the relative energy of product complexes, the transition state for the 1,4-addition reaction is expected to be lower in energy than the transition state for the 1,2-addition reaction.

The reactant complex for the unprotonated reactant complex is 17.44 kcal/mol lower than the energy of separated reactants (BQ and BMAT). This value is larger than the value obtained for the neutral system (6.17 kcal/mol) because the existence of changed species increases the strength of the hydrogen bonding interactions. With respect to separated reactants, the product complex for the 1,4-addition reaction is 48.45 kcal/mol lower in energy while the product complex for the 1,2-addition reaction is 42.82 kcal/mol lower in energy. With respect to the reactant complex, the product complex for the 1,4-addition reaction is 31.00 kcal/mol lower in energy while the product complex for the 1,2-addition reaction is 25.38 kcal/mol lower in energy. Similarly, with respect to separated reactants, the product for the 1,4-addition reaction is 19.86 kcal/mol lower in energy while the product for the 1,2-addition reaction is 10.99 kcal/mol lower in energy.

CHAPTER 4

REACTION STUDIES IN ACIDIC ENVIRONMENTS

4.1 Introduction

The results of the study of the reaction between benzoquinone (BQ) and methylamine (MA) in acidic environments are presented in this chapter. The acidic environment is modeled by considering a protonated system although, in reality, a protonated system is not very likely to be actually present in aqueous solutions of pH = 6. Like the neutral system, the first step of the reaction can lead to an 1,2-addition or an 1,4-addition as presented in Figure 4.1 below. The abbreviations for the acidic-modeled species can be found in Table 4.1 below, as well. Both reactions involve creation of a N–C bond between the N atom of methylamine and a C atom of benzoquinone. In the acidic-modeled reaction, an H atom is also transferred between the N atom of the amine and an O atom of benzoquinone. Like the neutral system, modeling the reactions requires the inclusion of two water molecules in computations.

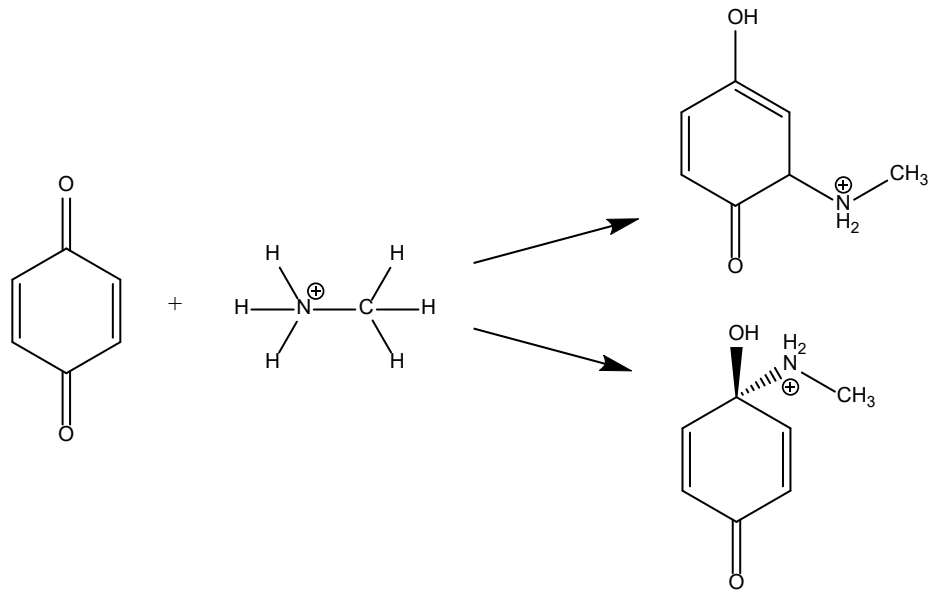

Figure 4.1 The first step of the reaction of benzoquinone with protonated MA leading to the acidic-modeled 1,4-addition product (top) and 1,2-addition product (bottom)

Table 4.1 Species labeling and chemical formulas for various stages of the reaction pathway in acidic environments

Formula	Name/Description & Label
$H_2O\cdots CH_3NH_3^+\cdots H_2O$	Protonated methylamine trimer (AMAT) (**AR**)
$C_6H_4O_2$	Benzoquinone (**BQ**)
$H_2O\cdots H_2O\cdots CH_3NH_3^+\cdots C_6H_4O_2$	Reactant complex (**ARC**)
$H_2O\cdots H_2O\cdots CH_3NH_2\cdots C_6H_5O_2H^+$	Transition state (**ATS**)
$H_2O\cdots H_2O\cdots CH_3NH_2–C_6H_5O_2H^+$	1,4-Product complex (**APCA**)
$H_2O\cdots H_2O\cdots CH_3NH_2–C_6H_5O_2H^+$	1,2-Product complex (**APCB**)
$CH_3NH_2–C_6H_5O_2H^+$	1,4-Product (**APA**)
$CH_3NH_2–C_6H_5O_2H^+$	1,2-Product (**APB**)
$H_2O\cdots H_2O$	Water dimer (**P**)

4.2 Acidic-Modeled Reactants and Products

4.2.1 Acidic-modeled reactants

For all low-energy conformations of AMAT a T-shaped geometry between the O atoms of water and the N atom of methylamine is obtained. Various starting geometries of AMAT were considered, some that were protonated at the amine group and some that were protonated at water. The T-shaped arrangement obtained in the optimized structures is preferred because it maximizes the number of hydrogen bonds to two and the positive charge is centered between all three molecules. The variation between these low-energy conformations comes from the different orientations of the water molecules configuring around the amine group. MAT is protonated at the amine and both water molecules for configuration verification. The lowest-energy conformation (**AR1**) is 30.55 kcal/mol lower in energy than the separated protonated MA and water dimer. The other low-energy conformation, **AR2,** is 1.99 kcal/mol higher in energy than **AR1**. **AR1** and **BQ** together form the reactant state, which is considered the zero of energy for the other stages of the reaction pathway in acidic environments.

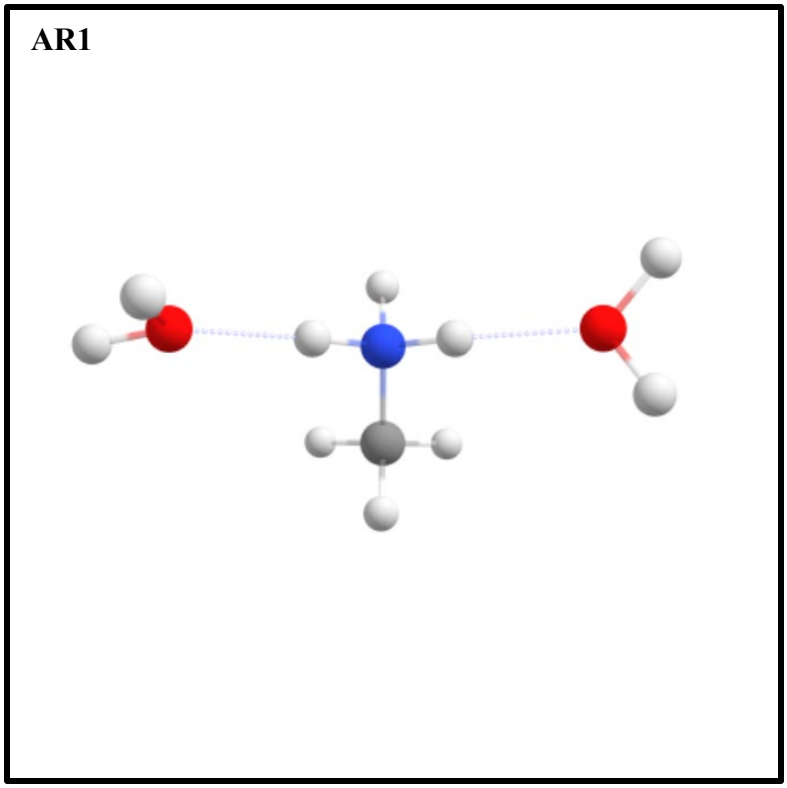

Figure 4.2 Lowest-energy acidic-modeled trimer **AR1**

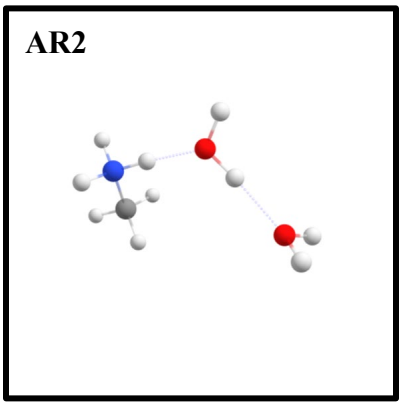

Figure 4.3 Other low-energy acidic-modeled trimer **AR2**

4.2.2 Acidic-modeled product of the 1,4-addition reaction

The product of the 1,4-addition reaction is a compound that has a new N–C bond and has an H atom connected to an O atom of benzoquinone as shown in Figure 4.4. The N–C bond is

two C atoms away from the new OH group. Multiple conformations are possible due to the rotation around the C–N bond and rotation around the C–OH bond. It is possible that two hydrogen atoms transfer to the C=O group of BQ. However, this is roughly 50 kcal/mol higher in energy than only one hydrogen atom transferred. The lowest-energy product conformation for the acidic-modeled 1,4-addition step is shown in Figure 4.4 and the next low-energy conformation is shown in Figure 4.5. For **APA1**, an H atom of the amine group is hydrogen-bonded to the neighboring C=O orienting both hydrogens away from the OH group of BQ. The methyl group is pointing towards the OH group. The next low-energy conformation in Figure 4.5, **APA2**, is 1.30 kcal/mol higher in energy than **APA1**.

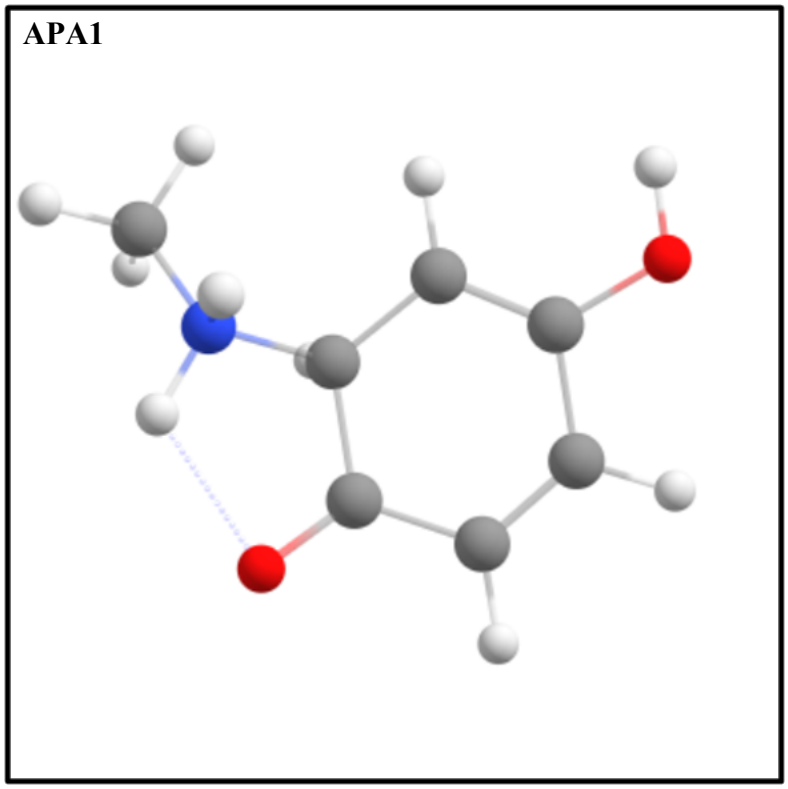

Figure 4.4 Lowest-energy conformation for the acidic-modeled product of the 1,4-addition of methylamine to benzoquinone (**APA1**)

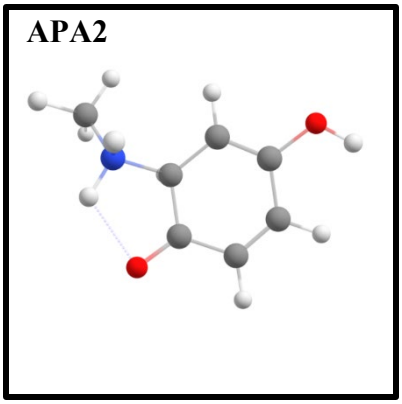

Figure 4.5 Another low-energy conformation for the acidic-modeled product of the 1,4-addition of methylamine to benzoquinone: **APA2**

4.2.3 Acidic-modeled product of the 1,2-addition reaction

The product of the 1,2-addition reaction is a compound that has a new N–C bond and has a H atom connected to an O atom of benzoquinone as shown in Figure 4.6. The N–C bond is now next to the new OH group. Multiple conformations are possible due to the rotation around the C–N bond and rotation around the C–OH bond. The lowest-energy product conformation of the acidic-modeled 1,2-addition product (**APB1**) is shown in Figure 4.6. For this conformation, the hydrogen atoms of the amine group are orienting away from the C=O group, the methyl group is pointing towards the C=O group, and the H atom of the OH group orients away from the protonated amino group. Another low-energy product for the 1,2-addition of AMAT to BQ can be seen in Figure 4.7. Conformation **APB2** is 0.89 kcal/mol higher in energy than **APB1**. Comparing the 1,2-addition product to the 1,4-addition product, the **APB1** is 9.85 kcal/mol higher in energy than **APA1**.

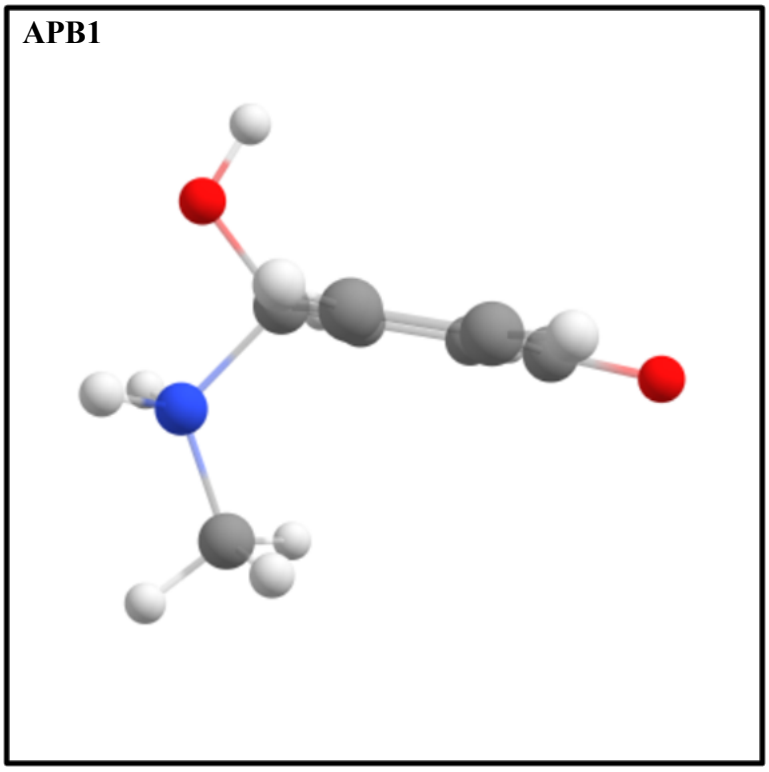

Figure 4.6 Lowest-energy conformation for the acidic-modeled product of the 1,2-addition of methylamine to benzoquinone (**APB1**)

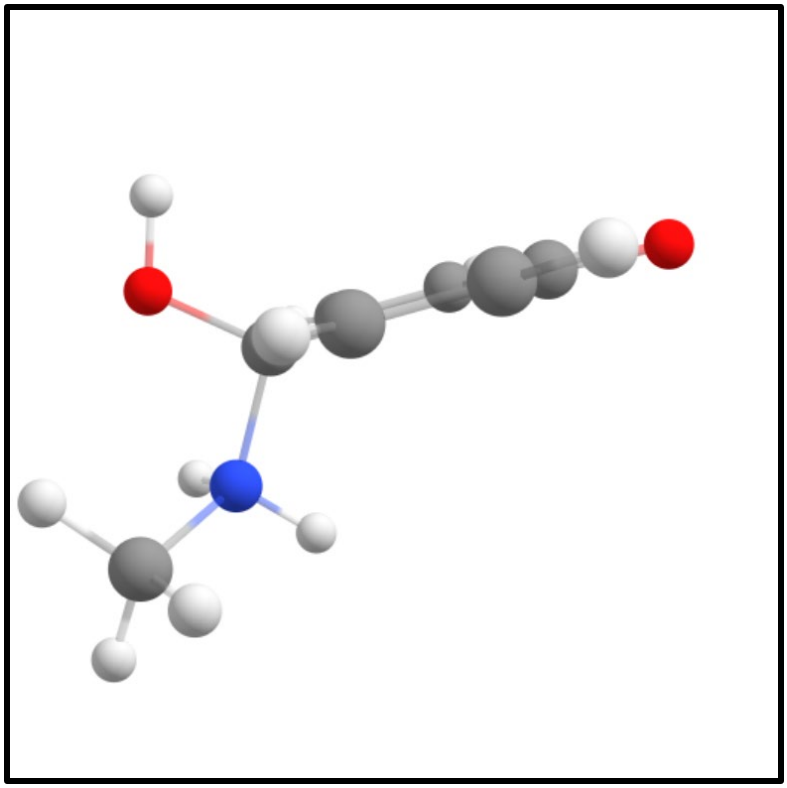

Figure 4.7 Other low-energy conformation for the acidic-modeled product of the 1,2-addition of methylamine to benzoquinone (**APB2**)

4.3 Acidic-Modeled Reactant and Product Complexes

4.3.1 Acidic-modeled reactant complexes

The reactant complex is a tetramer containing protonated methylamine, *p*-benzoquinone and two water molecules interacting with each other through non-covalent interactions, mainly hydrogen bonding. Optimization calculations for this tetramer under acidic-modeled conditions were carried out and a low-energy structure was obtained. The lowest-energy conformation for the reactant complex, **ARC1**, is shown in Figure 4.8. For **ARC1**, the tetramer structure appears to have the protonated MA surrounded and hydrogen bonded with two water molecules and BQ. Thus, the methyl group orients away from both water molecules and BQ. This arrangement is

very energy efficient because it maximizes the hydrogen bonds. No other conformations were searched or obtained. The lowest-energy conformation (**ARC1**) is 13.65 kcal/mol lower in energy than separated AMAT and BQ.

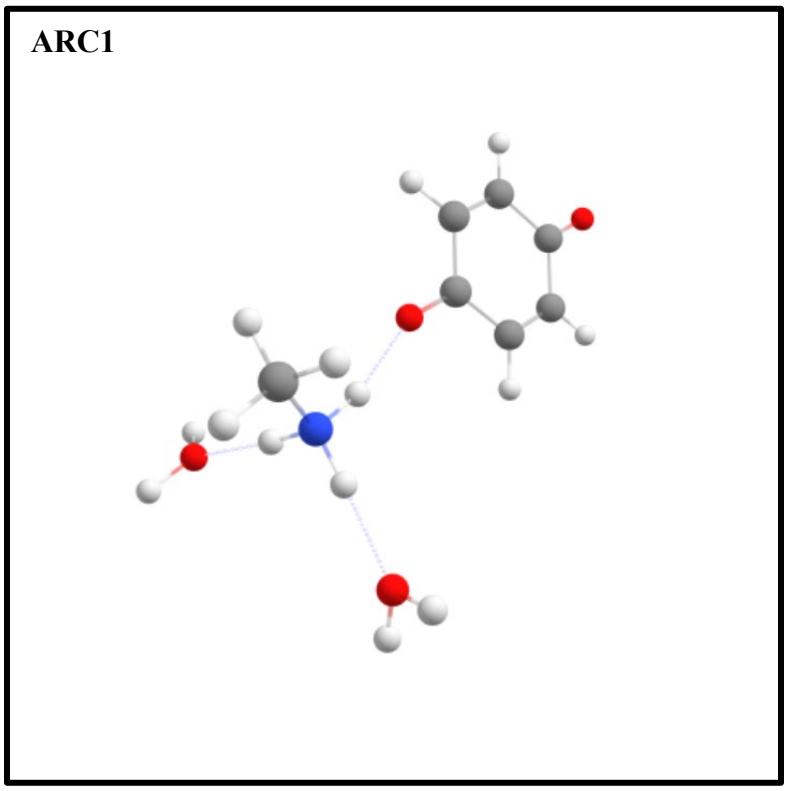

Figure 4.8 Lowest-energy conformation for the acidic-modeled reactant complex **ARC1**

4.3.2. Acidic-modeled product complex for the 1,4-addition reaction

The product complex stage for the 1,4-addition reaction contains the product for the 1,4-addition reaction in interaction with two water molecules. The lowest-energy acidic-modeled product complex geometry for the 1,4-addition of methylamine to benzoquinone is shown in Figure 4.9, and three other low-energy conformations are shown in Figure 4.10. For **APCA1**, the two water molecules arrange to both hydrogen bond with the cationic amine, in a similar T-shaped form as **ARC1**. The pattern of the two H bond interactions in **APCA1** appears to be

energetically preferred because this pattern does not appear in higher-energy conformations **APCA3** or **APCA4**. The lowest-energy conformation (**APCA1**) is 25.84 kcal/mol lower in energy than separated products (i.e., the 1,4-addition product, **APA1**, and water dimer). The other three low-energy conformations, **APCA2**, **APCA3**, and **APCA4**, are 0.66 kcal/mol, 1.17 kcal/mol, and 1.21 kcal/mol, respectively, higher in energy than **APCA1**.

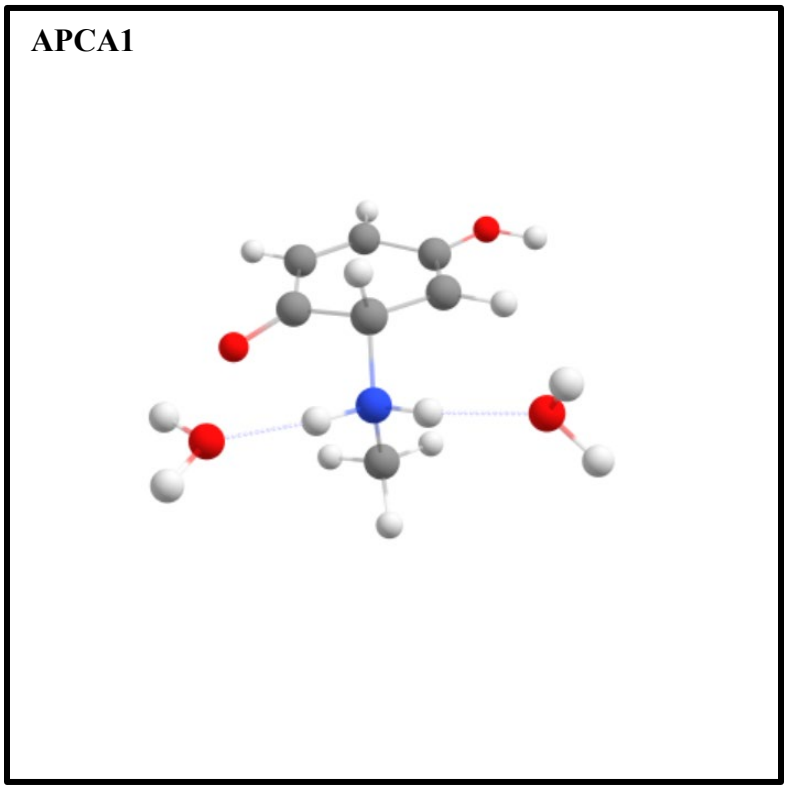

Figure 4.9 Lowest-energy conformation of the acidic-modeled product complex for the 1,4-addition of methylamine to benzoquinone **APCA1**

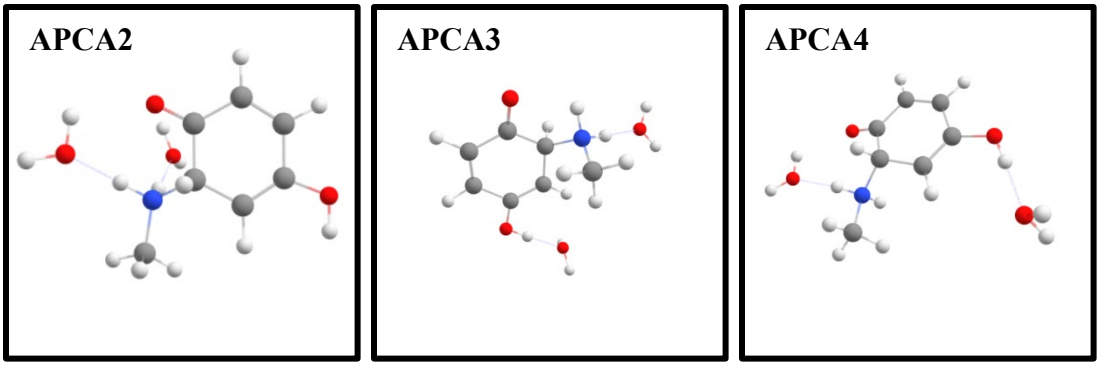

Figure 4.10 Other low-energy conformations for the acidic-modeled product complexes for the 1,4-addition of methylamine: **APCA2**, **APCA3**, **APCA4**

4.3.3 Acidic-modeled product complex for the 1,2-addition reaction

The lowest-energy product complex geometry for the acidic-modeled 1,2-addition of methylamine to benzoquinone is shown in Figure 4.11. For **APCB1**, both water molecules interact with the amine group in a T-shaped fashion**,** like the interaction in **ARC1**. The lowest-energy conformation (**APCB1**) is 26.66 kcal/mol lower in energy than separated products (i.e., the 1,2-addition product, **APB1**, and water dimer).

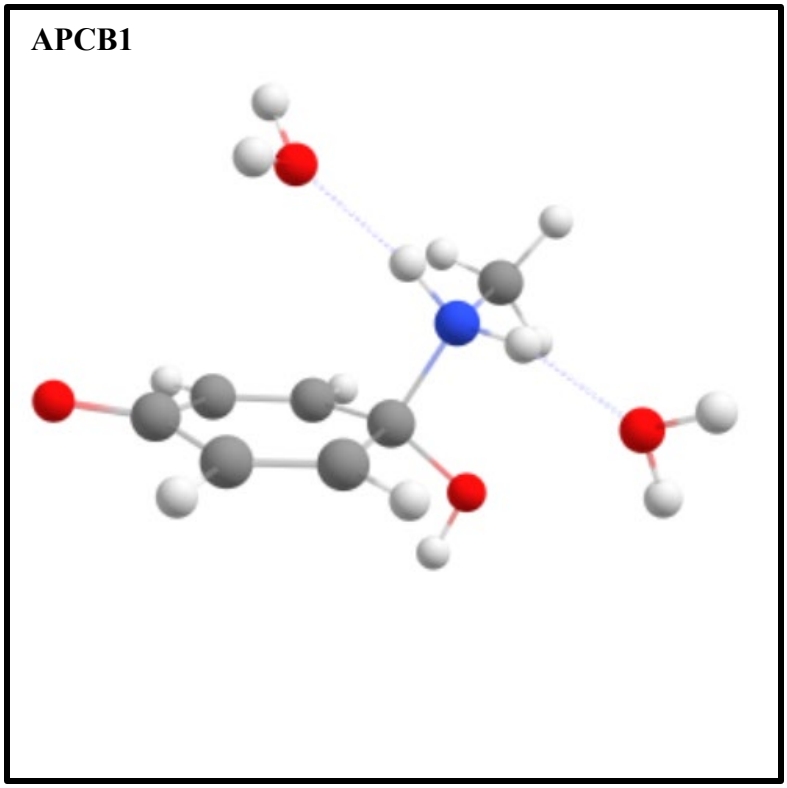

Figure 4.11 Lowest-energy conformation of the acidic-modeled product complex for the 1,2-addition of methylamine to benzoquinone **APCB1**

4.4 Acidic-Modeled Transition State

No transition states for either the 1,2-addition reaction or the 1,4-addition reaction were obtained in this study. Many computations were pursued but none of them optimized to the desired transition state. Initial attempts to identify transition states for the acidic-modeled system were carried out by protonating the geometry of the lowest-energy transition state structure for the neutral 1,4-addition reaction of methylamine to benzoquinone (**TSA1**) and analyzing the change in geometry. Few such starting geometries are shown in Figure 4.12 (**A**-**C**) while their corresponding output geometries are shown in Figure 4.12 (**D**-**F**). Conformations **D**-**F** in Figure 4.12 represent geometries after 30 cycles, because no initial geometries reached optimization. All

shown starting transition state geometries are protonated at the amine group. Various C–N bond length were tested in the starting geometries. Most calculations resulted in geometries where both water molecules break apart from their original hydrogen bond to the C=O group on BQ. A total of twenty-eight trials were carried out.

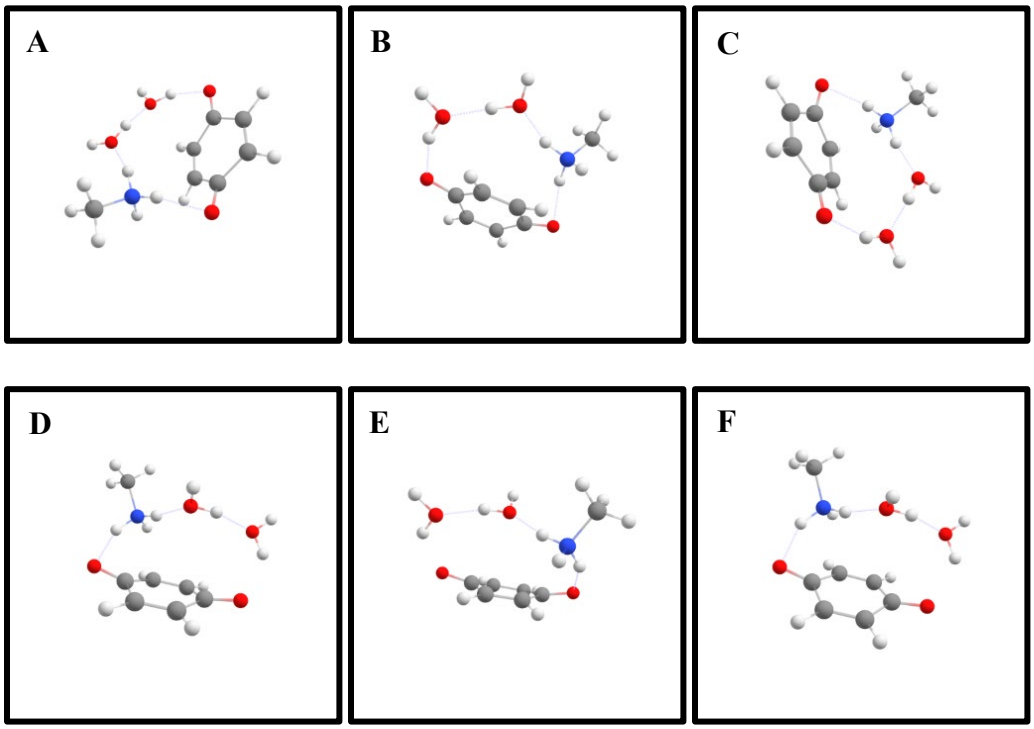

Figure 4.12 Acid-modeled variations of **TSA1** starting geometries: **A**, **B**, **C**, and corresponding output geometries **D**, **E**, **F**, respectively

Another study was carried out to determine a minimum estimate for the barrier height. In this study, the C–N distance was kept constant while all other parameters for the system were optimized with a bonding pattern of either reactant complex or 1,4-addition product complex. The bonding pattern of the reactant complex has the moving H atom covalently bonded to the N atom of amine while the pattern of the product complex has the moving H atom covalently bonded to the O atom of benzoquinone. As the C–N distances decreases from 2.50 A to 2.10 A, the structure with reactant complex pattern increases from about 1 kcal/mol to about 29 kcal/mol

relative to the separated reactant stage. On the other hand, as the C–N distance increases from 2.10 to 2.50 A, the structure with product complex pattern slightly increases in the range of around 16-20 kcal/mol relative to the separated reactant stage. At a C–N distance in the range of 2.2-2.3 A, the two patterns have similar energies, about 17-18 kcal/mol higher than the energy of separated reactant stage. This value of energy is the minimum necessary to go from reactant complex stage toward product complex stage therefore it is minimum estimate of the barrier height. Because additional atom rearrangements are necessary, an additional 5-10 kcal/mol is expected. Accordingly, the minimum estimate for the barrier height for acidic-modeled 1,4-addition reaction is about 20-25 kcal/mol higher than the separated reactant stage of the reaction.

4.5 Analysis of Acidic-Modeled Reaction Pathway

Even though no transition state has been identified, based on the energies of optimized reactants, products, and complexes, an overall energy diagram can be created for the reaction pathway for the addition of methylamine to benzoquinone in acidic environments. This diagram is presented in Figure 4.13. The zero of energy is considered to be the electronic energy of separated BQ and AMAT.

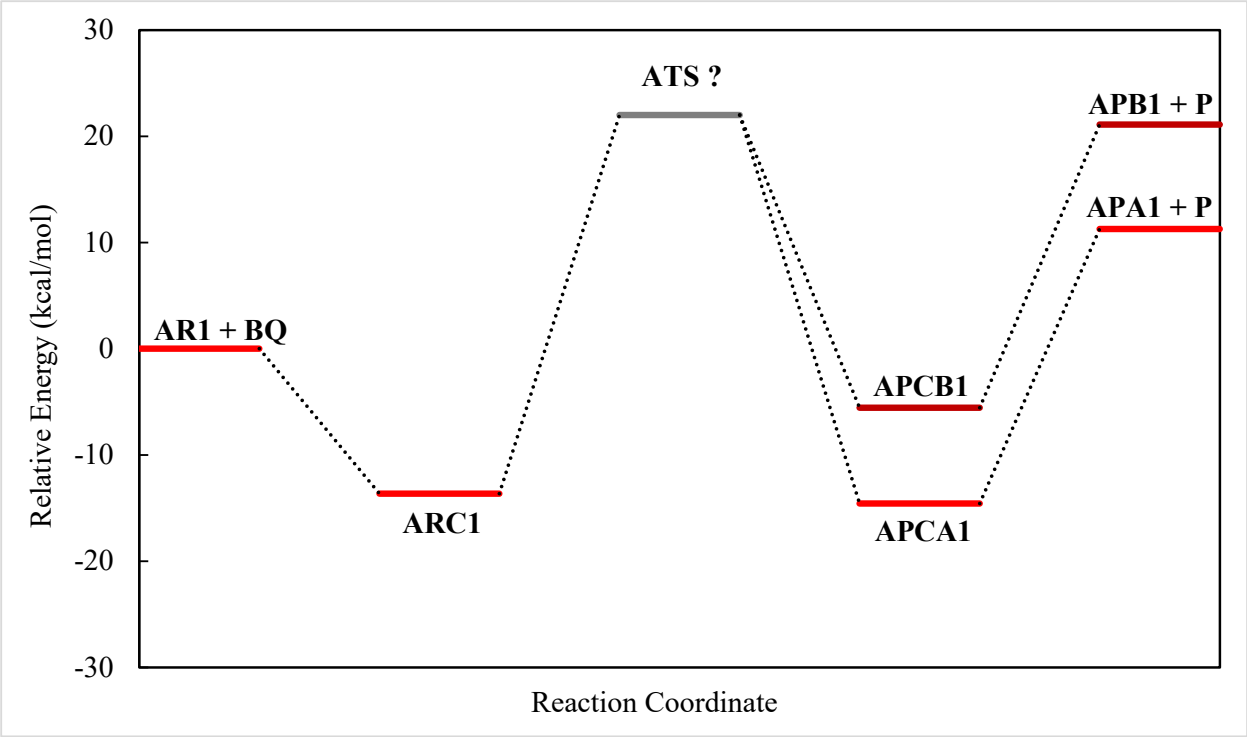

Figure 4.13 Acidic-modeled energy diagram calculated with protonated species

Considering that moving from the reactant complex to either one of product complexes involves not only the formation of the C–N bond but also the transfer of a H atom from the protonated amine to an oxygen atom of benzoquinone, the barrier heights are expected to be large. As presented in the previous section, they are estimated to be more than 30 kcal/mol higher than the reactant complex. Also, based on the relative energy of product complexes, the transition state for the 1,4-addition reaction is expected to be lower in energy than the transition state for the 1,2-addition reaction.

The reactant complex for the protonated reactant complex is 13.65 kcal/mol lower than the energy of separated reactants (BQ and AMAT). This value is larger than the value obtained for the neutral system (6.17 kcal/mol) because the existence of changed species increases the strength of the hydrogen bonding interactions. With respect to separated reactants, the product complex for the 1,4-addition reaction is 14.57 kcal/mol lower in energy while the product

complex for the 1,2-addition reaction is 5.55 kcal/mol lower in energy. With respect to the reactant complex, the product complex for the 1,4-addition reaction is 0.93 kcal/mol lower in energy while the product complex for the 1,2-addition reaction is 8.09 kcal/mol higher in energy. Similarly, with respect to separated reactants, the product for the 1,4-addition reaction is 11.26 kcal/mol higher in energy while the product for the 1,2-addition reaction is 22.11 kcal/mol higher in energy.

CHAPTER 5

ANALYSIS OF REACTION IN DIFFERENT ENVIRONMENTS

5.1 Introduction

The comparative analysis of results of the study of the reaction between benzoquinone (BQ) and methylamine (MA) in various environments are presented in this chapter. There are two main approaches to make the environment comparison. In the first approach, the energetics of the reaction in acidic, basic, and neutral environments is examined. In the second approach, small ions (hydronium or hydroxide ions) are placed in the proximity of the transition state obtained for the 1,4-addition reaction in neutral environment to estimate their influence on the energy of the transition state.

5.2 Reaction Path Energetics

5.2.1 Barrier heights

The easiest and most straightforward criteria of comparison between various pathways for a reaction, or different reactions is to compare their barrier height, which is the energy difference between the saddle point (or transition state) and the energy of reactants. Unfortunately, in the current study, no transition states were identified for the acidic-modeled or basic-modeled reactions. However, as presented in the earlier chapters, the barrier heights for acidic-modeled or basic-modeled reactions were estimated to be around –10 kcal/mol and +22 kcal/mol, respectively, with respect to separated reactants. The negative value for acidic-modeled reaction is due to transition state being around 7 kcal/mol above the energy of reactant complex, which is 17 kcal/mol lower in energy than separated reactants. For comparison, the

barrier height in neutral environments is 6.56 kcal/mol for the 1,4-addition reaction and 7.77 kcal/mol for the 1,2-addition reaction. The estimated barrier heights are consistent with the experimental observation of reaction occurring faster in basic environments than acidic environments.

5.2.2 Energies of reaction determined from reactants and products

In the absence of identifying transition states for acidic- and basic-modeled reactions, alternative methods of estimating to relative reactivity in different environments can be employed. Looking at the energy of reaction is one of these alternative methods. The classical energy of reaction is the energy difference between the products (1,2-addition product or 1,4-addition product and water dimer) and the reactants (MAT + BQ), and it is denoted as ΔE_{RP}. Because the reactants are considered the relative zero of energy, the energy of reaction is just the energy of the products. The energies of reaction for the 1,4-addition reaction of MAT to BQ in different environments (determined based on **PA1**, **APA1**, **BPA1**) are presented in Table 5.1. The energies of reaction for the 1,2-addition reaction of MAT to BQ in different environments (determined based on **PB1**, **APB1**, **BPB1**) are presented in Table 5.2. The range in relative energy for the products between the acid, neutral, and base 1,4-addition of MAT to BQ is 31.12 kcal/mol while the range in relative energy for the products between the acid, neutral, and base 1,2-addition of MAT to BQ is 32.10 kcal/mol. For both the 1,4-addition and 1,2-addition reaction of MAT to BQ, the basic-modeled pathway is the most favorable because the energy of reaction is the most exothermic. Moreover, the 1,4-addition basic-modeled pathway is 8.87 kcal/mol lower in energy than the 1,2-addition pathway. Both the 1,4-addition and 1,2-addition pathways followed the same ranking of basic-modeled being the lowest in relative energy, hence

the most favored, the neutral-modeled being in the middle, and the acidic-modeled having the highest energy of reaction, signifying the least favored environment. Also, the 1,4-addition acidic-modeled pathway is 9.85 kcal/mol lower in energy than the 1,2-addition pathway.

Table 5.1 Relative energy difference for the reactants to products reaction of the 1,4-addition of MA to PBQ

pH	Reactants	Products	ΔE_{RP} (kcal/mol)
Acid	0.00	11.26	11.26
Neutral	0.00	3.12	3.12
Base	0.00	-19.86	-19.86

Table 5.2 Relative energy difference for the reactants to products reaction of the 1,2-addition of MA to PBQ

pH	Reactants	Products	ΔE_{RP} (kcal/mol)
Acid	0.00	21.11	21.11
Neutral	0.00	2.97	2.97
Base	0.00	-10.99	-10.99

5.2.3 Energies of reaction determined from reactant and product complexes

An alternative way possible for calculating the energy of reaction is to look at the reaction occurring between reactant complex and the product complex. Accordingly, the energy of reaction is the energy difference between the product complex and the reactant complex, and it is denoted as ΔE_{RCPC}. These alternative energies of reaction for the 1,4-addition reaction of MAT to BQ in different environments (determined based on **PCA1**, **APCA1**, **BPCA1** and **RC1**,

ARC1, **BRC1**, respectively) are presented in Table 5.3. The alternative energies of reaction for the 1,2-addition reaction of MAT to BQ in different environments (**PCB1**, **APCB1**, **BPCB1** and **RC1**, **ARC1**, **BRC1**, respectively) are presented in Table 5.4. The range in relative energy for reactant complexes to product complexes between the acidic, neutral, and basic environments of 1,4-addition reaction of MAT to BQ is 30.09 kcal/mol. The range in relative energy for reactant complexes to product complexes between the acid, neutral, and base 1,2-addition of MAT to BQ is 33.48 kcal/mol. For both the 1,4-addition and 1,2-addition of MAT to BQ, the basic-modeled pathway is the most favorable yielding the lowest relative energy difference from reactant complexes to product complexes. However, the 1,4-addition basic-modeled pathway is 5.63 kcal/mol lower in energy than the 1,2-addition pathway. Both the 1,4-addition and 1,2-addition mechanisms followed the same pattern of basic-modeled being the most exothermic, hence the most favored, the neutral-modeled in the middle, and the acidic-modeled being the least exothermic, signifying the least favored pathway. Also, the 1,4-addition acidic-modeled pathway is 9.02 kcal/mol lower in energy than the 1,2-addition pathway.

Table 5.3 Relative energy difference for the reactant complex to product complex reaction of the 1,4-addition of MA to PBQ

pH	Reactant Complex	Product Complex	ΔE_{RCPC} (kcal/mol)
Acid	-13.65	-14.57	-0.92
Neutral	-6.17	-14.69	-8.52
Base	-17.44	-48.45	-31.01

Table 5.4 Relative energy difference for the reactant complex to product complex reaction of the 1,2-addition of MA to PBQ

pH	Reactant Complex	Product Complex	ΔE_{RCPC} (kcal/mol)
Acid	-13.65	-5.55	8.10
Neutral	-6.17	-10.78	-4.61
Base	-17.44	-42.82	-25.38

5.3 The Effect of Ionized Species on the Transition State of 1,4-Addition Reaction

5.3.1 Ionized species in cubic positions

Another approach to investigate the influence of pH on the reactivity of BQ towards amines is to take a previously determined transition state and place either a hydronium ion (to represent acidic conditions) or a hydroxide ion (to represent basic conditions) in its vicinity. These ionized species (hydronium and hydroxide) will be placed far enough from the transition state to produce an energetic influence, but not close enough to rearrange the atomic structure. The interaction between the ion and the transition state that lowers the energy of the combined system compared to the separated parts will be an indication that the environment which that ion is modeling will favor the reaction. To complete the comparative study, a water molecule was also used instead of hydronium or hydroxide ions. Because the 1,4-addition reaction has a lower barrier height than the 1,2-addition reaction in neutral environments, the lowest-energy transition state for 1,4-addition reaction (**TSA1**) was chosen for this study.

The oxygen atom of the hydronium ion, hydroxide or water was placed at 8.00 angstroms away from the “center” of the benzoquinone ring. The “center” of the benzoquinone ring was considered to be the point at the middle of the distance between atoms C1 and C4 of BQ. In the

study presented in this section, each species (H_2O, H_3O^+, or HO^-) were placed in a cubic position around **TSA1**, particularly, in positions consisting of each of the corners (a total of 8 different positions), the middle of each edge (a total of 12 different positions), and the center of each face (a total of 6 different positions). An example model of all employed corner positions is presented in Figure 5.1, and a different visualization of the corners of the cubic geometry is presented in Figure 5.2. A diagram can also be found in Figure 5.3 representing all individual cubic positions (corners, edges, and faces) for placement of H_2O, H_3O^+, or HO^- species.

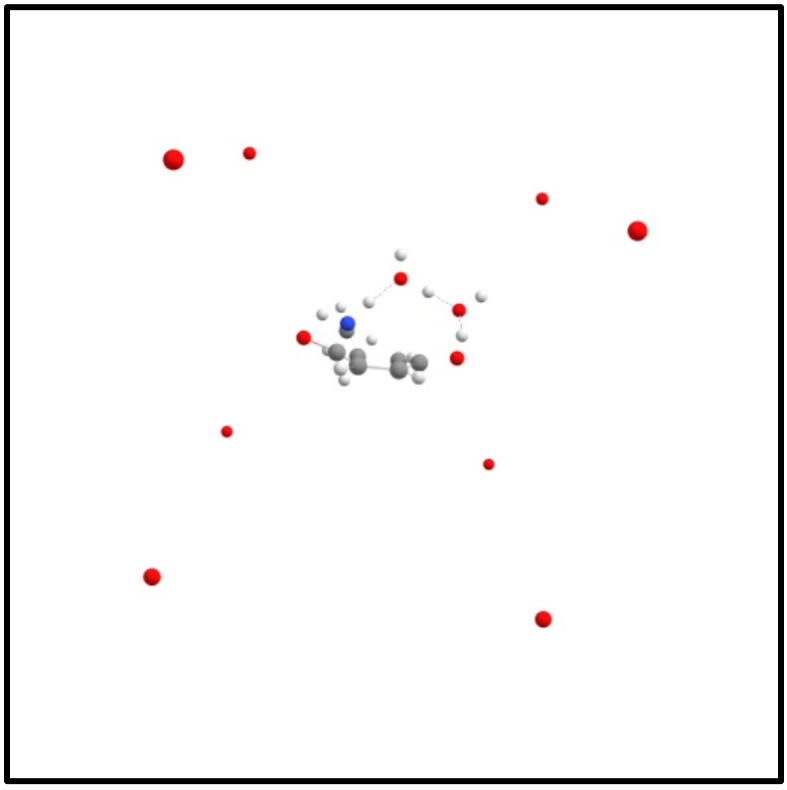

Figure 5.1 Geometric positioning of H_2O, H_3O^+, or HO^- species in the corners of the cubic model

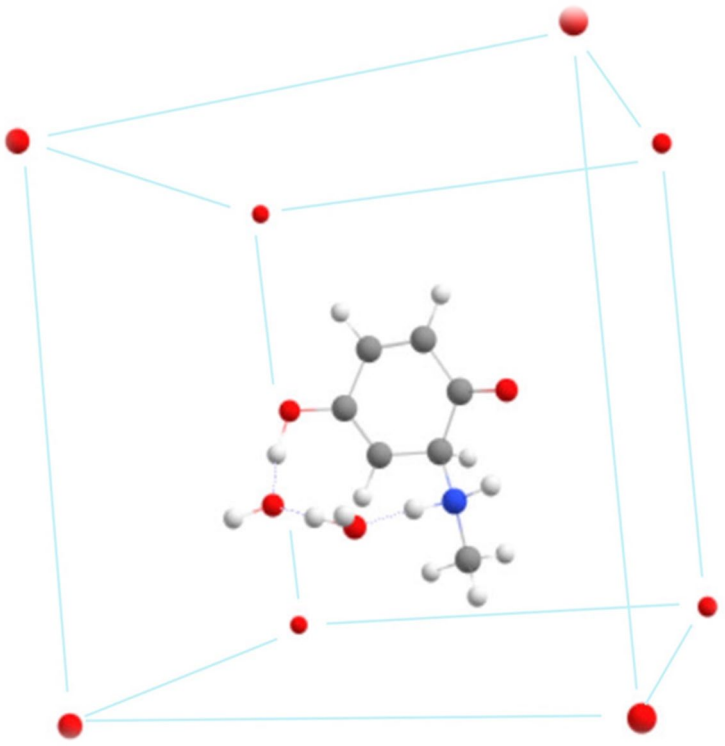

Figure 5.2 Another representation of the geometric positioning of H_2O, H_3O^+, or HO^- species in the corners of the cubic model

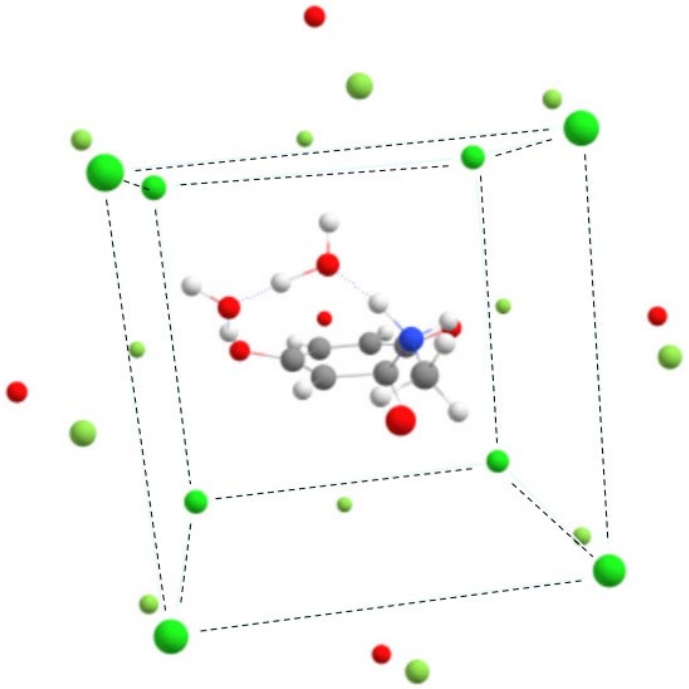

Figure 5.3 Representation of all geometric (corners, edges, and faces) positioning of H_2O, H_3O^+, or HO^- species in the cubic model

The position of H_2O, H_3O^+, or HO^- species influencing the transition state is defined by the oxygen atom of these species. This oxygen atom is labeled as O_{26}. As mentioned earlier, O_{26} is at the same distance of 8.00 A from the "center" of the transition state structure but it is at different distances from the main atoms involved in the hydrogen transfer. The number labeling for all atoms of **TSA1** is given in Figure 5.4, and the distances between O_{26} and the main atoms involved in hydrogen transfer are given in Tables 5.5 and 5.6. The smallest three average distances are presented in bold in these two tables.

The energy of the system containing **TSA1** and influencing species (H_2O, H_3O^+, or HO^-) is then compared with the values of separated **TSA1** and influencing species. A negative value of this interaction energy should indicate that the presence of the influencing species lowers the energy of the transition state therefore speeding the reaction. The interaction energies for

individual position of influencing species as well as the average obtained for each type of positions are given in Table 5.7. The presence of water (modeling the neutral system) has the smallest contribution, and that contribution is positive, on average. Not surprisingly, the small ions (H_3O^+, or HO^-) will have a higher influence, and this influence will be negative, as the presence of the **TSA1** near these small ions will stabilize them. However, the influence of HO^- ion (modeling the basic environment) is slightly more negative than the influence of H_3O^+ ion (modeling the basic environment) suggesting that the reaction will be favored in basic environments. The same result is obtained independent of the influencing species being placed in a corner, an edge, or a face of the cube.

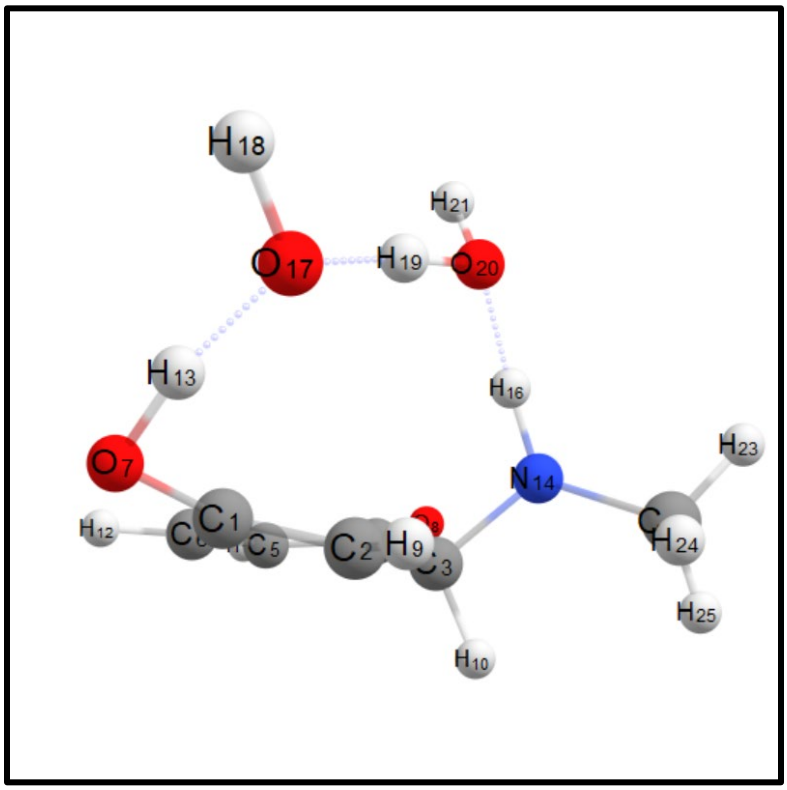

Figure 5.4 Lowest energy neutral transition state with oxygen, nitrogen, and hydrogens numbered for reference of Table 5.5 and Table 5.8 **TSA1**

Table 5.5 Distances between O_{26} and the N_{14}, O_{17}, and O_{20} atoms that are involved in hydrogen transfer process of the transition state

Position	$N_{14}\cdots O_{26}$ (Å)	$O_{17}\cdots O_{26}$ (Å)	$O_{20}\cdots O_{26}$ (Å)	Average (Å)
Face 1	**7.95**	**7.23**	**6.22**	**7.13**
Face 2	8.88	10.20	10.68	9.92
Face 3	**5.80**	**6.88**	**5.97**	**6.22**
Face 4	10.41	10.44	10.82	10.56
Face 5	**9.44**	**5.78**	**8.19**	**7.80**
Face 6	7.27	11.09	9.26	9.21
Corner 1	9.92	7.43	8.53	8.63
Corner 2	**7.44**	**4.42**	**5.07**	**5.64**
Corner 3	**8.02**	**7.03**	**8.32**	**7.79**
Corner 4	10.37	9.22	10.79	10.13
Corner 5	8.81	10.34	9.14	9.43
Corner 6	**5.87**	**8.44**	**6.04**	**6.78**
Corner 7	6.59	10.06	8.95	8.53
Corner 8	9.31	11.70	11.27	10.76
Edge 1	10.50	8.27	9.93	9.57
Edge 2	**8.85**	**5.31**	**6.57**	**6.91**
Edge 3	**7.57**	**4.97**	**6.40**	**6.32**
Edge 4	9.45	8.05	9.82	9.11
Edge 5	9.20	11.48	10.57	10.42
Edge 6	7.25	9.57	7.50	8.11
Edge 7	**5.63**	**9.38**	**7.36**	**7.46**
Edge 8	7.98	11.32	10.47	9.93
Edge 9	9.59	9.04	8.86	9.16
Edge 10	**6.24**	**6.17**	**4.57**	**5.66**
Edge 11	7.08	8.64	8.62	8.11
Edge 12	10.15	10.88	11.48	10.84

Table 5.6 Distances between O_{26} and the H_{13}, H_{19}, and H_{16} atoms that are involved in hydrogen transfer process of the transition state

Position	$H_{13}\cdots O_{26}$ (Å)	$H_{19}\cdots O_{26}$ (Å)	$H_{16}\cdots O_{26}$ (Å)	Average (Å)
Face 1	**7.66**	**6.55**	**7.05**	**7.09**
Face 2	9.43	10.45	9.68	9.85
Face 3	**7.77**	**6.30**	**5.82**	**6.63**
Face 4	9.34	10.60	10.46	10.13
Face 5	**5.28**	**7.08**	**8.89**	**7.08**
Face 6	10.95	10.10	8.02	9.69
Corner 1	6.81	7.93	9.22	7.99
Corner 2	**5.55**	**4.58**	**6.44**	**5.52**
Corner 3	**6.95**	**7.70**	**8.18**	**7.61**
Corner 4	7.99	10.06	10.51	9.52
Corner 5	9.97	9.64	8.75	9.45
Corner 6	**9.16**	**7.14**	**5.74**	**7.34**
Corner 7	10.07	9.44	7.64	9.05
Corner 8	10.81	11.45	10.10	10.79
Edge 1	7.13	9.13	10.18	8.81
Edge 2	**5.54**	**5.86**	**7.83**	**6.41**
Edge 3	**5.64**	**5.66**	**7.09**	**6.13**
Edge 4	7.21	9.01	9.62	8.61
Edge 5	10.76	10.96	9.65	10.46
Edge 6	9.78	8.43	7.13	8.45
Edge 7	**9.84**	**8.29**	**6.31**	**8.15**
Edge 8	10.82	10.85	9.06	10.24
Edge 9	8.52	8.85	9.10	8.82
Edge 10	**7.33**	**5.19**	**5.42**	**5.98**
Edge 11	8.66	8.59	7.78	8.34
Edge 12	9.70	11.19	10.67	10.52

Table 5.7 Energetic effect on **TSA1** from the influencing species (H_2O, OH^-, H_3O^+) in cubic positions

Influencing species position	H_2O (neutral) effect (kcal/mol)	OH^- (basic) effect (kcal/mol)	H_3O^+ (acidic) effect (kcal/mol)
Face 1	0.07	-2.11	0.37
Face 2	0.19	-1.69	0.22
Face 3	0.52	-8.12	3.75
Face 4	0.08	-1.27	-0.67
Face 5	0.29	5.44	-8.90
Face 6	0.39	-1.29	-1.22
Face average	**0.26**	**-1.51**	**-1.08**
Corner 1	0.41	1.92	-4.24
Corner 2	-0.23	-0.04	-4.25
Corner 3	0.63	0.42	-2.65
Corner 4	0.39	1.52	-3.62
Corner 5	-0.09	-0.23	-1.07
Corner 6	-0.32	-6.58	4.09
Corner 7	-0.45	-7.56	5.10
Corner 8	-0.07	-1.55	-0.16
Corner average	**0.03**	**-1.51**	**-0.85**
Edge 1	0.55	2.37	-4.99
Edge 2	0.30	1.23	-4.31
Edge 3	0.56	2.83	-6.43
Edge 4	0.51	2.46	-4.57
Edge 5	-0.16	-1.09	-1.02
Edge 6	-0.19	-1.64	0.17
Edge 7	-1.00	-9.93	6.48
Edge 8	-0.17	-3.09	1.39
Edge 9	0.11	-0.45	-1.29
Edge 10	0.49	-2.74	-0.63
Edge 11	0.23	-5.43	3.21
Edge 12	0.13	-0.84	-0.82
Edge average	**0.11**	**-1.36**	**-1.07**

5.3.2 Ionized species in special positions

A more intuitive approach to species placement can be used to further investigate the interactions between **TSA1** and influencing species. These special positions of influencing species are obtained along the direction of the "center" of **TSA1** and each of the seven main atoms involved in hydrogen transfer in the transition state **TSA1**. The oxygen atom of the hydronium ion, hydroxide or water was placed at 6.00 angstroms away from the main atom, opposite from the "center" of **TSA1**. A sample representation of one of these special positions in shown Figure 5.5. Like the cubic positioning of the influencing species, the energy interaction between influencing species and TSA1 were calculated, and these energies are presented in Table 5.8 along with the numeric labeling of their corresponding main atoms of **TSA1** involved in the hydrogen transfer process. The results of the special positioning of the influencing species shows that water have again the smallest influence while OH^- and H_3O^+ have essentially the same influence (-1.21 kcal/mol for OH^- influence and -1.33 kcal/mol for H_3O^+ influence, respectively), although a slightly more negative value for acidic modelling. Unfortunately, no definitive conclusions can be drawn from the study of these special positions.

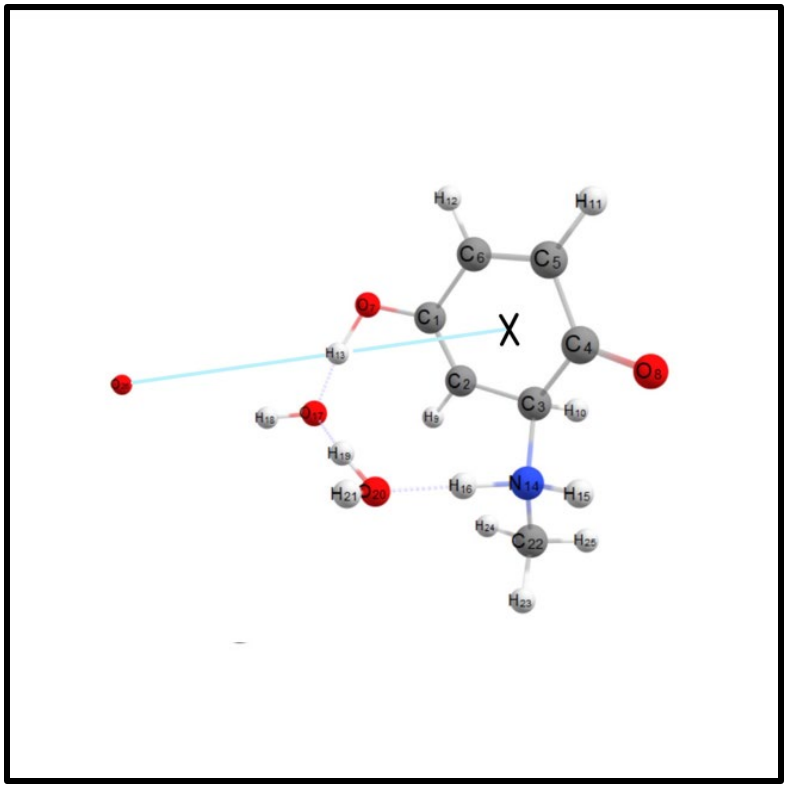

Figure 5.5 Special positioning of influencing species and their linear relationship with the main atoms involved in hydrogen transfer process, where X is the "center" of the **TSA1**

Table 5.8 Energetic effect on **TSA1** from the influencing species (H_2O, OH^-, H_3O^+) in special positions

Atom collinear to influencing species position	H_2O (neutral) effect (kcal/mol)	OH^- (basic) effect (kcal/mol)	H_3O^+ (acidic) effect (kcal/mol)
H_{13}	0.44	1.95	-4.73
N_{14}	-0.31	-9.04	5.81
H_{16}	0.36	-4.44	2.08
O_{17}	0.17	0.57	-2.91
H_{19}	0.15	-0.16	-2.09
O_{20}	0.27	-1.39	-0.59
O_7	0.32	4.03	-6.85
Special position average	0.20	-1.21	-1.33

5.3 Future Work and Concluding Remarks

The study presented here investigated computationally the influence of acidic and basic environments of the reaction of BQ with MA. All theoretical calculations were performed using a hybrid density functional theory method, MPW1K, in conjunction with the 6-31+G(d,p) basis set. Two main approaches were applied, one focusing on the reaction energetics and the other on the effect of ionized species on the transition state obtained for neutral species. On the approach looking at reaction energetics, new transition states were found for the neutral-modeled 1,2-addition reaction of MA with BQ, and new reaction profiles were determined for the basic-modeled of 1,2- and 1,4-addition reactions of MA with BQ and the acidic-modeled 1,2- and 1,4-addition reactions of MA with BQ. Both employed approaches showed that the reaction is predicted to be faster in basic environments, which is consistent with experimental results of protein modifications by BQ. Future work might involve looking in more detail on the distance,

position and/or orientation of the influencing species or carrying out additional computations to identify transition states for acidic or basic-modeled systems.

BIBLIOGRAPHY

Adamo, C.; Barone, V. “Exchange Functionals with Improved Long-range Behavior and Adiabatic Connection Methods without Adjustable Parameters: The mPW and mPW1PW Models,” *J. Chem. Phys.,* **1998**, 108, 664-675.

Albu, T. V.; Mikel, S. E., "Performance of Hybrid Density Functional Theory Methods Toward Oxygen Electroreduction Over Platinum". *Electrochim. Acta.* **2007,** *52* (9), 3149-3159.

Becke, A. D. “Density-functional Thermochemistry. IV. A New Dynamical Correlation Functional and Implications for Exact-exchange Mixing,” *J. Chem. Phys.,* **1996**, 104, 1040.

Dohi, T.; Hu, Y.; Kamitanaka, T.; Kita, Y. Controlled Couplings of Quinone Monoacetals Using Reusable Polystyrene-Anchored Specific Proton Catalyst. *Tetrahedron* **2012**, *68* (40), 8424–8430.

Fernando, J. R. C. “Theoretical Studies on Quinone Reactivity,” Master of Science Thesis, Tennessee Tech University, Cookeville, TN, 2009.

Frisch, G. W.; Gaussian 09, M. J. Frisch, G. W. Trucks, H. B. Schlegel, G. E. Scuseria, M. A. Robb, J. R. Cheeseman, G. Scalmani, V. Barone, B. Mennucci, G. A. Petersson, H. Nakatsuji, M. Caricato, X. Li, H. P. Hratchian, A. F. Izmaylov, J. Bloino, G. Zheng, J. L. Sonnenberg, M. Hada, M. Ehara, K. Toyota, R. Fukuda, J. Hasegawa, M. Ishida, T. Nakajima, Y. Honda, O. Kitao, H. Nakai, T. Vreven, J. A. Montgomery, Jr., J. E. Peralta, F. Ogliaro, M. Bearpark, J. J. Heyd, E. Brothers, K. N. Kudin, V. N. Staroverov, R. Kobayashi, J. Normand, K. Raghavachari, A. Rendell, J. C. Burant, S. S. Iyengar, J. Tomasi, M. Cossi, N. Rega, J. M. Millam, M. Klene, J. E. Knox, J. B. Cross, V. Bakken, C. Adamo, J. Jaramillo, R. Gomperts, R. E. Stratmann, O. Yazyev, A. J. Austin, R. Cammi, C. Pomelli, J. W. Ochterski, R. L. Martin, K. Morokuma, V. G. Zakrzewski, G. A. Voth, P. Salvador, J. J. Dannenberg, S. Dapprich, A. D. Daniels, Ö. Farkas, J. B. Foresman, J. V. Ortiz, J. Cioslowski, and D. J. Fox, Gaussian, Inc., Wallingford, CT, **2009.**

He, Y.; Xu, D.-H.; Zhang, Y.-J.; Zhang, C.; Guo, J.-M.; Li, L.; Liang, X.-Q. Microscopic Mechanism of Light-Induced Tetrazole-Quinone 1,3-Dipolar Cycloaddition: A MS-CASPT2 Theoretical Investigation. *RSC Adv.* **2021**, *11* (52), 32792–32798.

Kim, J.; Vaughn, A. R.; Cho, C.; Albu, T. V.; Carver, E. A. "Modifications of Ribonuclease A Induced by p-benzoquinone," *Bioorg. Chem.* **2012,** *40*, 92-98.

Kim, J. “Biological implications of benzoquinones.” Quinone: Occurrence, Medicinal Uses and Physiological Importance. Nova Science Publishers, Inc. 2013.

Lee, C. H. K. “Theoretical Studies of Naphthoquinone Reactivity Toward Amines.” Departmental Honors Thesis, The University of Tennessee at Chattanooga, Chattanooga, TN, 2019.

Li, J.; Xu, H.; Wang, J.; Wang, Y.; Lu, D.; Liu, J.; Wu, J. Theoretical Insights on the Hydration of Quinones as Catholytes in Aqueous Redox Flow Batteries. *Chin. J. Chem. Eng.* **2021**, *37*, 72–78.

Nawrat, C. C.; Moody, C. J. Quinones as Dienophiles in the Diels-Alder Reaction: History and Applications in Total Synthesis. *Angew. Chem. Int. Ed.* **2014**, *53* (8), 2056–2077.

Rathnayake, L. “Theoretical Investigations of p-Benzoquinones and Thiosemicaarbazones.” Master of Science Thesis, Tennessee Tech University, Cookeville, TN, 2013.

Tarumi, M.; Matsuzaki, Y.; Suzuki, K. Theoretical Study on the Redox Reaction Mechanism of Quinone Compounds in Industrial Processes. *Chem. Eng. Sci.* **2019**, *199*, 381–387.

Teixeira-Dias, J. J. C. *MOLECULAR PHYSICAL CHEMISTRY: A Computer-Based Approach Using Mathematica(R) and Gaussian.*; 2019.

Zhang, L.; Zhang, G.; Xu, S.; Song, Y. Recent Advances of Quinones as a Privileged Structure in Drug Discovery. *European Journal of Medicinal Chemistry* **2021**, *223*, 113632.

Zhao, Y.; Truhlar, D. G. “Hybrid Meta Density Functional Theory Methods for Thermochemistry, Thermochemical Kinetics, and Noncovalent Interactions: The MPW1B95 and MPWB1K Models and Comparative Assessments for Hydrogen Bonding and van der Waals Interactions,” *J. Phys. Chem. A*. **2004**, *108*, 6908-6918.

Zhen, F.; Hapiot, P. “Electrochemical Reduction of Quinones is Ethylene Chosen as an Example of Deep Eutectic Solvent”. *Electrochem. Sci. Adv.* **2022,** 00.

APPENDIX A

SUPPLEMENTARY INFORMATION FOR CHAPTER 2, 3, 4, AND 5

This appendix includes the optimized geometries in Cartesian coordinates for minimum-energy structures and transition states in gas-phase using the mPW1B95-44/6-31+G(d,p) level of theory.

Cartesian coordinates of neutral reaction pathway

TSB1

C	-0.674146	-0.249922	-0.245349
C	0.793392	-0.535751	-0.177767
C	1.724207	0.406362	-0.250540
C	1.364999	1.824725	-0.416106
C	-0.059294	2.128293	-0.623676
C	-0.991877	1.186034	-0.551399
O	-1.264298	-1.125410	-1.078012
O	2.207227	2.695559	-0.401971
N	-1.252953	-0.528796	1.159872
H	-0.296377	3.154016	-0.861470
H	-2.036122	1.394485	-0.741121
H	-1.214214	-1.538871	1.248302
C	-0.629457	0.131566	2.307058
H	-2.319653	-0.278971	1.135230
H	-2.294788	-0.825452	-1.305120
O	-3.531945	-0.351503	-1.374508
O	-3.762877	-0.068011	0.979075
H	-3.820256	-0.198823	-0.125445
H	-4.231154	0.715032	1.253133
H	-4.138254	-0.880154	-1.884614
H	1.047997	-1.583703	-0.090994
H	2.779316	0.182208	-0.215620
H	-1.213814	-0.082902	3.195107
H	-0.626324	1.201836	2.132109
H	0.389883	-0.210105	2.441874

TSB2

C	0.641326	-0.076488	0.213283
C	-0.813761	-0.422412	0.125423
C	-1.774438	0.491219	0.066926
C	-1.470235	1.931065	0.122692
C	-0.069772	2.301015	0.377059
C	0.893842	1.389252	0.435110
O	1.246086	-0.874483	1.105432
O	-2.337847	2.766086	-0.009659
N	1.246576	-0.353413	-1.189612
H	0.122832	3.350684	0.537619
H	1.920229	1.647622	0.658208
C	1.221132	-1.767322	-1.577186
H	0.760261	0.216063	-1.872105
H	2.293706	-0.031094	-1.172372
H	2.256085	-0.525529	1.321679
O	3.484068	0.002971	1.370009
O	3.734673	0.188342	-0.990676
H	3.778353	0.108477	0.123242
H	4.194107	0.965928	-1.293912
H	4.111845	-0.465876	1.911510
H	-1.035655	-1.479879	0.137076
H	-2.819253	0.227505	0.008057
H	1.893778	-1.911378	-2.414657
H	0.216745	-2.072447	-1.848917
H	1.567667	-2.342784	-0.727058

TSB3

C	-0.674615	-0.243754	-0.225184
C	0.793638	-0.527005	-0.151903
C	1.726997	0.409003	-0.260275
C	1.371969	1.824678	-0.450282
C	-0.058122	2.137731	-0.590894
C	-0.993374	1.202071	-0.480764
O	-1.235767	-1.098127	-1.098937
O	2.220472	2.688183	-0.497965
N	-1.277584	-0.569998	1.157336
H	-0.300152	3.169410	-0.795457
H	-2.044513	1.433184	-0.581436
H	-1.229859	-1.581644	1.216156
C	-0.676668	0.068727	2.329216
H	-2.341651	-0.307440	1.117405
H	-2.289205	-0.857120	-1.313110
O	-3.566970	-0.567556	-1.345552
O	-3.711529	0.191951	0.898906
H	-3.802535	-0.119697	-0.175529
H	-4.457089	-0.124839	1.400791
H	-3.898355	-0.088341	-2.098380
H	1.047834	-1.574245	-0.054664
H	2.781388	0.179713	-0.241428
H	-1.247411	-0.201930	3.210546
H	-0.721073	1.143631	2.196023
H	0.356165	-0.237736	2.446848

TSB4

C	-0.674495	-0.259157	-0.221400
C	0.795113	-0.536940	-0.165198
C	1.721280	0.407738	-0.257145
C	1.353914	1.824067	-0.423967
C	-0.076013	2.123909	-0.586768
C	-1.005763	1.180432	-0.495205
O	-1.255907	-1.128699	-1.068083
O	2.195894	2.695269	-0.441043
N	-1.246906	-0.573721	1.179041
H	-0.324160	3.152076	-0.801138
H	-2.055828	1.396546	-0.637485
H	-1.142448	-1.578452	1.269193
C	-0.675580	0.131179	2.327335
H	-2.322603	-0.376658	1.138580
H	-2.273460	-0.819255	-1.320272
O	-3.502440	-0.319731	-1.411909
O	-3.716997	0.049573	0.926828
H	-3.797438	-0.139084	-0.170879
H	-4.468339	-0.297679	1.397800
H	-4.120917	-0.787183	-1.964117
H	1.055804	-1.583827	-0.081625
H	2.777561	0.187018	-0.239850
H	-1.197354	-0.177911	3.226216
H	-0.818982	1.195729	2.184174
H	0.383066	-0.082208	2.420291

TSB5

C	-0.645534	-0.072301	-0.195143
C	0.807290	-0.425135	-0.094294
C	1.778374	0.479002	-0.076451
C	1.490023	1.919237	-0.174438
C	0.085403	2.299673	-0.384037
C	-0.888683	1.397706	-0.399242
O	-1.228436	-0.864334	-1.106208
O	2.371583	2.746940	-0.101695
N	-1.277853	-0.359136	1.194433
H	-0.105080	3.351429	-0.532709
H	-1.921685	1.677337	-0.550539
C	-1.292752	-1.779883	1.552742
H	-0.785951	0.186069	1.892772
H	-2.312099	0.006434	1.167787
H	-2.268825	-0.582743	-1.305642
O	-3.546353	-0.252664	-1.319484
O	-3.664460	0.528384	0.918350
H	-3.763836	0.207261	-0.156901
H	-4.428049	0.264456	1.423277
H	-3.875438	0.235624	-2.067561
H	1.020427	-1.484420	-0.081663
H	2.820818	0.204766	-0.023940
H	-1.948911	-1.921632	2.404188
H	-0.294682	-2.123895	1.799788
H	-1.671455	-2.328050	0.698246

RC1

C	3.361005	0.423372	0.462740
C	2.128641	1.173635	0.166079
C	1.016599	0.563149	-0.240417
C	0.987997	-0.900997	-0.398262
C	2.219424	-1.658612	-0.110640
C	3.327029	-1.042309	0.292098
O	4.368540	0.982780	0.832580
O	-0.015936	-1.487106	-0.752044
H	2.182384	2.243641	0.296087
H	0.109603	1.110379	-0.464980
H	2.159055	-2.727663	-0.245583
H	4.243486	-1.568080	0.512099
N	-4.566476	-0.665640	0.638070
C	-4.060167	0.160023	1.721806
H	-3.160773	-0.295215	2.126028
H	-3.778589	1.132597	1.329144
H	-4.766310	0.306449	2.540476
H	-4.794784	-1.591423	0.962564
O	-2.636693	-0.308673	-1.409567
H	-3.294533	-0.563461	-0.738541
H	-5.411285	-0.273949	0.253083
O	-1.725844	2.211731	-0.944998
H	-2.141557	1.362698	-1.178604
H	-1.889536	2.803919	-1.672781
H	-1.846596	-0.829763	-1.248344

RC2

C	2.301479	-0.771977	-0.442413
C	1.058362	-0.616142	-1.218706
C	0.250590	0.421048	-1.023465
C	0.571198	1.441805	-0.014042
C	1.851209	1.338087	0.699930
C	2.656911	0.299451	0.505270
O	3.021389	-1.731998	-0.600230
O	-0.190185	2.365614	0.211004
H	0.849385	-1.394134	-1.936762
H	-0.673346	0.555214	-1.566432
H	2.071948	2.132347	1.395876
H	3.593023	0.177914	1.027900
H	-3.401800	2.416815	-0.809539
O	-2.762120	1.720607	-0.692464
H	-1.950509	2.132657	-0.368017
H	-0.093180	-1.138243	2.609165
O	-0.105937	-0.920767	1.681776
H	-1.037376	-0.995182	1.392293
H	-2.880830	-0.119945	0.242907
N	-2.742250	-1.031150	0.663107
H	-3.457429	-1.141157	1.364364
C	-2.850155	-2.076605	-0.336960
H	-2.061873	-1.948991	-1.073789
H	-2.700165	-3.047397	0.127697
H	-3.804837	-2.093501	-0.865785

RC3

C	2.282735	-0.738686	-0.464267
C	1.024688	-0.588267	-1.217727
C	0.213972	0.443381	-1.005481
C	0.545623	1.463657	0.000457
C	1.833133	1.359758	0.700229
C	2.641450	0.326202	0.489639
O	3.011524	-1.687229	-0.646792
O	-0.215536	2.384534	0.238185
H	0.808766	-1.364570	-1.935562
H	-0.718705	0.573668	-1.534593
H	2.058227	2.150191	1.399108
H	3.583888	0.206006	1.001044
H	-3.483801	2.394923	-0.650930
O	-2.792246	1.739794	-0.645339
H	-1.987487	2.175771	-0.336292
H	-0.008304	-1.358073	2.584101
O	-0.036662	-1.055997	1.681169
H	-0.971616	-1.107465	1.399624
H	-2.708187	-0.138566	0.222038
N	-2.667020	-1.057081	0.646535
H	-3.418561	-1.098178	1.316194
C	-2.823742	-2.091192	-0.358245
H	-1.988321	-2.045351	-1.051907
H	-2.794234	-3.070006	0.112883
H	-3.746303	-2.016724	-0.936870

RC4

C	0.098415	-1.048146	-0.535095
C	0.026376	-0.649232	0.881017
C	-1.135449	-0.321687	1.441664
C	-2.379957	-0.277500	0.656680
C	-2.291444	-0.607215	-0.776055
C	-1.132042	-0.943280	-1.335744
O	1.099556	-1.563549	-1.001884
O	-3.436646	0.027541	1.166705
H	0.951404	-0.675655	1.437023
H	-1.223175	-0.059094	2.484716
H	-3.214361	-0.554398	-1.332962
H	-1.037983	-1.195997	-2.380707
H	3.422642	1.875502	1.464859
O	2.983500	1.473101	0.721921
H	3.288749	0.555921	0.670889
H	2.671000	-1.479516	-0.110875
O	3.429084	-1.243812	0.446593
H	4.195164	-1.668448	0.071364
H	0.756117	1.624172	-1.958862
N	0.480984	1.535363	-0.994430
H	1.301753	1.686330	-0.421778
C	-0.587061	2.442737	-0.658808
H	-1.460290	2.232099	-1.273063
H	-0.875089	2.290645	0.379712
H	-0.339797	3.500593	-0.777939

TSA1

C	1.071066	-1.209735	-0.476765
C	0.419270	-0.123591	-0.933134
C	-1.020074	0.066143	-0.668884
C	-1.685708	-0.983332	0.210549
C	-1.015010	-2.256504	0.341927
C	0.290026	-2.336271	0.040366
O	2.368062	-1.322364	-0.413727
O	-2.728213	-0.691861	0.765295
H	0.979527	0.691062	-1.365386
H	-1.616991	0.079009	-1.588632
H	-1.559404	-3.066310	0.800240
H	0.845712	-3.243955	0.227911
H	2.725009	-0.285561	-0.153447
N	-1.240177	1.372517	0.006469
H	-2.093867	1.268210	0.554380
H	-0.367191	1.554031	0.669078
O	2.842079	0.937579	0.219722
H	3.705660	1.176859	0.541230
H	1.820727	1.469305	0.837415
O	0.894291	1.889012	1.291113
H	0.967714	1.825883	2.239457
C	-1.338763	2.514681	-0.903642
H	-1.456944	3.420257	-0.320334
H	-0.420561	2.587762	-1.474824
H	-2.182743	2.388556	-1.574102

TSA2

C	1.154795	-1.127500	-0.508454
C	0.412258	-0.090035	-0.939636
C	-1.033310	-0.013265	-0.648633
C	-1.593768	-1.104842	0.252144
C	-0.830643	-2.326854	0.357472
C	0.467945	-2.310446	0.020170
O	2.456418	-1.148100	-0.476797
O	-2.636830	-0.888177	0.839146
H	0.894521	0.768005	-1.381661
H	-1.644906	-0.066451	-1.557696
H	-1.301365	-3.174856	0.828135
H	1.093532	-3.175491	0.187863
H	2.756008	-0.108329	-0.110200
N	-1.351336	1.279109	0.011592
H	-2.161391	1.099972	0.604864
H	-0.463942	1.571140	0.624424
O	2.835386	1.030238	0.421760
H	3.502672	1.602967	0.057430
H	1.751531	1.595805	0.808722
O	0.777065	2.043729	1.152024
H	0.851131	2.233244	2.083477
C	-1.618822	2.378920	-0.915378
H	-1.793843	3.285203	-0.347470
H	-0.748069	2.526613	-1.543811
H	-2.483568	2.151028	-1.530390

TSA3

C	1.200683	-1.129508	-0.361783
C	0.506232	-0.301910	-1.168498
C	-0.926106	-0.021607	-0.926698
C	-1.643470	-0.964136	0.036849
C	-0.846768	-1.933920	0.761868
C	0.472827	-2.013459	0.553540
O	2.500561	-1.168970	-0.279138
O	-2.847340	-0.873537	0.156169
H	1.043998	0.343948	-1.847475
H	-1.530691	-0.017230	-1.834469
H	-1.371739	-2.581436	1.446229
H	1.079806	-2.730070	1.087883
H	2.820180	-0.077075	-0.240775
N	-0.976783	1.383765	-0.383271
H	-0.604124	1.963782	-1.126245
H	-0.189979	1.507501	0.411860
O	2.879625	1.176873	-0.077806
H	3.735888	1.493281	0.193775
H	1.892235	1.558329	0.646535
O	0.941789	1.827765	1.190711
H	0.997433	1.515224	2.089651
C	-2.274263	1.935046	0.027479
H	-3.012249	1.795174	-0.754590
H	-2.620155	1.431840	0.919586
H	-2.135004	2.990292	0.234907

TSA4

C	-1.226906	-1.107830	0.404895
C	-0.481416	-0.302954	1.189153
C	0.955426	-0.070628	0.917108
C	1.609180	-1.006687	-0.097779
C	0.762580	-1.944673	-0.805424
C	-0.549751	-1.994648	-0.549098
O	-2.527530	-1.130238	0.376879
O	2.809465	-0.940774	-0.263773
H	-0.971087	0.334015	1.912017
H	1.580827	-0.134917	1.809123
H	1.245126	-2.591749	-1.520758
H	-1.194386	-2.687183	-1.070740
H	-2.855550	-0.036225	0.168995
N	1.056713	1.351646	0.435209
H	0.747534	1.913670	1.219270
H	0.236760	1.563488	-0.326887
O	-2.968104	1.126508	-0.215202
H	-3.500934	1.694443	0.332067
H	-1.893575	1.611134	-0.634599
O	-0.880135	1.982107	-1.018614
H	-0.893892	2.008664	-1.971272
C	2.362854	1.860258	-0.001591
H	3.124087	1.651068	0.741846
H	2.650735	1.384508	-0.928648
H	2.265990	2.929712	-0.154780

Cartesian coordinates of basic reaction pathway

BR1

H	-2.635381	-0.920677	-1.510100
O	-2.930677	-0.833381	-0.609112
H	-2.234746	-0.181075	-0.199198
H	-1.535646	1.610778	0.441002
O	-1.170937	0.748555	0.259800
H	0.541464	0.537045	0.649499
H	1.518252	-0.515779	1.416993
N	1.535805	0.273752	0.790232
C	2.089078	-0.134082	-0.476178
H	1.562587	-0.962338	-0.967831
H	2.056763	0.708151	-1.165468
H	3.138208	-0.423478	-0.372651

BR2

H	0.523947	-0.945776	0.653053
O	-1.332514	1.261410	-0.161238
H	-1.450281	1.742985	-0.975412
H	-1.620029	-0.135663	-0.308906
O	-1.809954	-1.175061	-0.321599
H	-2.545224	-1.280371	0.274177
C	2.007348	-0.066458	-0.373759
H	2.737186	-0.872191	-0.269819
H	1.558152	-0.153370	-1.371357
H	2.567313	0.869223	-0.353336

BR3

H	-0.489641	1.782364	-0.109334
N	1.193799	-0.063899	0.893928
H	1.605690	-0.664963	1.590555
H	0.244432	-0.429870	0.695835
O	-1.143654	1.551774	-0.765631
H	-1.294055	0.561983	-0.566175
O	-1.280429	-0.915721	-0.088897
H	-2.063925	-1.121445	0.414047
C	1.958364	-0.131644	-0.328907
H	2.114496	-1.145331	-0.719235
H	1.423616	0.421111	-1.097699
H	2.939861	0.333282	-0.204939

BR4

N	1.182613	-0.099752	-0.712408
H	0.468483	0.618178	-0.542539
H	0.607541	-0.944000	-0.713561
O	-1.171096	1.281469	0.137215
H	-1.727792	1.931447	-0.282622
H	-1.497884	-0.114960	-0.013433
O	-1.818057	-1.100305	0.002844
H	-1.928739	-1.262420	0.934524
C	2.099111	-0.110949	0.398682
H	1.631045	-0.250520	1.382303
H	2.847002	-0.897584	0.273492
H	2.640606	0.834505	0.436123

BPA1

C	-0.556675	-0.576337	0.640672
C	-0.656891	0.931360	0.491528
C	0.381810	1.593827	-0.283235
C	1.537354	0.953997	-0.503086
C	1.861984	-0.429759	-0.044648
C	0.825876	-1.113355	0.547298
H	0.205507	2.617953	-0.582994
H	2.349122	1.442945	-1.027812
H	0.979783	-2.138256	0.852073
O	3.050523	-0.807041	-0.247317
O	-1.611427	1.543135	0.945865
N	-1.414924	-1.205093	-0.381028
H	-1.026856	-0.807522	1.600759
C	-2.784529	-0.769927	-0.466770
H	-2.934311	0.270130	-0.775559
H	-3.249430	-0.871923	0.512791
H	-3.318354	-1.418436	-1.161410
H	-0.934564	-1.162858	-1.265993

BPA2

C	-0.629143	-0.420124	0.731735
C	-0.546311	1.089632	0.617791
C	0.604826	1.641403	-0.081740
C	1.667175	0.865267	-0.321633
C	1.795871	-0.571868	0.065701
C	0.666960	-1.135277	0.612738
H	0.572450	2.692545	-0.333197
H	2.548376	1.269356	-0.804624
H	0.698169	-2.169165	0.930550
O	2.927412	-1.093927	-0.130599
O	-1.439313	1.798501	1.053193
N	-1.566688	-0.807881	-0.341326
H	-1.106091	-0.625886	1.701264
C	-2.953673	-0.781742	0.033436
H	-3.567361	-1.123277	-0.799057
H	-3.246307	0.237457	0.273344
H	-3.184742	-1.402072	0.913315
H	-1.276246	-1.710419	-0.677197

BPB1

C	0.000000	0.000000	0.000000
C	0.000000	0.000000	1.499820
C	1.104778	0.000000	2.233527
C	2.438122	0.009102	1.610550
C	2.485234	-0.096204	0.145034
C	1.372599	-0.157287	-0.576305
O	-0.756822	-1.068503	-0.496969
O	3.447697	0.082641	2.277267
H	-0.980049	0.010905	1.958433
H	1.083289	-0.000906	3.312453
H	3.467348	-0.154690	-0.298187
H	1.401138	-0.277092	-1.651122
N	-0.637058	1.219357	-0.463390
C	-0.094624	2.466036	0.033906
H	-0.572204	3.284716	-0.494682
H	0.988219	2.556561	-0.089809
H	-0.323282	2.574862	1.089743
H	-0.628360	1.207781	-1.472776

BPA3

C	-0.603038	-0.427536	0.227885
C	-0.563248	1.068185	-0.019554
C	0.717353	1.706908	0.232643
C	1.837278	0.967003	0.194778
C	1.902329	-0.501820	-0.029438
C	0.677487	-1.127881	-0.084094
H	0.733273	2.786802	0.289463
H	2.807164	1.441511	0.284990
H	0.623463	-2.203636	-0.157394
O	3.057192	-1.001218	-0.152782
O	-1.542241	1.695604	-0.393887
N	-1.754243	-1.089196	-0.351038
H	-1.808054	-0.841993	-1.326519
H	-0.770356	-0.455952	1.323898
C	-3.010675	-0.827373	0.307354
H	-3.802267	-1.374558	-0.203970
H	-3.289924	0.227412	0.354071
H	-2.960716	-1.214628	1.325888

BPB2

C	-0.019133	0.003299	0.020393
C	-0.022507	-0.084427	1.525961
C	1.065304	-0.124715	2.298999
C	2.409764	-0.056388	1.724302
C	2.501863	-0.003674	0.265693
C	1.402790	0.054939	-0.491046
O	-0.621957	-1.046198	-0.518942
O	3.411160	-0.072289	2.431597
H	-1.017975	-0.159806	1.942019
H	1.018254	-0.244999	3.372750
H	3.500437	-0.047688	-0.147381
H	1.471114	0.066472	-1.572501
N	-0.742956	1.260072	-0.316110
C	-0.011467	2.494881	-0.209135
H	-0.680669	3.341200	-0.368335
H	0.838555	2.600910	-0.896459
H	0.389290	2.582641	0.800811
H	-1.100004	1.090875	-1.245124

BPA4

C	-1.557580	-0.731763	-0.094595
C	-0.335066	-0.986462	-0.674884
C	0.809140	-0.037665	-0.570687
C	0.398605	1.408324	-0.368669
C	-0.819495	1.623660	0.406784
C	-1.704369	0.625768	0.517379
O	-2.577806	-1.471372	-0.029839
O	1.060512	2.332975	-0.798328
H	-0.172596	-1.949065	-1.138589
H	1.429052	-0.040906	-1.468869
H	-1.000547	2.619476	0.787085
H	-2.644515	0.774683	1.034251
N	1.749358	-0.314262	0.548294
C	2.501592	-1.522550	0.318724
H	3.125378	-1.736985	1.185370
H	1.877760	-2.400937	0.115915
H	3.164681	-1.374366	-0.533411
H	1.165834	-0.460871	1.360723

BPB3

C	0.027558	-0.001168	-0.064854
C	-0.020737	-0.016339	1.441057
C	1.042781	-0.069149	2.246535
C	2.404120	-0.060693	1.710110
C	2.539027	-0.054878	0.253743
C	1.463275	-0.013547	-0.538162
O	-0.614674	-1.041437	-0.565035
O	3.384491	-0.078382	2.446157
H	-1.029538	-0.036354	1.830013
H	0.960663	-0.144085	3.322195
H	3.549371	-0.117390	-0.127276
H	1.568243	-0.045706	-1.615593
N	-0.594872	1.311316	-0.455561
C	-0.960331	1.357458	-1.847025
H	-1.641368	2.189620	-2.029747
H	-1.466773	0.421198	-2.067164
H	-0.116888	1.453041	-2.546598
H	0.031905	2.067075	-0.217885

BRC1

C	-2.418501	0.595403	0.318707
C	-1.047166	0.943453	-0.069677
C	-0.189672	0.020573	-0.519946
C	-0.600870	-1.386819	-0.632006
C	-1.980252	-1.746023	-0.230127
C	-2.827566	-0.822514	0.211123
O	-3.218264	1.417446	0.722174
O	0.140476	-2.258873	-1.039535
H	-0.729185	1.975298	0.025614
H	0.832624	0.307124	-0.796213
H	-2.243018	-2.789778	-0.321774
H	-3.840868	-1.047498	0.510154
N	3.159979	-1.242491	0.268094
C	2.601683	-1.312383	1.594312
H	2.697808	-2.321009	1.999686
H	3.154108	-0.647099	2.256047
H	1.543434	-1.027629	1.670384
H	2.620983	-1.828594	-0.350636
O	2.448811	1.367593	-0.815215
H	2.991274	1.589814	-1.567299
H	3.054591	-0.289620	-0.097298
O	1.057442	3.316499	-0.065418
H	1.657186	2.538137	-0.404745
H	1.487000	3.621951	0.727353

BRC2

C	-2.235651	0.279828	-0.763491
C	-1.084898	0.877476	-0.082226
C	-0.289690	0.150460	0.707999
C	-0.566247	-1.273782	0.948539
C	-1.667499	-1.901730	0.185559
C	-2.453992	-1.174522	-0.600385
O	-3.003920	0.924347	-1.452600
O	0.042055	-1.932533	1.767539
H	-0.869949	1.924223	-0.254080
H	0.597531	0.584613	1.165605
H	-1.804076	-2.962585	0.335513
H	-3.284984	-1.592007	-1.149939
N	2.336435	-1.034519	-0.398822
C	3.461653	-1.257567	-1.267389
H	3.435105	-2.265698	-1.685092
H	3.409451	-0.563731	-2.104538
H	4.448003	-1.121907	-0.802171
H	2.369657	-1.653359	0.396220
H	2.357849	-0.075500	-0.023011
O	2.306513	1.571125	0.815806
H	3.153070	1.848584	1.154861
O	0.753101	3.500541	0.320498
H	1.433422	2.741809	0.482637
H	0.577296	3.844889	1.190691

BRC3

C	-4.088975	0.736036	0.708585
N	-3.146077	0.503682	-0.361066
H	-3.618836	0.577780	-1.249517
H	-4.600284	1.704556	0.655955
H	-4.850002	-0.044939	0.740622
H	-3.557270	0.709127	1.657258
H	-2.424168	1.275650	-0.349702
O	-1.273156	2.457290	-0.271355
H	-1.607667	3.349254	-0.228480
H	-2.742993	-1.333579	-0.300477
O	-2.622864	-2.304548	-0.266386
H	-1.681653	-2.446842	-0.166478
O	0.469826	-2.493782	0.030241
C	1.080105	-1.439781	0.030939
C	0.418584	-0.138553	-0.055971
C	1.104026	1.008751	-0.058162
C	2.570616	0.992985	0.031931
C	3.249591	-0.322447	0.122500
C	2.556084	-1.456108	0.122604
O	3.244599	2.003759	0.036322
H	-0.660487	-0.114716	-0.121137
H	0.518201	1.936822	-0.128854
H	4.327576	-0.294317	0.187528
H	3.017909	-2.430325	0.187193

BPCA1

C	0.658503	-1.225931	-0.358599
C	0.189786	0.045454	-0.547914
C	-1.277938	0.358933	-0.569987
C	-2.102187	-0.596573	0.251110
C	-1.636185	-1.977119	0.262225
C	-0.346399	-2.240895	0.013286
O	1.863758	-1.641134	-0.468398
O	-3.089424	-0.242771	0.869040
H	0.864517	0.780106	-0.962852
H	-1.638278	0.123278	-1.592669
H	-2.324661	-2.727310	0.623300
H	0.040257	-3.247166	0.109353
N	-1.699875	1.712083	-0.287683
C	-0.801246	2.759651	-0.689376
H	-1.279457	3.721037	-0.509025
H	0.169529	2.758831	-0.185332
H	-0.616461	2.687159	-1.761458
H	-1.968494	1.784940	0.679915
H	2.891387	1.188672	0.928499
O	2.244534	1.638211	1.492097
H	1.428576	1.174250	1.298319
O	3.823418	0.014144	-0.224878
H	3.050176	-0.602963	-0.397328
H	4.437747	-0.514135	0.275702

BPCA2

C	0.716588	-0.299201	-0.075313
C	-0.177233	0.650715	-0.463959
C	-1.611060	0.354290	-0.728906
C	-2.119597	-0.977220	-0.195787
C	-1.126982	-1.986142	0.109905
C	0.169964	-1.645150	0.179801
O	1.980977	-0.162797	0.103677
O	-3.319934	-1.171114	-0.076138
H	0.165910	1.644045	-0.714612
H	-1.734851	0.215617	-1.815772
H	-1.480252	-2.975139	0.364171
H	0.910533	-2.381716	0.464341
N	-2.492198	1.452601	-0.372853
C	-2.458426	1.753743	1.041263
H	-3.140266	2.575865	1.249974
H	-2.735105	0.906404	1.678956
H	-1.452959	2.063065	1.314065
H	-3.428246	1.160699	-0.612512
O	3.705785	1.796996	-0.247332
H	2.965437	1.143052	-0.196941
O	4.613692	-1.050373	0.143633
H	3.646622	-1.042950	0.182856
H	3.695370	2.227907	0.601948
H	4.795700	-0.135270	-0.075719

BPCA3

C	0.865740	-0.136176	-0.157705
C	-0.090868	0.802151	-0.385503
C	-1.525880	0.462579	-0.581058
C	-1.935301	-0.940322	-0.155820
C	-0.879930	-1.921443	-0.018997
C	0.404270	-1.527953	-0.000911
O	2.137590	0.059221	-0.060982
O	-3.115227	-1.205605	0.019100
H	0.189707	1.835555	-0.530350
H	-1.722071	0.427162	-1.665488
H	-1.170626	-2.946566	0.160276
H	1.190338	-2.254137	0.165023
N	-2.424616	1.473681	-0.053698
C	-2.290155	1.640411	1.376963
H	-2.994356	2.396820	1.717809
H	-2.469979	0.720901	1.945663
H	-1.283541	1.982040	1.602335
H	-3.362023	1.153850	-0.248612
H	2.979754	2.575861	-1.450262
O	3.147730	2.506874	-0.515428
H	2.783675	1.624179	-0.276836
H	3.171517	-1.218491	0.239585
O	3.760279	-1.971359	0.488159
H	4.296088	-1.627842	1.196229

BPCA4

C	0.758651	-1.416815	-0.420045
C	0.340115	-0.153026	-0.707649
C	-1.062944	0.301663	-0.523535
C	-1.959569	-0.619310	0.272651
C	-1.540736	-2.000330	0.380778
C	-0.278331	-2.342397	0.072729
O	1.951239	-1.880346	-0.507587
O	-3.002533	-0.201636	0.753861
H	1.044865	0.553915	-1.121291
H	-1.571001	0.274304	-1.515293
H	-2.245153	-2.699001	0.808445
H	0.060868	-3.360347	0.217377
N	-1.164219	1.637172	0.030046
C	-0.860046	2.680484	-0.914616
H	-1.085069	3.646668	-0.468235
H	0.203256	2.677246	-1.147803
H	-1.419914	2.589152	-1.857997
H	2.284873	1.508338	0.849512
O	1.695198	2.197629	1.184809
H	0.805300	1.859373	1.049887
O	3.468599	0.124642	0.176428
H	3.961026	-0.221716	0.916051
H	2.929207	-0.650346	-0.154949
H	-2.101607	1.738283	0.392006

BPCB1

C	-0.264497	-0.040627	0.183021
C	0.538323	1.221370	0.008667
C	1.867366	1.290407	0.060822
C	2.684720	0.091257	0.266624
C	1.969325	-1.168052	0.485002
C	0.638435	-1.219048	0.440962
O	-1.115511	0.093146	1.216278
O	3.906079	0.144218	0.276695
H	-0.072748	2.104285	-0.128204
H	2.408057	2.222396	-0.022636
H	2.582557	-2.029169	0.709705
H	0.107271	-2.144198	0.629023
N	-1.017450	-0.241901	-1.081381
C	-0.254019	-0.615845	-2.246661
H	-0.914952	-0.672687	-3.109943
H	0.277624	-1.570196	-2.160347
H	0.492224	0.149734	-2.453245
H	-1.737214	-0.922279	-0.870651
H	-2.311445	1.321675	0.689685
O	-2.911632	1.760390	0.050628
H	-2.545964	1.409502	-0.764710
H	-3.830725	-0.475325	0.479925
O	-3.366059	-1.268368	0.745959
H	-2.512151	-0.898312	1.069604

BPCB2

C	0.174154	0.002477	-0.359263
C	-0.892115	-0.709258	-1.148416
C	-2.144626	-0.904069	-0.738180
C	-2.599110	-0.422800	0.568956
C	-1.597011	0.220704	1.421819
C	-0.347655	0.408967	0.997790
O	1.247188	-0.799052	-0.211376
O	-3.754766	-0.573083	0.939596
H	-0.539867	-1.074601	-2.102942
H	-2.876355	-1.441346	-1.324835
H	-1.927904	0.503452	2.411185
H	0.397688	0.858978	1.642549
N	0.540698	1.192611	-1.149067
C	-0.359275	2.314549	-1.124784
H	-0.025155	3.063059	-1.841735
H	-0.471364	2.802881	-0.148870
H	-1.352088	1.987092	-1.432615
H	1.483697	1.439288	-0.884282
H	2.839668	-0.191122	-0.919506
O	3.708161	0.245905	-0.856388
H	3.886836	0.163433	0.081685
O	2.778872	-0.548588	1.852237
H	2.123793	-0.666321	1.100364
H	2.887141	-1.416691	2.227793

BPCB3

C	0.254225	-0.047468	-0.358142
C	-0.675142	-0.964801	-1.107165
C	-1.956319	-1.168661	-0.803754
C	-2.585157	-0.489254	0.331917
C	-1.723623	0.368335	1.149216
C	-0.443625	0.563025	0.833249
O	1.340195	-0.730975	0.053207
O	-3.767772	-0.649900	0.598587
H	-0.195061	-1.473132	-1.931663
H	-2.586377	-1.854339	-1.352507
H	-2.182600	0.803557	2.025688
H	0.197338	1.174733	1.456740
N	0.652862	1.000632	-1.315816
C	-0.297509	2.042012	-1.601488
H	0.081977	2.668133	-2.407642
H	-0.547956	2.691727	-0.753793
H	-1.229738	1.594806	-1.945902
H	1.544730	1.357244	-1.003396
H	2.973538	-0.152706	-0.583046
O	3.806034	0.348388	-0.511568
H	3.876380	0.451880	0.438720
O	2.603069	0.000159	2.183437
H	2.708549	-0.774689	2.726438
H	2.048024	-0.299004	1.401945

BPCB4

C	0.046811	0.364731	-0.084576
C	-0.841801	0.706559	-1.250661
C	-2.075662	0.239693	-1.428697
C	-2.710640	-0.637886	-0.443737
C	-1.892789	-1.036823	0.700943
C	-0.659541	-0.563735	0.867062
O	1.172767	-0.218442	-0.554395
O	-3.859707	-1.031740	-0.584743
H	-0.372392	1.319400	-2.008350
H	-2.659440	0.460958	-2.310683
H	-2.342328	-1.740172	1.386436
H	-0.053327	-0.884174	1.705764
N	0.278323	1.599473	0.692017
C	0.983586	2.621292	-0.051209
H	1.389386	3.351204	0.645423
H	0.296889	3.151015	-0.710197
H	1.805238	2.221165	-0.652148
H	0.875368	1.320049	1.458598
H	1.734010	-1.942114	-0.106647
O	2.302806	-2.584693	0.351094
H	2.901220	-2.001922	0.819236
O	3.221785	0.226554	0.939692
H	2.429683	0.089037	0.331747
H	3.919543	0.551926	0.379271

Cartesian coordinates of acidic reaction pathway

AR1

N	2.931897	-0.093894	0.295398
C	3.271552	-0.664568	1.615965
H	2.898208	-1.678875	1.673885
H	4.348186	-0.662093	1.726474
H	2.823933	-0.060096	2.394386
H	1.927875	-0.053052	0.162908
H	3.322315	-0.671230	-0.466486
H	3.297738	0.867375	0.199187
O	3.948510	2.502050	0.101162
H	4.427710	2.864414	-0.642616
H	3.849227	3.213300	0.732356
O	3.979423	-1.746203	-1.708315
H	3.516770	-2.070899	-2.479564
H	4.860522	-2.115442	-1.746251

AR2

H	3.214821	-0.697245	-0.062587
O	2.303529	-0.984215	-0.100239
H	2.320624	-1.909046	-0.343108
H	-2.847146	-1.444538	0.535430
O	-2.293360	-0.981860	-0.092329
H	-2.699434	-1.097065	-0.949930
H	0.858335	-0.046091	0.269707
N	0.010935	0.503994	0.489168
H	0.014881	0.685868	1.486267
C	-0.019932	1.764711	-0.281937
H	0.004811	1.524849	-1.337053
H	-0.928522	2.304675	-0.048379
H	0.843689	2.364443	-0.024643
H	-0.820362	-0.073480	0.282300

AR3

C	-2.203942	-1.032808	-0.531681
N	-1.412382	-0.512963	0.606162
H	-1.769997	0.381329	0.924268
H	-1.443192	-1.144800	1.398925
H	-3.238735	-1.147640	-0.235491
H	-1.795316	-1.989810	-0.829188
H	-2.126060	-0.332839	-1.353351
O	1.104709	-0.120920	-0.121381
H	-0.399761	-0.375612	0.336341
O	2.251876	2.305378	0.146264
H	1.560408	0.737594	-0.040906
H	1.738479	-0.759199	-0.441291
H	2.837963	2.556830	0.857754
H	2.417791	2.909107	-0.575489

APA1

C	-0.718249	-0.090446	0.338236
C	-0.436919	1.303928	-0.221368
C	0.936772	1.758291	-0.204152
C	1.912450	0.857293	-0.054614
C	1.653187	-0.565223	0.157477
C	0.411374	-1.047293	0.302948
H	1.128808	2.796358	-0.420903
H	2.952283	1.142092	-0.111562
H	0.235441	-2.083726	0.551397
O	2.777402	-1.269492	0.202974
O	-1.376195	1.932167	-0.653249
N	-1.929195	-0.559784	-0.395285
H	-2.423626	0.310750	-0.641485
H	2.627262	-2.202942	0.354595
H	-1.049300	0.074140	1.369098
C	-2.807022	-1.497028	0.336089
H	-3.642714	-1.763579	-0.299376
H	-3.167048	-1.005600	1.231652
H	-2.245701	-2.385427	0.597922
H	-1.630667	-0.975135	-1.274571

APA2

C	-0.727556	-0.053545	0.338418
C	-0.456299	1.326372	-0.252374
C	0.912212	1.801051	-0.206405
C	1.896793	0.917511	-0.009858
C	1.655026	-0.505715	0.219283
C	0.414541	-0.992326	0.345430
H	1.096265	2.837167	-0.439096
H	2.925013	1.251556	-0.045471
H	0.267546	-2.030533	0.599460
O	2.695915	-1.326897	0.324785
O	-1.387546	1.932482	-0.729255
N	-1.919159	-0.567374	-0.395879
H	-2.431409	0.280585	-0.676845
H	-1.073777	0.134400	1.360954
C	-2.783218	-1.503826	0.354213
H	-3.602354	-1.812403	-0.283703
H	-3.168066	-0.993523	1.228610
H	-2.201284	-2.367458	0.651412
H	-1.599070	-1.004805	-1.256830
H	3.536116	-0.885705	0.207987

APB1

C	-0.272993	-0.082350	-0.270990
C	0.536097	-1.327287	-0.108938
C	1.861949	-1.313234	-0.075359
C	2.623649	-0.049749	-0.169217
C	1.845127	1.186102	-0.397175
C	0.519264	1.173634	-0.430957
O	-1.254850	-0.214406	-1.245265
O	3.822024	-0.028973	-0.070502
H	-0.025264	-2.251973	-0.067461
H	2.443778	-2.218149	0.011398
H	2.414774	2.091102	-0.543462
H	-0.054361	2.071151	-0.624108
N	-1.171666	0.068205	0.945249
C	-0.502700	0.241145	2.253398
H	-1.262804	0.334624	3.019123
H	0.106193	1.135584	2.217914
H	0.118043	-0.624967	2.444603
H	-1.789287	0.853982	0.746966
H	-1.778490	-0.750277	0.953531
H	-0.867367	-0.323860	-2.115579

ARC1

C	-3.885177	0.273274	-0.164640
C	-2.882420	1.184785	-0.755157
C	-1.579165	0.973150	-0.587157
C	-1.099151	-0.173613	0.191546
C	-2.084946	-1.084146	0.782895
C	-3.389545	-0.877344	0.617953
O	-5.065598	0.464227	-0.318054
O	0.096909	-0.372989	0.348686
H	-3.272330	2.016837	-1.321066
H	-0.827585	1.623088	-1.007993
H	-1.692437	-1.914670	1.348632
H	-4.142171	-1.526231	1.038662
N	2.887502	-0.108179	0.289087
C	3.237398	-0.586895	1.638426
H	2.838072	-1.583557	1.773872
H	4.314716	-0.603932	1.743637
H	2.806683	0.078723	2.375467
H	1.867981	-0.077212	0.180184
H	3.266235	-0.739454	-0.426756
H	3.265666	0.831186	0.122779
O	4.025470	2.480348	-0.083444
H	4.428004	2.816085	-0.882433
H	4.092935	3.178077	0.566042
O	3.962805	-1.951257	-1.592935
H	3.455176	-2.557282	-2.129848
H	4.882492	-2.124450	-1.785861

APCA1

C	-0.351065	-0.343527	0.306971
C	0.163620	0.227462	1.400825
C	1.635782	0.378718	1.520156
C	2.438162	0.211746	0.235788
C	1.804737	-0.508554	-0.851290
C	0.488332	-0.738539	-0.817336
O	-1.636046	-0.633257	0.100076
O	3.555105	0.675175	0.178929
H	-0.443524	0.464031	2.263185
H	2.023567	-0.398785	2.187211
H	2.414899	-0.758020	-1.704060
H	-0.018050	-1.217738	-1.641769
N	2.025323	1.664812	2.151423
C	1.661252	2.862393	1.369979
H	1.919069	3.742054	1.946692
H	2.221221	2.860758	0.443283
H	0.596924	2.843942	1.167304
H	3.049967	1.657931	2.307828
H	1.579597	1.712264	3.075647
H	-2.187093	-0.394026	0.844837
O	4.759465	1.515711	2.555273
H	5.128654	1.248265	1.713144
H	5.470967	1.824601	3.111906
O	0.584992	1.657089	4.618488
H	0.790746	1.093817	5.363512
H	0.064120	2.378578	4.968557

APCA2

C	-0.023337	-0.111388	0.047282
C	-0.009136	-0.136093	1.384250
C	1.274600	0.055734	2.105390
C	2.402414	0.669734	1.285511
C	2.331633	0.526329	-0.154855
C	1.172432	0.189438	-0.727638
O	-1.074176	-0.368012	-0.731959
O	3.299080	1.249536	1.859779
H	-0.880491	-0.447704	1.939540
H	1.656468	-0.920143	2.428351
H	3.204049	0.798979	-0.726014
H	1.067794	0.144066	-1.801228
N	1.164072	0.867796	3.343747
C	0.147375	0.427651	4.311151
H	0.265803	1.007838	5.218250
H	-0.844089	0.590934	3.909385
H	0.294676	-0.623387	4.532373
H	1.015055	1.847634	3.063050
H	2.090179	0.830637	3.801913
H	-1.858581	-0.583425	-0.228035
O	1.184069	3.366509	2.109480
H	0.633499	4.140340	2.004006
H	2.080533	3.626773	1.898465
O	3.627691	0.341698	4.493968
H	4.300436	0.651156	3.887280
H	4.044270	0.178084	5.337732

APCA3

C	-0.071615	-0.275486	-0.049904
C	0.134455	0.263137	1.161361
C	1.513364	0.311364	1.696902
C	2.644045	0.112218	0.691221
C	2.323911	-0.574079	-0.540962
C	1.040724	-0.719411	-0.887902
O	-1.247105	-0.490213	-0.617167
O	3.736466	0.549026	0.979302
H	-0.694596	0.509959	1.808185
H	1.650634	-0.483677	2.437455
H	3.138949	-0.858113	-1.186347
H	0.764901	-1.165092	-1.831944
N	1.850655	1.571656	2.416672
C	1.529279	2.808351	1.676039
H	1.835296	3.657823	2.274116
H	2.071562	2.805050	0.738072
H	0.464325	2.840177	1.486636
H	2.867281	1.525848	2.533593
H	1.416031	1.585739	3.349259
H	-1.990352	-0.220903	-0.050046
O	-3.318517	0.253143	1.003431
H	-3.859849	-0.457050	1.345709
H	-3.924525	0.907112	0.657739
O	0.745017	1.563458	5.011731
H	1.208596	1.257056	5.789905
H	-0.064061	1.966867	5.322041

APCA4

C	-1.699595	-0.832599	-0.007840
C	-0.940810	0.265411	0.133515
C	0.519918	0.119181	0.338365
C	1.111391	-1.242498	-0.016733
C	0.210140	-2.376408	-0.026149
C	-1.109346	-2.167420	-0.054187
O	-3.017691	-0.857016	-0.099140
O	2.291484	-1.313559	-0.278117
H	-1.406143	1.230965	0.257722
H	0.773464	0.274551	1.392975
H	0.647452	-3.357543	-0.113994
H	-1.805918	-2.988471	-0.133672
N	1.319919	1.136128	-0.401641
C	1.092568	2.534265	0.008537
H	1.772237	3.169804	-0.545851
H	0.070351	2.821610	-0.199577
H	1.299191	2.619494	1.068643
H	1.126483	1.034069	-1.393914
H	2.329132	0.921391	-0.271820
H	-3.409957	0.031995	-0.044796
O	-4.049416	1.665419	0.084608
H	-4.570011	1.860465	0.862856
H	-4.551973	1.991344	-0.660908
O	4.001255	0.824905	0.149024
H	4.215612	-0.105466	0.075710
H	4.818371	1.317992	0.182251

APCB1

C	-0.023337	-0.111388	0.047282
C	-0.009136	-0.136093	1.384250
C	1.274600	0.055734	2.105390
C	2.402414	0.669734	1.285511
C	2.331633	0.526329	-0.154855
C	1.172432	0.189438	-0.727638
O	-1.074176	-0.368012	-0.731959
O	3.299080	1.249536	1.859779
H	-0.880491	-0.447704	1.939540
H	1.656468	-0.920143	2.428351
H	3.204049	0.798979	-0.726014
H	1.067794	0.144066	-1.801228
N	1.164072	0.867796	3.343747
C	0.147375	0.427651	4.311151
H	0.265803	1.007838	5.218250
H	-0.844089	0.590934	3.909385
H	0.294676	-0.623387	4.532373
H	1.015055	1.847634	3.063050
H	2.090179	0.830637	3.801913
H	-1.858581	-0.583425	-0.228035
O	1.184069	3.366509	2.109480
H	0.633499	4.140340	2.004006
H	2.080533	3.626773	1.898465
O	3.627691	0.341698	4.493968
H	4.300436	0.651156	3.887280
H	4.044270	0.178084	5.337732

Cartesian coordinates of cubic positions

Fig. 5.3

C	1.351136	0.625389	0.123214
C	2.573240	0.014259	-0.138632
C	3.716353	0.782510	-0.255579
C	3.639512	2.156943	-0.111049
C	2.421744	2.767207	0.151569
C	1.276692	2.002578	0.271179
H	4.650365	0.282498	-0.458353
H	4.531799	2.756786	-0.202887
H	2.367920	3.838843	0.263751
H	0.319124	2.454007	0.477979
C	0.133816	-0.186672	0.261792
C	0.233631	-1.659157	0.052889
C	1.431897	-2.227817	-0.186618
C	2.656504	-1.463745	-0.296545
H	1.505046	-3.294941	-0.319309
O	-0.941577	0.310010	0.538173
O	-0.854029	-2.374873	0.141369
O	3.727091	-1.993227	-0.516827
H	-1.723064	-1.892244	0.222085
O	-3.307968	-1.564134	0.268729
H	-3.606579	-1.353930	1.153743
H	-3.510149	-0.752548	-0.247107
O	-3.302835	0.662978	2.119598
H	-3.147805	0.989585	3.001481
H	-2.441482	0.564144	1.703203
N	-3.827650	0.911694	-0.876482
H	-4.089731	1.344793	-0.002979
H	-2.939890	1.307110	-1.142856
C	-4.830680	1.120282	-1.902776
H	-5.023928	2.169303	-2.133726
H	-5.765146	0.665442	-1.587306
H	-4.521452	0.622598	-2.817337

Face 1: H_2O

C	1.071066	-1.209735	-0.476765
C	0.419270	-0.123591	-0.933134
C	-1.020074	0.066143	-0.668884
C	-1.685708	-0.983332	0.210549
C	-1.015010	-2.256504	0.341927
C	0.290026	-2.336271	0.040366
O	2.368062	-1.322364	-0.413727
O	-2.728213	-0.691861	0.765295
H	0.979527	0.691062	-1.365386
H	-1.616991	0.079009	-1.588632
H	-1.559404	-3.066310	0.800240
H	0.845711	-3.243955	0.227911
H	2.725009	-0.285561	-0.153447
N	-1.240177	1.372517	0.006469
H	-2.093867	1.268210	0.554380
H	-0.367191	1.554031	0.669078
O	2.842079	0.937579	0.219722
H	3.705660	1.176858	0.541230
H	1.820727	1.469305	0.837415
O	0.894291	1.889012	1.291113
H	0.967714	1.825883	2.239457
C	-1.338763	2.514681	-0.903642
H	-1.456943	3.420257	-0.320334
H	-0.420561	2.587762	-1.474824
H	-2.182743	2.388556	-1.574102
O	1.719712	0.835450	7.360795
H	0.786985	0.800268	7.167226
H	1.791902	1.075508	8.280494

Face 1: H_3O

C	1.027333	1.560662	0.724973
C	1.513644	0.789242	-0.265599
C	1.749933	-0.652780	-0.059986
C	1.333533	-1.215721	1.291893
C	1.168948	-0.275150	2.376467
C	0.997849	1.024043	2.087948
O	0.527595	2.752717	0.557266
O	1.145884	-2.414054	1.383003
H	1.590370	1.190654	-1.264283
H	2.807915	-0.922772	-0.160940
H	1.061822	-0.671384	3.373324
H	0.766450	1.736856	2.866538
H	0.003267	2.696950	-0.438770
N	1.005575	-1.435779	-1.081751
H	0.817721	-2.345295	-0.660606
H	0.057668	-0.894453	-1.288010
O	-0.568783	2.335148	-1.530049
H	-1.207360	2.953463	-1.871078
H	-0.858591	1.067181	-1.655381
O	-1.013561	-0.032737	-1.735658
H	-1.905135	-0.232224	-1.463568
C	1.706456	-1.584830	-2.358117
H	1.072028	-2.130913	-3.046287
H	1.897725	-0.600636	-2.769775
H	2.642915	-2.113580	-2.212536
O	-6.746721	-0.797456	0.539958
H	-6.610235	0.148609	0.366757
H	-6.392371	-1.382429	-0.149902
H	-6.524700	-1.071325	1.445147

Face 1: HO

C	0.887438	1.595344	0.660223
C	1.372004	0.801470	-0.313316
C	1.650539	-0.625750	-0.062315
C	1.278811	-1.150181	1.317779
C	1.113400	-0.175750	2.371907
C	0.901951	1.107460	2.041632
O	0.353006	2.767491	0.461948
O	1.124744	-2.348857	1.455452
H	1.416244	1.168568	-1.327057
H	2.712778	-0.872163	-0.177811
H	1.038603	-0.538515	3.384334
H	0.669039	1.841660	2.799623
H	-0.191391	2.662642	-0.519253
N	0.904777	-1.463652	-1.038490
H	0.750156	-2.361941	-0.581278
H	-0.061315	-0.954402	-1.242041
O	-0.777532	2.247418	-1.583705
H	-1.439453	2.836618	-1.931696
H	-1.036616	0.968798	-1.657486
O	-1.164366	-0.136884	-1.695273
H	-2.044213	-0.349108	-1.396001
C	1.581175	-1.640564	-2.324472
H	0.946371	-2.226997	-2.978233
H	1.737456	-0.667243	-2.774923
H	2.534165	-2.139723	-2.181728
O	-6.824186	-0.965112	0.736358
H	-7.770489	-1.107248	0.706123

H_{13}: H_3O

C	1.071066	-1.209735	-0.476765
C	0.419270	-0.123591	-0.933134
C	-1.020074	0.066143	-0.668884
C	-1.685708	-0.983332	0.210549
C	-1.015010	-2.256504	0.341927
C	0.290026	-2.336271	0.040366
O	2.368062	-1.322364	-0.413727
O	-2.728213	-0.691861	0.765295
H	0.979527	0.691062	-1.365386
H	-1.616991	0.079009	-1.588632
H	-1.559404	-3.066310	0.800240
H	0.845711	-3.243955	0.227911
H	2.725009	-0.285561	-0.153447
N	-1.240177	1.372517	0.006469
H	-2.093867	1.268210	0.554380
H	-0.367191	1.554031	0.669078
O	2.842079	0.937579	0.219722
H	3.705660	1.176858	0.541230
H	1.820727	1.469305	0.837415
O	0.894291	1.889012	1.291113
H	0.967714	1.825883	2.239457
C	-1.338763	2.514681	-0.903642
H	-1.456943	3.420257	-0.320334
H	-0.420561	2.587762	-1.474824
H	-2.182743	2.388556	-1.574102
O	8.521164	1.264637	-0.192287
H	8.483433	0.463801	-0.740833
H	8.065318	2.031248	-0.577225
H	8.319773	1.112994	0.745855

Cartesian coordinates of special positions

H_{13}: H_2O

C	1.071066	-1.209735	-0.476765
C	0.419270	-0.123591	-0.933134
C	-1.020074	0.066143	-0.668884
C	-1.685708	-0.983332	0.210549
C	-1.015010	-2.256504	0.341927
C	0.290026	-2.336271	0.040366
O	2.368062	-1.322364	-0.413727
O	-2.728213	-0.691861	0.765295
H	0.979527	0.691062	-1.365386
H	-1.616991	0.079009	-1.588632
H	-1.559404	-3.066310	0.800240
H	0.845711	-3.243955	0.227911
H	2.725009	-0.285561	-0.153447
N	-1.240177	1.372517	0.006469
H	-2.093867	1.268210	0.554380
H	-0.367191	1.554031	0.669078
O	2.842079	0.937579	0.219722
H	3.705660	1.176858	0.541230
H	1.820727	1.469305	0.837415
O	0.894291	1.889012	1.291113
H	0.967714	1.825883	2.239457
C	-1.338763	2.514681	-0.903642
H	-1.456943	3.420257	-0.320334
H	-0.420561	2.587762	-1.474824
H	-2.182743	2.388556	-1.574102
O	8.521164	1.264637	-0.192287
H	7.933830	1.823816	0.308755
H	9.391853	1.641167	-0.098417

H_{13}: HO

C	1.071066	-1.209735	-0.476765
C	0.419270	-0.123591	-0.933134
C	-1.020074	0.066143	-0.668884
C	-1.685708	-0.983332	0.210549
C	-1.015010	-2.256504	0.341927
C	0.290026	-2.336271	0.040366
O	2.368062	-1.322364	-0.413727
O	-2.728213	-0.691861	0.765295
H	0.979527	0.691062	-1.365386
H	-1.616991	0.079009	-1.588632
H	-1.559404	-3.066310	0.800240
H	0.845711	-3.243955	0.227911
H	2.725009	-0.285561	-0.153447
N	-1.240177	1.372517	0.006469
H	-2.093867	1.268210	0.554380
H	-0.367191	1.554031	0.669078
O	2.842079	0.937579	0.219722
H	3.705660	1.176858	0.541230
H	1.820727	1.469305	0.837415
O	0.894291	1.889012	1.291113
H	0.967714	1.825883	2.239457
C	-1.338763	2.514681	-0.903642
H	-1.456943	3.420257	-0.320334
H	-0.420561	2.587762	-1.474824
H	-2.182743	2.388556	-1.574102
O	8.521164	1.264637	-0.192287
H	9.446033	1.511993	-0.198487

APPENDIX B

SAMPLE GAUSSIAN INPUT FILES

This appendix includes different sample input files that were used in the calculations of energies of the energy minima and transition states.

A sample input file for reactant complex calculation in gas-phase using Cartesian coordinates system: neutral (**RC1**)

```
# mPWB95/6-31+G(d,p) IOp(3/76=0560004400)
SCF=(Conver=9,MaxCycle=200) Integral=(grid=ultrafine)
OPT=(Verytight,Calcall,Maxcycle=40)

reactant complex neutral v1

0 1
6         3.382804000      0.435179000      0.429216000
6         2.144677000      1.179534000      0.141918000
6         1.029224000      0.563060000     -0.245813000
6         1.003282000     -0.902527000     -0.391999000
6         2.239832000     -1.654517000     -0.111538000
6         3.350668000     -1.032050000      0.272289000
8         4.393395000      1.000486000      0.781370000
8        -0.002823000     -1.495254000     -0.728870000
1         2.196818000      2.250605000      0.263556000
1         0.117680000      1.106948000     -0.460830000
1         2.180306000     -2.724898000     -0.235865000
1         4.270945000     -1.553609000      0.486291000
7        -4.597554000     -0.666374000      0.620380000
6        -4.089852000      0.162321000      1.700756000
1        -3.191761000     -0.293896000      2.106923000
1        -3.801469000      1.130376000      1.300492000
1        -4.795192000      0.315912000      2.518680000
1        -4.837702000     -1.588650000      0.946095000
8        -2.622914000     -0.320188000     -1.369716000
1        -3.289291000     -0.584777000     -0.711635000
1        -5.433085000     -0.270288000      0.220353000
8        -1.729450000      2.198064000     -0.886287000
1        -2.150138000      1.348883000     -1.109319000
1        -1.922958000      2.794297000     -1.603355000
1        -1.830756000     -0.837153000     -1.204998000
```

A sample input file for reactant complex calculation in gas-phase using Cartesian coordinates system: acid (**ARC1**)

```
 # mPWB95/6-31+G(d,p) IOp(3/76=0560004400)
SCF=(Conver=9,MaxCycle=200) Integral=(grid=ultrafine)
OPT=(Verytight,Calcall,Maxcycle=30)

Reactant complex in acidic media

1 1
6                  -3.869124    0.206063   -0.104972
6                  -2.921177    1.299850   -0.407887
6                  -1.606024    1.111560   -0.327556
6                  -1.060360   -0.190662    0.065782
6                  -1.989839   -1.285806    0.360338
6                  -3.306262   -1.102571    0.282702
8                  -5.059939    0.380625   -0.173657
8                   0.147163   -0.371087    0.147668
1                  -3.361440    2.242649   -0.694080
1                  -0.893668    1.891885   -0.546083
1                  -1.546506   -2.228967    0.639150
1                  -4.019160   -1.884479    0.494232
7                   2.866160   -0.003378    0.294598
6                   3.158755   -0.332503    1.702805
1                   2.629359   -1.235986    1.976755
1                   4.225437   -0.471847    1.823547
1                   2.826432    0.488145    2.325485
1                   1.851660    0.092417    0.154050
1                   3.180310   -0.743459   -0.321682
1                   3.350818    0.873418    0.014204
8                   4.235832    2.270677   -0.302399
1                   4.436742    2.649069   -1.154992
1                   4.666426    2.824547    0.369302
8                   3.714898   -2.015637   -1.326778
1                   3.594029   -2.958143   -1.228829
1                   4.256996   -1.867811   -2.099182
```

A sample input file for reactant complex calculation in gas-phase using Cartesian coordinates system: base (**BRC1**)

```
# mPWB95/6-31+G(d,p) IOp(3/76=0560004400)
SCF=(Conver=9,MaxCycle=200) Integral=(grid=ultrafine)
OPT=(Verytight,Calcall,Maxcycle=30)

rc v8 basic

-1 1
6       -2.423114000      0.598104000      0.312715000
6       -1.052430000      0.948781000     -0.075464000
6       -0.190675000      0.026594000     -0.518984000
6       -0.596782000     -1.382817000     -0.623775000
6       -1.974765000     -1.745128000     -0.219649000
6       -2.826256000     -0.822155000      0.214677000
8       -3.226848000      1.419928000      0.708727000
8        0.147309000     -2.254287000     -1.027513000
1       -0.738233000      1.982086000      0.015015000
1        0.831627000      0.314650000     -0.794288000
1       -2.233227000     -2.790515000     -0.304611000
1       -3.838920000     -1.049158000      0.514343000
7        3.164164000     -1.243478000      0.266455000
6        2.599546000     -1.322878000      1.589410000
1        2.697609000     -2.333360000      1.989644000
1        3.145848000     -0.659070000      2.257679000
1        1.539736000     -1.042937000      1.661668000
1        2.630667000     -1.828717000     -0.357775000
8        2.449323000      1.369032000     -0.810827000
1        2.994128000      1.590087000     -1.561575000
1        3.056455000     -0.289274000     -0.094762000
8        1.056696000      3.320386000     -0.068549000
1        1.656828000      2.541145000     -0.404551000
1        1.483351000      3.625941000      0.725750000
```

A sample input file for a product complex calculation in gas phase using mixed coordinates system: neutral product complex

```
#HF/STO-3G

starting geometry manipulated towards product

0 1
 6      0.36249  -1.37667  -0.05285
 6      0.17191  -0.19218  -0.78716
 6     -1.05826   0.39057  -0.77565
 6     -2.22466  -0.28396  -0.13128
 6     -1.95935  -1.52643   0.61512
 6     -0.73018  -2.0381    0.64613
 8      1.48735  -1.96982   0.03544
 8     -3.33194   0.17846  -0.22564
 1      0.99523   0.21623  -1.35034
 1     -1.30876   1.19034  -1.45295
 1     -2.80061  -1.99132   1.10473
 1     -0.48565  -2.94892   1.16977
 7     -1.12822   1.53245   0.34293
 6     -0.45368   2.70306  -0.18127
 1     -0.30485   3.48611   0.56014
 1      0.51489   2.41885  -0.5911
 1     -1.03412   3.11912  -0.99806
 1     -0.72883   1.2188    1.21444
 1      2.19937   2.03402   0.98929
 8      2.90913   1.40273   1.08503
 1      3.36506   1.62317   1.89524
 8      3.32203  -0.48283  -0.8378
 1      4.13226  -0.66957  -1.30706
H 7 0.9 1 114.140 2 7.246
H 22 0.9 24 109.809 7 24.290
```